Neuronal Flt1 controls spinal cord vascularization involving venous endothelium with high angiogenic potential

Zur Erlangung des akademischen Grades eines

DOKTORS DER NATURWISSENSCHAFTEN

(Dr. rer. nat.)

von der KIT-Fakultät für Chemie und Biowissenschaften

des Karlsruher Instituts für Technologie (KIT)

genehmigte

DISSERTATION

von

Raphael Wild

aus

Berlin

KIT-Dekan: Prof. Dr. Willem Klopper

Referent: Prof. Dr. Ferdinand le Noble

Korreferent: Prof. Dr. Stefan Schulte-Merker

Tag der mündlichen Prüfung: 21.10.2016

Acknowledgments

I would like to express my deep gratitude to Prof. Dr. Ferdinand le Noble who gave me the opportunity to pursue my PhD in his lab in Berlin and later in Karlsruhe. With his endless scientific enthusiasm, positive energy and the many hours we discussed on the interpretation of results, he greatly promoted the success of my work. Ferdinand gave me the chance to freely develop my own ideas, scrutinize existing models and encouraged me on every step towards my PhD with constructive comments.

My special thanks goes to Alina Klems, who constantly gave me input with new ideas and thoughts for the development of my project. I am so grateful that you were part of the team moving to Karlsruhe and that I could share with you the nice little office in 439. Without you, the fast and efficient buildup of the lab in Karlsruhe would not have been possible and the coffee breaks on the terrace in the 5th floor at campus north would have been only half as nice.

This work could not have been completed without the great collaborators, Dr. Masanari Takamiya, who provided great genetic tools for the paper and most importantly, shared his long research experience with me. I would also like to thank Prof. Dr. Stefan Schulte-Merker, who helped with great discussions, reagents and zebrafish lines. Furthermore, I am very grateful to Dr. Tilmann Breiderhoff, who helped me countless times in troubleshooting my experiments.

I want to thank all the lab members from the le Noble group, especially Janine and Katja without whom many of my experiments would not have been possible. They also created a great working environment making it a pleasure to work in the lab. Many thanks go as well to Dr. Janna Krüger, who showed me how to work with zebrafish and produce all these beautiful images at the confocal microscope.

I am very thankful to my family and friends for their cheerful support, confidence and encouragement. Lastly, I want to thank Caroline for being on my side during these challenging years while completing my PhD. You kept me sane and showed me what really matters in life.

Erklärung

Der experimentelle Teil der vorliegenden Arbeit wurde am Max-Delbrück-Centrum für Molekulare Medizin in Berlin, am Institut für Toxikologie und Genetik des Karlsruher Instituts für Technologie (KIT) sowie am Zoologischen Institut, Abteilung für Zell- und Entwicklungsbiologie am (KIT) in der Zeit von September 2012 bis August 2016 durchgeführt.

Ich versichere, dass ich meine Doktorarbeit selbstständig angefertigt und keine anderen als die angegebenen Quellen und Hilfsmittel benutzt, sowie die wörtlichen oder inhaltlich übernommenen Stellen als solche kenntlich gemacht und die Satzung des Karlsruher Instituts für Technologie (KIT) zur Sicherung guter wissenschaftlicher Praxis in der jeweils gültigen Fassung beachtet habe.

Raphael Wild, August 2016

Table of Contents

1 Summary 8

2 Zusammenfassung 9

3 Introduction 11

3.1 A historical perspective on vascular research 12
3.2 The vascular system 14
3.3 Zebrafish trunk vascular development 14
3.3.1 Zebrafish trunk vasculogenesis 14
3.4 Arteriovenous differentiation 16
3.5 Arteriolar and venular differences 18
3.6 Angiogenesis 19
3.6.1 Spouting angiogenesis and the tip cell concept 20
3.7 Zebrafish trunk angiogenesis 25
3.7.1 Primary and secondary sprouting 25
3.7.2 Decision making – becoming vein or lymphatic? 26
3.7.3 Bmp signaling drives caudal vein plexus formation 27
3.7.4 Directional migration of angiogenic sprouts 28
3.8 The zebrafish spinal cord – development and function 30
3.9 A late friendship – neurovascular development 31
3.9.1 VEGF receptors 32
3.10 The master regulators of angiogenesis – VEGF receptors 32
3.10.1 Expression and Regulation of VEGFRs 34
3.10.2 VEGFR-1 (FLT1, Flt1) function and signaling 34
3.10.3 Clinical implications of angiogenesis and Flt1 39
3.10.4 VEGFR-2 (Kdr/Kdrl) – the focal point of vascular biology 40
3.10.5 VEGFR-3 (FLT4,Flt4) function in vascular biology 42
3.10.6 VEGF ligands 43
3.10.7 Expression and regulation of VEGFs 45
3.11 Dll4-Notch signaling 46
3.11.1 Notch signaling in AVD 46
3.11.2 The role of Notch in angiogenesis 47
3.12 Anastomosis and lumen formation 48
3.12.1 Vascular lumen formation 48
3.13 Endothelial cell junctions 48
3.14 Morpholinos – friend or foe? 49
3.15 Aim of the work 51

4 Results 52

4.1 Loss of Flt1 induces massive hypervascularization of the spinal cord 52

4.1.1 Generation of *flt1* full mutants 52
4.1.2 Generation of *mflt1*-specific mutants 63
4.2 Spinal cord neurons express Flt1 and Vegfaa 64
4.2.1 Analysis of *flt1*^{ka601}; *vhl*^{hu2117} double mutants 68
4.3 Ectopic neurovascular networks in *flt1*^{ka601} and other Vegfaa gain-of-function scenarios originate from venous ISVs 70
4.4 Ectopic sprouts in *flt1*^{ka601} mutants display distinctive angiogenic cell behaviors 73
4.4.1 Nuclear migration and positioning is linked to ectopic sprout initiation 75
4.5 *flt1*^{ka601} ectopic sprouts are blood flow dependent 77
4.5.1 Ectopic *flt1*^{ka601} sprouts originate from remodeled arterial or purely venous ECs 78
4.5.2 Spinal cord vascularization in WT larvae involves venous sprouting 80
4.5.3 Notch related genes are not deregulated in *flt1*^{ka601} mutants 81
4.6 Artery-vein differences in Vegfaa responsiveness can be explained with notch 84
4.7 Neuronal sFlt1 and Vegfaa determine angiogenic sprouting at the neurovascular interface 86
4.7.1 Transplanted *flt1*^{ka601} neurons but not ECs are competent to induce hypersprouting 87
4.8 Neuronal soluble Flt1 controls spinal cord vascularization 88
4.9 Neuronal Vegfaa drives spinal cord vascularization in *flt1*^{ka601} mutants 90

5 Discussion 92

5.1 Distinctive angiogenic cell behaviors in *flt1*^{ka601} tertiary sprouts 92
5.2 Neuronal Flt1 – a new cellular source of an old player 97
5.3 The tip cell concept – we need new models for an old question 101
5.4 Veins not arteries make new vessels 104
5.5 Finding the balance – safeguarding supply without disrupting neuronal differentiation 106

6 Materials and Methods 109

6.1 Materials 109
6.1.1 Transgenic lines 109
6.2 Methods 114
6.2.1 Ethics statement 114
6.2.2 Morpholino injections 114
6.2.3 mRNA injection and generation of transgenic/mutant lines 114
6.2.4 Generating *flt1* mutants 114
6.2.5 Generation of *mflt1 specific* mutants 115
6.2.6 Generation of p5E_ Xla.Tubb-3.8 and p5E_flt1^{enh} 116
6.2.7 Generation of pME_eGFP-p2A_SmaI 116
6.2.8 pME_eGFP-p2A_*vegfaa* 165, vegfc and *sflt1* cloning 116
6.2.9 Generation of gateway expression clones 117
6.2.10 Generation of tissue-specific KO constructs 117

6.2.11 FACS analysis 118
6.2.12 Gene expression analysis by real-time qPCR 118
6.2.13 RNA-Seq library preparation and sequencing 118
6.2.14 Identification of differentially expressed genes 119
6.2.15 Zebrafish histological sectioning 119
6.2.16 Inhibitor treatments 119
6.2.17 Gal4ERT2 endoxifen activation 119
6.2.18 Vascular network analysis 120
6.2.19 Imaging 120
6.2.20 Statistical analysis 120

7 Bibliography 121

8 Abbreviations 136

9 Publications 139

10 Curriculum Vitae 140

1 Summary

Whole body homeostasis requires the coordinated actions of multiple organs to sustain blood perfusion, maintenance of blood oxygenation and nutrient supply. Each organ has an unique role herein and in order to fulfill this task efficiently, tissue-specific vascular networks with defined functional properties and branching architecture have emerged during evolution. Organ-specific vascular networks and tissue functions are dependent on angiocrine mechanisms and intensive cross-talk between vascular cells and cells of the surrounding organs. Nerves critically depend on blood vessels, as small changes in vascular supply can have profound effects on neuronal function, survival and regeneration. While it is appreciated that neurons can secrete vascular growth factors, little is known how the developing nervous system becomes vascularized. In the present work, we focused on neurovascular cross-talk between the developing spinal cord and surrounding blood vessels in the trunk of the zebrafish. Using tissue-specific and inducible loss- and gain-of-function approaches, we show that neurons produce Vegfaa and sFlt1 to dynamically regulate spinal cord vascularization. Loss of sFlt1 or gain of Vegfaa promotes angiogenesis along the spinal cord, whereas combining both promotes ingrowth into the neural tube. This suggests that these events correlate with neuronal differentiation and associated changes in neuronal metabolism. High-resolution *in vivo* analysis of cellular behavior at single cell level within growing angiogenic sprouts shows that neurons attract new blood vessels exclusively from veins. The process of venous sprouting requires adequate nuclear positioning prior to sprout initiation, which is driven by the Vegfaa-Kdrl-PI3/Akt pathway and is independent of Notch. Based on the differences of the cellular and molecular signature – with previously described primary and secondary sprouting modes – we termed the process 'tertiary sprouting'. We propose that the spinal cord uses a two-tiered mechanism to regulate lateral and internal vascularization involving neuronal sFlt1 and Vegfaa. Altogether, we show that spinal cord neurons and tertiary sprout-capillaries form a neurovascular unit, which is tightly regulated by neurovascular cross-talk.

2 Zusammenfassung

Die Homöostase des Körpers erfordert das koordinierte Zusammenspiel verschiedener Organe, um die Durchblutung, die Sauerstoffversorgung und die Nährstoffversorgung auf zellulärer Ebene zu gewährleisten. Jedes Organ spielt hierbei eine spezifische Rolle und hat im Laufe der Evolution ein gewebespezifisches Blutgefäßsystem mit einzigartiger Morphologie und funktionalen Eigenschaften entwickelt. Organspezifische vaskuläre Netzwerke und die Funktion von Geweben sind von angiokrinen Mechanismen und dem engen cross-talk zwischen Endothelzellen und Zellen des umgebenden Organs abhängig. Nerven reagieren besonders empfindlich auf Schwankungen in der Blutversorgung und nur geringe Veränderungen können deren Funktion beeinträchtigen oder sogar zum Absterben führen. Es ist hinreichend bekannt, dass Neuronen vaskuläre Wachstumsfaktoren sekretieren, jedoch der genaue Ablauf der Vaskularisierung des Nervensystems und deren molekulare Steuerung ist weitgehend unbekannt.

In der vorliegenden Arbeit untersuchen wir den neurovaskulären cross-talk zwischen dem sich entwickelnden Neuralrohr und den unmittelbar angrenzenden Blutgefäßen im Modelsystem Zebrafisch. Durch die Verwendung von gewebespezifischen, induzierbaren loss- und gain-of-function Experimenten konnten wir zeigen, dass Neuronen Vegfaa und sFlt1 produzieren und so die Vaskularisierung des Neuralrohr dynamisch steuern können. Der Verlust von sFlt1 oder die Hochregulation von Vegfaa regte die laterale Vaskularisierung entlang des Neuralrohrs an, wohingegen die Kombination von beidem das Einwachsen von Gefäßen in das Neuralrohr bewirkte. Dies legt nahe, dass diese Ereignisse mit der neuronalen Differenzierung und der anschließenden Änderung der metabolen Aktivität von Neuronen korrelieren. Hochaufgelöste *in vivo* Analysen der zellulären Verhaltensmuster in angiogenen Gefäßsprossen zeigte, dass ausschließlich venöse Gefäßsprosse zur Bildung des perineuralen vaskulären Netzwerkes beitragen können. Diese venöse Gefäßsprossung erfordert die adäquate Positionierung des endothelialen Zellkerns in unmittelbarer Nähe zum Ort der Sprossungsinitiierung, die durch den Vegfaa-Kdrl-PI3K/Akt Signalweg unabhängig von Notch induziert wird. Bedingt durch die molekularen und zellulären Unterschiede zu den bekannten primären und sekundären Sprossungsprozessen bezeichnen

wir den Prozess als `tertiäre Sprossung'. Wir postulieren, dass das Neuralrohr einen zweistufigen sFlt1/Vegfaa-abhängigen Mechanismus verwendet um die laterale und interne Vaskularisierung zu steuern. Zusammenfassend zeigen wir, dass Neuronen des Neuralrohrs und perineuralen Kapillaren, die aus den tertiären Sprossen gebildet werden, eine neurovaskuläre Einheit bilden, welche durch die fein abgestimmte Regulation der Neuronen gesteuert wird.

3 Introduction

The vascular system supplies organs throughout the entire human body and is estimated to have a total length of more than 100,000 km in an average human being (Aird 2005). It supplies oxygen, nutrients, signaling molecules and immune cells to its target organs and removes CO_2 and waste products (Carmeliet 2003; Adams & Eichmann 2010).

The circulation connects the heart, lungs and target tissues and consists of a hierarchical system of arteries, arterioles, capillaries, venules and veins to safeguard the function of organs and cells (Adams & Eichmann 2010; Herbert & Stainier 2011). In adults, growth of blood vessels is tightly controlled and an imbalance in this process contributes to various inflammatory, ischemic, infectious and immune disorders as well as cancer (Carmeliet 2003; Carmeliet 2005).

Blood vessel growth and the integrity of the vascular homeostasis have tremendous effects on disease progression. When a tumor lesion exceeds a few millimeters in diameter, hypoxia and nutrient deprivation can trigger an 'angiogenic switch' and the tumor starts to secret molecules to activate vascularization from adjacent tissues to promote its growth and finally becomes harmful (Hanahan & Folkman 1996; Bergers & Benjamin 2003). The relatively simple but ingenious idea to block this process in order to restrict tumor growth was already put forward in 1971 (Folkman 1971). In 2004, the first anti-angiogenic agents were approved by the U.S. Food and Drug Administration (FDA) for the treatment of cancer and eye disease (Al-Husein et al. 2012). Anti-angiogenic therapy is nowadays routinely used as adjuvant therapy for the treatment of many cancers (Al-Husein et al. 2012).

Despite these encouraging advances, tumor resistance and compensation by alternative signaling pathways as well as side effects such as bleeding require angiogenesis research to identify therapeutic targets exclusively present in growing blood vessels (Elice et al. 2012). Recent research identified promising targets such as glycolytic endothelial metabolism and molecules specific to pathological angiogenesis, which can possibly be targeted with fewer

side effects and cannot be compensated by the tumor (De Bock et al. 2013; Dewerchin & Carmeliet 2012).

Coronary artery disease (CAD) was the leading cause of death worldwide in 2010 (Moran et al. 2014). CAD is characterized by an atherosclerotic occlusion of a coronary artery resulting in hypoperfusion and ischemia in the heart myocardium with subsequent infarct and heart failure (Ambrose & Singh 2015). Stimulation of collateralization (arteriogenesis) or therapeutic angiogenesis could be used to prevent or treat CAD in a non-invasive manner (Simons 2005; Degen et al. 2014). However, to effectively treat CAD using pro-angiogenic or pro-arteriogenic agents many hurdles have to be overcome and more research is needed (Rubanyi 2013). Another approach is the ischemic organ revascularization with vascular progenitor cells injected into the blood of the patient (Rafii & Lyden 2003; Nolan et al. 2013; Rafii et al. 2016). In addition, sufficient blood vessel supply is extremely important to protect neurons from neurodegenerative processes (Storkebaum & Carmeliet 2004; Oosthuyse et al. 2001; Lange, Storkebaum, et al. 2016).

In the future it will be important to develop effective pro- and antiangiogenic agents, ideally locally modulating vascular growth.

3.1 A historical perspective on vascular research

Judah Folkman was one of the first investigators exploring the field of vascular development (Folkman 1971; Ribatti 2008). He hypothesized that a tumor could not grow to a larger volume than 1 mm^3 without vascularization and thus could not be harmful in a prevascular state (Folkman 1971; Hanahan & Folkman 1996). This idea and the identification of collateralization as an important mechanism to evade arterial occlusions from Wolfgang Schaper boosted vascular research by the end of the 1980s (Schaper et al. 1988).

Our knowledge of vascular development was and is vastly dependent on suitable model systems, which can be used to elucidate the underlying processes of vascular growth (Santhakumar et al. 2012). The first model systems used in vascular research were the frog, the pig and the chick embryo (Thoma 1873; Sabin 1917). The vessels of the chick

chorioallantoic membrane (CAM) are readily accessible and can therefore be easily studied without the vascular plexus formed in the CAM rapidly acquires a hierarchical organization with emerging arteries and veins, a process known as vasculogenesis followed by flow-induced vascular remodeling (le Noble et al. 2004; Nowak-Sliwinska et al. 2014).

As a consequence, most early (end of 1980s) research investigated a process termed vasculogenesis, the de novo formation of blood vessels (Risau & Flamme 1995). In the middle of the 1990s, mouse mutants became available and vasculogenesis was studied in the primitive vascular plexus of the mouse yolk sac (Fong et al. 1995; Shalaby et al. 1995; Carmeliet et al. 1996; Ferrara et al. 1996). Mouse vascular research was mainly restricted to the yolk vascular plexus and gross vascular anatomy, thus only severe developmental defects could be identified at this time (Fong et al. 1995; Carmeliet et al. 1996). The major breakthrough came with the development of the mouse retinal vascular model, a postnatal model characterized by a defined vascular plexus formed by angiogenesis in the retina of the eye (Stone & Dreher 1987; Ruhrberg et al. 2002; Gerhardt et al. 2003). The mouse is a particularly attractive model for vascular research since genetic techniques are far advanced, facilitating genetic interventions (Davis 2004). The major disadvantage of the retinal vascular model is that vessel growth cannot be analyzed in a dynamic manner, because the retina has to be prepared from euthanized neonates (Stone & Dreher 1987).

By 2000, the first zebrafish vascular reporter lines were established (Isogai 2001). Using zebrafish as a model system brings several advantages. They are transparent, develop ex-utero and all organ primordia are developed before 36 hours post fertilization (hpf) (Lieschke & Currie 2007; Veldman & Lin 2008). Hence, vascular development can be followed dynamically in all organs, using time-lapse imaging (Kamei & Weinstein 2005). Since 2013, zebrafish can be easily genetically manipulated using CRISPR/Cas (Clustered Regularly Interspaced Short Palindromic Repeats), revolutionizing the use of zebrafish as a vascular model system (Hwang et al. 2013; Auer & Bene 2014; Ablain et al. 2015).

3.2 The vascular system

The heart pumps blood into the lungs to be enriched with oxygen. The oxygen-rich blood is then spread throughout our body into arteries and smaller arterioles (Carmeliet 2003; Adams & Eichmann 2010). From arterioles the blood is drained into the smallest blood vessels – the capillaries, which are in contact with single cells and have small diameters in the size range of an erythrocyte (Y C Fung & Zweifach 1971). Cells are supplied with nutrients and oxygen by capillaries and secrete carbon dioxide and waste products into the blood, which is carried by venules and veins into the vena cava to be eventually released by the lungs (Carmeliet 2003; Herbert & Stainier 2011). The lymphatic vascular system is important for the reuptake of extravasated fluid from blood vessels and its drainage back into the blood circulation together with the transport of immune cells (Adams & Alitalo 2007; Tammela & Alitalo 2010).

3.3 Zebrafish trunk vascular development

The zebrafish vasculature constitutes an ideal model system to study developmental angiogenesis (Isogai et al. 2001; Veldman & Lin 2008). Zebrafish embryos develop externally and can therefore be dynamically imaged. They are transparent and thus easy to access and in addition, they are readily genetically modified (Veldman & Lin 2008; Isogai et al. 2001; Kamei & Weinstein 2005; Hwang et al. 2013). In contrast to the mouse model, zebrafish embryos develop ex utero and do not form a yolk vascular plexus.

3.3.1 Zebrafish trunk vasculogenesis

Vasculogenesis in zebrafish starts with the differentiation of two distinct subpopulations of angioblasts in the head and the trunk (Jin et al. 2005; Proulx et al. 2010). Trunk angioblasts are specified in the lateral plate mesoderm and migrate towards the midline to coalesce into the dorsal aorta (DA) (Isogai et al. 2003).

3.3.1.1 From mesodermal precursors to endothelial cells

The zebrafish cloche (*npas4*) mutant fails to generate the hematopoietic lineage and angioblasts and was shown to be the master regulator of hematopoietic and endothelial development (Stainier et al. 1995; Reischauer et al. 2016). The gene *npas4* (Cloche) is a bHLH PAS transcription factor upstream of *etv2* and *tal1* driving commitment of mesodermal cells to endothelial and hematopoietic cells. *npas4* is thus the earliest known angioblast marker activating *etv2* (Patterson & Patient 2006; Reischauer et al. 2016). However, how *npas4* expression and angioblast specification is activated in mesodermal cells is unknown. Cells expressing transcription factors of the ETS family such as *etv2* upregulate the endothelial markers *kdrl* and *fli1a* in order to initiate endothelial differentiation (Sumanas & Lin 2006; Reischauer et al. 2016). Quadruple knockdown of all ETS transcription factors expressed in the zebrafish, namely *etv2, ets1, fli1a and fli1b* as well as ectopic *etv2* expression showed that ETS transcription factors are necessary and sufficient to drive angioblast differentiation in zebrafish (Pham et al. 2007).

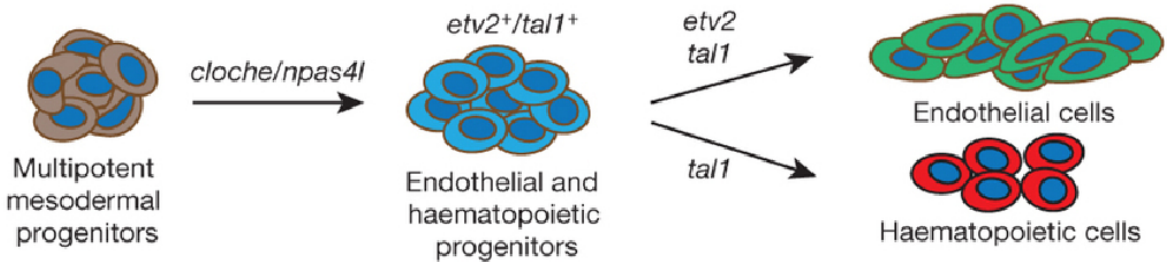

Figure 3-1 Angioblast differentiation from mesodermal precursors

Multipotent mesodermal progenitors upregulate the transcription factor *npas4l* (cloche) to differentiate into endothelial and hematopoietic progenitors by a yet unknown mechanism. These progenitors upregulate the transcription factors *tal1* to differentiate into hematopoietic cells or *tal1* and *etv2* to become endothelial cells. It is unknown how the selective upregulation of etv2 is achieved. Modified from (Reischauer et al. 2016).

3.3.1.2 From angioblasts to functional vessels

Following angioblast specification angioblasts migrate to the midline. This process is regulated by Elabela (Ela)-Apelin (Apln) receptor (Aplnr) signaling in zebrafish (Helker et al. 2015). Apelin and Elabela are expressed at the midline and function as a chemoattractants by activating directed Apelin receptor-mediated migration (Helker et al. 2015). Angioblast eventually coalesce at the midline to form a chord-like structure. This precursor vessel is

separated into the DA and posterior cardinal vein (PCV) by a process termed selective cell sprouting (Herbert et al. 2009). This process is considered to be dependent on EphrinB2-EphB4's repulsive action. Repulsive EphrinB2-EphB4 forward signaling in venous cells expressing EphB4 segregates them ventrally from the DA where they form the PCV (Herbert et al. 2009; Kania & Klein 2016). DA and PCV formation is completed by 24hpf and this simple vascular system consisting of the heart, DA and PCV starts to carry blood flow (Isogai et al. 2001; Isogai et al. 2003).

In summary, zebrafish mesodermal precursor cells are specified by an unknown stimulus and start to express *npas4* and *tal1*. In a subpopulation of these *npas4*$^{+}$, *tal1*$^{+}$ cells *etv2* is upregulated, which activates endothelial genes resulting in endothelial specification. However, how only some *npas4*$^{+}$, *tal1*$^{+}$ cells are activated to upregulate *etv2* in order to produce the endothelial lineage is currently unknown. The *etv2*$^{+}$ angioblasts migrate in an Ela-Apelin-APJ-receptor-dependent manner to the midline to coalesce into the DA and PCV forming a simple circulation.

3.4 Arteriovenous differentiation

Arteries and veins were historically defined by parameters such as direction of flow and oxygenation level together with their anatomical and functional differences (Wang et al. 1998). Wang and colleagues were the first to show that arteries and veins are genetically hardwired prior to the onset of flow. Their studies show that already prior to the onset of flow Ephrin-B2 is specifically expressed in arteries, whereas EphB4 is mainly found in veins (Wang et al. 1998). In EphrinB2$^{-/-}$ KO mice angiogenesis but not vasculogenesis is affected, suggesting that arteriovenous differentiation is not required for vasculogenesis (Wang et al. 1998).

Since then, a variety of artery- and vein-specific markers such as Notch, Dll4, Flt4, Flt1, NRPs, COUP-TFII, connexins and other factors have been described (Lawson et al. 2001; le Noble et al. 2004; Siekmann & Lawson 2007; Swift & Weinstein 2009). Notch has been identified as the main driver of arterial differentiation, whereas venous differentiation was assumed to be the default pathway inhibited by Notch in arterial ECs (Lawson et al. 2001; Torres-Vázquez et al. 2003). However, COUP-TFII, an orphan nuclear receptor, was later found to be

expressed specifically in veins releasing venous ECs from the Notch-mediated repression, thus showing that the venous status is not default, but rather has to be activated (You et al. 2005; Swift & Weinstein 2009). How COUP-TFII is activated in venous ECs and why it is only activated in a subset of ECs is yet poorly understood.

On the other hand, the process of arterial differentiation is far better appreciated. In zebrafish sonic hedgehoc (Shh) was shown to be upstream of Vegfa and to be expressed in the notochord where it induces *vegfaa* expression in adjacent somites (Lawson et al. 2002). In turn, Vegfaa secreted from the somites activates *notch* and *dll4* expression in the adjacent DA but not in the PCV, which is possibly too distant to experience sufficient Vegfaa levels. VEGFR2 and NRP1 were shown to upregulate *NOTCH1* and *DLL4* in arteries (Liu et al. 2003). NRP1 acts hereby as a coreceptor enhancing VEGF-A-VEGFR2 signaling to promote arterial differentiation (Mukouyama et al. 2005; Jones et al. 2008). DLL4-NOTCH signaling in turn activates arterial markers such as *FLT1* and *EFNB2* (Funahashi et al. 2010; Jakobsson et al. 2010; Siekmann & Lawson 2007). After arteriovenous differentiation (AVD) is completed, ECs have to be separated from each other to form arteries and veins, respectively. This separation is considered to be driven by EphrinB2-EphB4-mediated EC repulsion (Füller et al. 2003; Herbert et al. 2009). Interestingly, *ephB4* knockdown in zebrafish leads to increased venous intersegmental vessel (vISV) numbers similar to *dll4*^{j16e1} mutants (Leslie et al. 2007; Kawasaki et al. 2014). As EphrinB2 is known to be downstream of Dll4/Notch signaling it is tempting to suggest that EphrinB2-EphB4's repulsive actions in aISVs and secondary sprouts regulate venous remodeling in zebrafish (Lawson et al. 2001; Siekmann & Lawson 2007). Interestingly, EphrinB2 was also shown to be involved in VEGFR-2 internalization and thereby enhances VEGFR2 signaling (Wang et al. 2010; Sawamiphak et al. 2010); however how these two functions are connected remains elusive.

In addition, the importance of genetic determinants in arteriovenous differentiation (AVD) is emphasized by the fact that hemodynamic forces are not the driver of AVD during development. Strikingly, le Noble and coworkers showed that ligated chicken arteries which reroute blood flow (arteries with venous flow) rapidly downregulate arterial markers and induce venous markers at a somewhat slower pace (le Noble et al. 2004). This experiment clearly demonstrates the remarkable plasticity of blood vessels, i.e. differentiation status is not ultimate but can be switched by hemodynamic forces (le Noble et al. 2004).

In summary, the formation of the initial blood vessels during development is genetically hardwired, but vascular remodeling and thus changing hemodynamic forces can rapidly reprogram vessel identity. However, the exact function of EphrinB2 and EphB4 in AVD remains elusive. In addition, how flow regulates AVD mechanistically is poorly understood. Arteries and veins have different susceptibility to a disease such as atherosclerosis, which cannot be explained solely by differences in blood flow. Thus, understanding the differences in endothelial cell function and vascular architecture between arteries and veins could be key to a better comprehension of disease conditions (Cui et al. 2015).

3.5 Arteriolar and venular differences

Arteries branch into smaller arterioles feeding the capillary bed, which drains into post-capillary-, collecting- and paramuscular venules with increasing diameter. Arterioles express markers such as Flt1, Nrp1, Gja5 (connexin 40), Notch1, Dll4 and Efnb2 (Wang et al. 1998; le Noble et al. 2004; Siekmann & Lawson 2007; Bussmann et al. 2010; Buschmann et al. 2010). However, the expression level of these genetic markers is highly dependent on the model organism (le Noble et al. 2004; Siekmann & Lawson 2007). Moreover, arterioles experience higher shear stress and blood pressure and are covered by more pericytes than venules. In addition, higher VE-cadherin levels in arterioles prevent immune cell extravasation and decrease vascular permeability (Vestweber 2015; Orsenigo et al. 2012).

Venules, in contrast, express genetic markers such as Flt4, Dab2, Ephb4 and CoupTFII, experience low shear stress and low blood pressure (Wang et al. 1998; You et al. 2005; L. D. Covassin et al. 2006; Hogan et al. 2009). Flt4 is downregulated during vein maturation and is only a marker for early venous development and angiogenic endothelia and the lymphatic system (Hogan et al. 2009; Adams & Alitalo 2007; Herbert & Stainier 2011). Venules are covered by few pericytes and express low VE-cadherin levels; thus leucocyte extravasation occurs mainly in post-capillary venules (Vestweber 2015). Of note, also angiogenesis and inflammation reactions occur predominantly in post-capillary venules and capillaries and not in arterioles (Risau 1995; Bergers & Benjamin 2003).

In conclusion, even small blood vessels such as arterioles and venules exhibit great genetic and functional differences with extensive physiological consequences. Although it is known for decades that angiogenesis during wound healing or tumorangiogenesis occurs from capillaries and the venular side this phenomenon is largely ignored in angiogenesis research. Most sprouting angiogenesis models do not differentiate between arteries and veins and sprouting enhancement or decrease is typically quantified in all vessels, but not specifically for arteries and veins. If we understood better the differences between arteries and veins and their sprouting behavior we could presumably target veins specifically or enhance vein formation to induce angiogenesis.

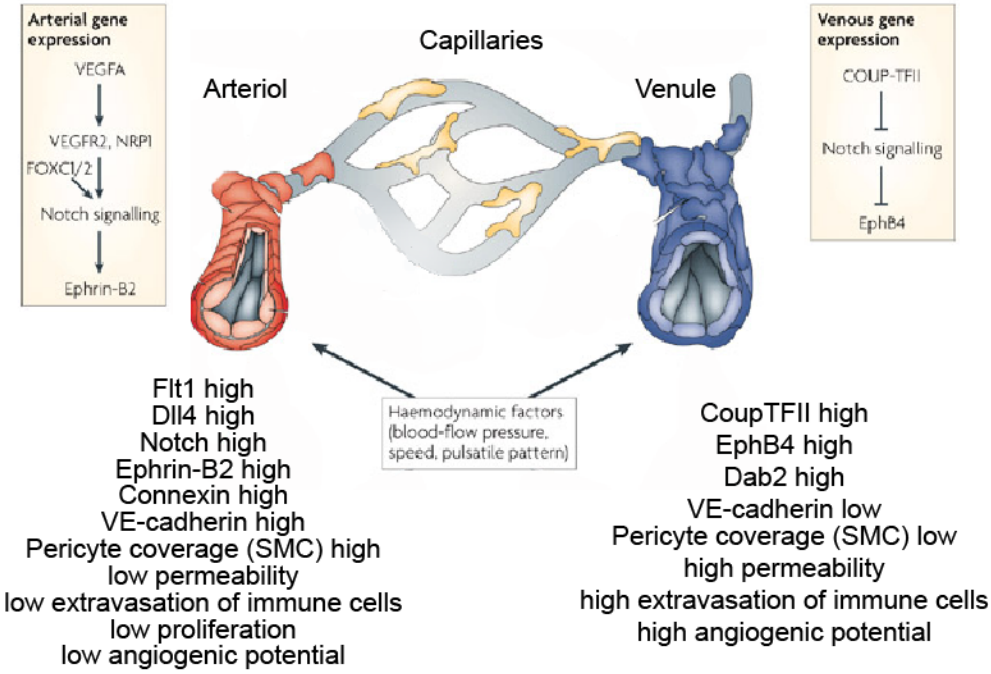

Figure 3-2. Differences between arterioles and venules

Arterioles and venules express distinct set of markers and display different characteristics regarding permeability, extravasation capacity and angiogenic potential. Modified from (Adams & Alitalo 2007).

3.6 Angiogenesis

In the early embryo, the first blood vessel structures are formed by vasculogenesis (Risau & Flamme 1995). Vasculogenesis forms the major large vessels such as the primary vascular plexus, the DA, the CV, the perineural vascular plexus (PNVP) surrounding the central bervous system (CNS) and the early cranial vasculature (Herbert & Stainier 2011). These

primitive structures serve as a template and are expanded by a process called angiogenesis (Folkman & Shing 1992; Flamme et al. 1997; Carmeliet 2003). Angiogenesis is defined as the growth of vessels from pre-existing ones (Folkman & Shing 1992; Flamme et al. 1997). Large vessels have a stereotyped pattern, which is comparable in different individuals from the same species (Carmeliet 2003; Eichmann 2010). These stereotyped vessels are formed by vasculogenic processes such as angioblast aggregation or plexus formation and subsequent vascular remodeling (Carmeliet 2003; Eichmann 2010). Growth of most small vessels is non-stereotyped and mainly governed by metabolic demand (Adams & Eichmann 2010). Two types of angiogenesis have been described sprouting angiogenesis and the less well-understood but possibly important intussuseptive angiogenesis (Burri et al. 2004).

3.6.1 Spouting angiogenesis and the tip cell concept

Sprouting angiogenesis is a highly complex process involving the selection of an endothelial cell (EC), the guided migration of this EC and its subsequent connection with other sprouts forming an anastomosis and a functional vascular loop (Ruhrberg et al. 2002; Gerhardt et al. 2003; De Smet et al. 2009). Even after years of quiescence, blood vessels retain the capability to propagate and to form angiogenic sprouts (De Bock et al. 2013). These sprouts are formed predominantly in small vessels at the capillary- and venular side (Risau 1995; Bergers & Benjamin 2003). Contradictory, most vascular research in zebrafish is focused on arterial primary sprouting, which is presumably a very rare process with limited relevance for health and disease (Ellertsdóttir et al. 2010).

To activate sprouting from a parent vessel, pericytes have to be removed and the basement membrane and surrounding extracellular matrix (ECM) need to be degraded (Adams & Alitalo 2007; Herbert & Stainier 2011). Growth factors such as VEGF-A, VEGF-C, Angiopoetin 2 (ANG-2) and bone morphogenetic proteins (BMPs) are capable to activate sprouting angiogenesis (Herbert & Stainier 2011; Wiley et al. 2011). Tightly regulated EC selection ensures that only some ECs are selected upon growth factor exposure (Ruhrberg et al. 2002; Gerhardt et al. 2003; Siekmann & Lawson 2007; Siekmann et al. 2013). Pro-angiogenic growth factors activate a so-called ‘tip cell’ for sprouting. VEGF-A activates VEGFR-2 in competing ECs, resulting in upregulation of delta like 4 (DLL4) (Roca & Adams 2007; Phng &

Gerhardt 2009). DLL4 in turn inhibits adjacent endothelial cells from sprout formation by activation of the NOTCH pathway in these cells, a process known as lateral inhibition (Gerhardt et al. 2003; Jakobsson et al. 2010; Herbert & Stainier 2011). Thereby, ECs experiencing the highest growth factor concentration are thought to be selected to become tip cells and inhibit their adjacent ECs, the so-called 'stalk cells', from adopting a tip cell fate (Siekmann & Lawson 2007; Hellström et al. 2007; Suchting et al. 2007).

Stalk cells are considered to proliferate and follow the guiding tip cell (Gerhardt 2008; Blanco & Gerhardt 2013). The inhibition of tip cell formation in stalk cells is thought to be realized via a NOTCH1-mediated *Flt4* down- and *Flt1* (*Vegfr-1*) upregulation (Siekmann & Lawson 2007; Funahashi et al. 2010). In stalk cells *Dll4* is similarly upregulated to inhibit adjacent ECs, not in direct contact with the tip cell. *Jag1* which is predominantly expressed in stalk cells is thought to block DLL4 –NOTCH1 signaling specifically in the tip cell (Benedito et al. 2009), and the deacetylase SIRT1 may deacetylate the notch intracellular domain (NICD) in the tip cell to accelerate proteasomal NICD degradation and thus destabilizing it, and consolidating tip cell identity (Guarani et al. 2011). Tip cell-enriched expression of *flt4* in zebrafish has been observed in primary sprouts and its expression is expanded to stalk cells in the absence of Notch signaling (Siekmann & Lawson 2007). Remarkably, in *flt4*^{hu4602} zebrafish mutants no primary sprouting phenotype could be observed, suggesting a minor role for Flt4 in this particular sprouting event. It is currently debated if and how *flt4*-deficient ECs can initiate sprouting angiogenesis and whether FLT4 can replace VEGFR-2 in retinal ECs (Tammela et al. 2008; Hogan et al. 2009; Benedito et al. 2012; Zarkada et al. 2015). VEGFR-1 is thought to act as a decoy receptor scavenging VEGFA in the microenvironment of stalk cells and thereby limiting VEGFA bioavailability and VEGFR-2 signaling in these cells (Funahashi et al. 2010; Herbert & Stainier 2011; Krueger et al. 2011).

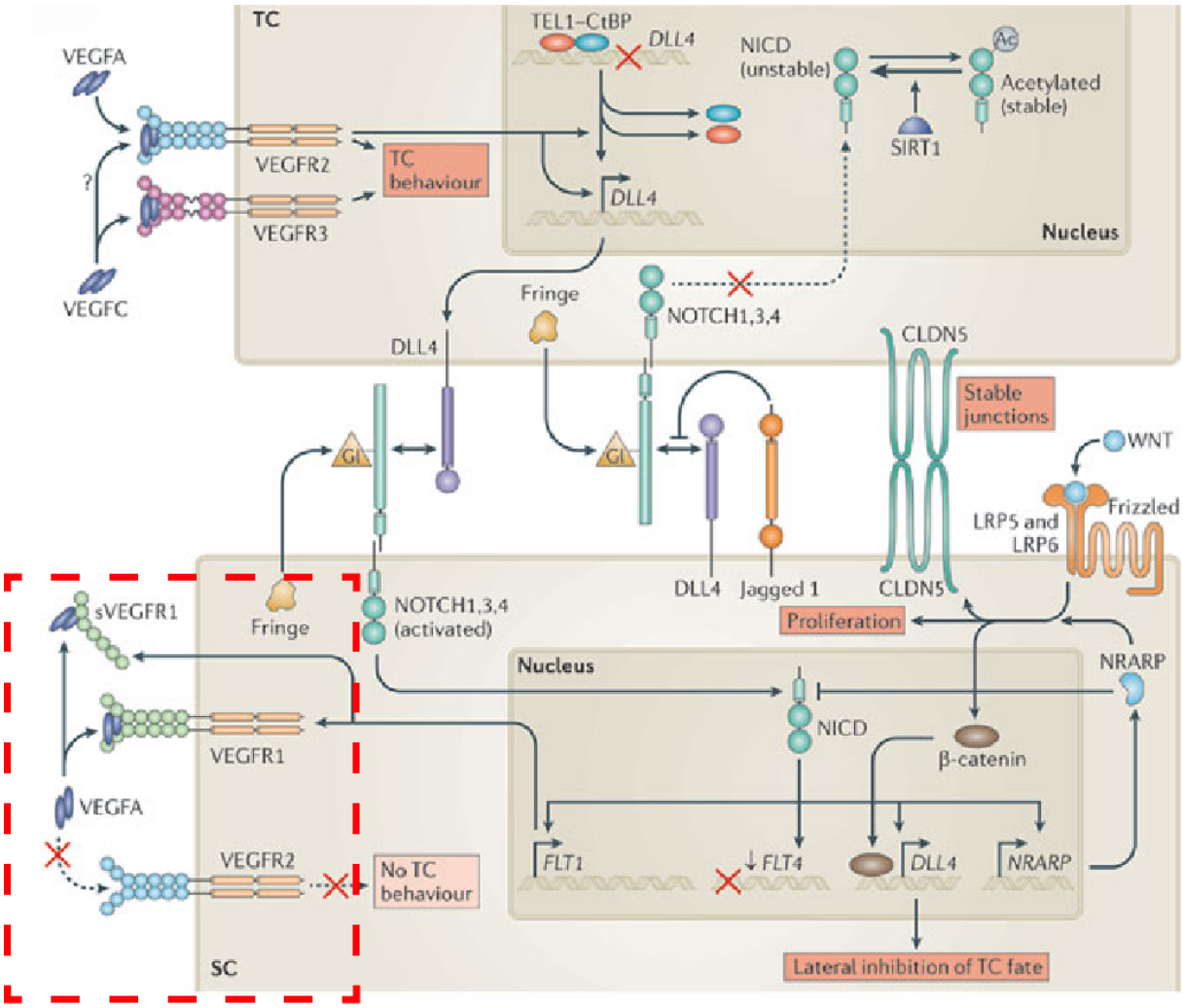

Figure 3-3. The tip cell concept

The tip cell concept is a model to explain how ECs select only a limited number of TCs to expand a vascular network in a coordinated manner. VEGFA activates VEGFR2, upregulating DLL4. The ECs experiencing the highest VEGFA levels upregulate DLL4 most rapidly and block sprouting and TC-formation in adjacent cells via NOTCH-mediated lateral inhibition. Notch target genes such as DLL4, FLT1 and NRARP activate SC-characteristics such as proliferation (NRARP) and prevent tip cell formation by limiting VEGFR2 signaling in the close microenvironment of the SC (FLT1), emphasized by the red dotted box. DLL4 is thought to block adjacent cells from becoming TCs. The TC is though to be protected from SC differentiation by SIRT1 mediated NICD destabilization and Jagged1 mediated blockade of DLL4-Notch signaling in the TC. TC, tip cell, SC, stalk cell. Modified from (Herbert & Stainier 2011).

Strikingly, *dll4*, *flt1* and *notch1a* are arterial markers in zebrafish and other organisms, and at least Dll4 and Notch1a are major regulators of arterial differentiation (le Noble et al. 2004; Lawson et al. 2001; Siekmann & Lawson 2007; Leslie et al. 2007). This questions the general validity of the tip cell concept for arteries and veins (Siekmann et al. 2013). In addition, *Flt1* upregulation in stalk cells could only be shown in embryoid body experiments or in cell

culture which are highly artificial and do not take into account AVD and blood flow (Jakobsson et al. 2010; Funahashi et al. 2010). Flow also influences the expression of arteriovenous markers, thus the interpretation of the data from Jakobsson and Funahashi and coworkers may be misleading (le Noble et al. 2004; Jakobsson et al. 2010; Funahashi et al. 2010). Moreover, in zebrafish primary sprouts *flt1, dll4* and *notch* are ubiquitously expressed in the sprout and not restricted to the tip or stalk cell (Krueger et al. 2011; Leslie et al. 2007). Furthermore, venous sprouts, which originate from the PCV, do not express either of the typical tip or stalk cell markers (*flt1, dll4, notch1a*), and still only a limited number of ECs and not every EC in the PCV forms sprouts. Thus, one could speculate that either venous ECs use a different mode for tip cell selection than arteries independent of Dll4/Notch and Flt1, or that the model deduced by the experiments is misleading. In the mouse retina the differences in arteriovenous marker expression are not as clear-cut as in the zebrafish vasculature and flow-dependent AVD possibly takes place coincidently with sprouting and plexus formation. Thus, as potentially the same genes are implied in two processes occurring at the same time, it seems to be extremely difficult to differentiate between arteriovenous differentiation processes and tip cell formation. In addition, old literature emphasized that venules and capillaries are normally the vessels that generate new sprouts, therefore it is at least surprising that arterial genes regulate this process (Risau 1995; Bergers & Benjamin 2003).

Furthermore, it is unclear if, for instance zebrafish primary sprouts follow a Vegfaa gradient. Vegfaa is expressed in the somites, thus the bioavailability of secreted Vegfaa in the corridors between the somites at the somite boundary should be uniform. Why the primary sprouts migrate dorsally is therefore unclear. One possibility is that they follow the path with the least physical constraints and that they are not guided but solely activated by Vegfaa to make a sprout.

In the future it will be important to clearly differentiate between angiogenic processes and AVD, which is possibly not trivial since not all vascular systems are as clearly separated into arteries and veins as the zebrafish trunk vasculature before 3 days post fertilization (dpf). In conclusion, tip cell models are taken for granted, but the underlying processes and genes

involved are far from being understood. Especially the differentiation between tip cell selection and AVD remains elusive.

3.6.1.1 Venous sprouting angiogenesis

Secondary venous sprouts in the zebrafish emanate from the PCV to form the lymphatic system and the vISVs and are regulated by Vegfc-Flt4 signaling. Specifically, hypochord-Vegfc activates dorsal PCV sprouting towards the horizontal myoseptum (HMS) (Isogai et al. 2003; Hogan et al. 2009; Ellertsdóttir et al. 2010). Why only a subset of venous ECs make secondary sprouts in the PCV and if adjacent cells are laterally inhibited or unable to sprout due to physical constraints is poorly understood (Koltowska et al. 2015).

Recent findings revealed a novel Bmp2b-dependent type of venous sprouting in zebrafish, which is independent of Vegfa-Kdrl and Notch signaling (Wiley et al. 2011). Furthermore, also other receptor tyrosine kinases (RTKs) such as the fibroblast growth factor receptor (FGFR) and other signaling pathways play a role in tumor angiogenesis and other pathological conditions (Welti et al. 2013).

In summary, ECs show a high degree of heterogeneity, which is even enhanced in different organ tissues. This complexity is currently heavily debated, and possibly one concept for all sprouting processes oversimplifies the complex nature of endothelial cells (Nolan et al. 2013; Rafii et al. 2016). The remarkable diversity of ECs entails chances for tissue specific vascular repair since they could potentially allow for localized induction of vascularization, e.g. in ischemic myocardium after artery occlusion. On the downside, it makes tumor angiogenesis extremely intricate to target as vascularization-inducing tumor cells, depending on the tumor location and origin, can exploit many different subtypes of ECs and pathways.

3.7 Zebrafish trunk angiogenesis

3.7.1 Primary and secondary sprouting

The simple zebrafish trunk vasculature is formed by two subsequent sprouting events, termed primary or arterial and secondary or venous sprouting (Isogai et al. 2003). *Vegfaa* expressed in somites drives dorsal arterial sprouting from the DA, a process termed primary sprouting (Isogai et al. 2001; Isogai et al. 2003; Ellertsdóttir et al. 2010). Arterial sprouts form a T-structure at the most dorsal region of the trunk and anastomose with adjacent sprouts forming the left and right dorsal longitudinal anastomotic vessel (DLAV) (Isogai et al. 2001). In a second wave of sprouting, venous sprouts emanate from the PCV and migrate dorsally in a Vegfc-dependent manner starting at 32 hpf (Isogai et al. 2003; Ellertsdóttir et al. 2010). *Vegfc* expressed in the hypochord activates Flt4 signaling in some venous ECs. Venous sprouts connect with aISVs at the level between the DA and HMS to form the vISVs (Hogan et al. 2009; Küchler et al. 2006). The anastomosis of a venous sprout with an aISV and the immediate onset of flow lead to subsequent pruning of the DA connection, and as a consequence a vISV is formed. This process is called arteriovenous remodeling and is mostly completed between 36-48 hpf (Isogai et al. 2003; Ellertsdóttir et al. 2010).

Notably, only 50 % of the venous sprouts connect to aISVs. The remaining 50% of sprouts migrate to the HMS forming together with later appearing lymphatic sprouts, which emanate from the vISVs the parachordal lymphangioblasts (PLs) at the level of the HMS (Isogai et al. 2003; van Impel et al. 2014). PLs differentiate into lymphatic endothelial cells (LECs) and form the lymphatic system (Küchler et al. 2006; Yaniv et al. 2006; Yaniv et al. 2007; Okuda et al. 2012).

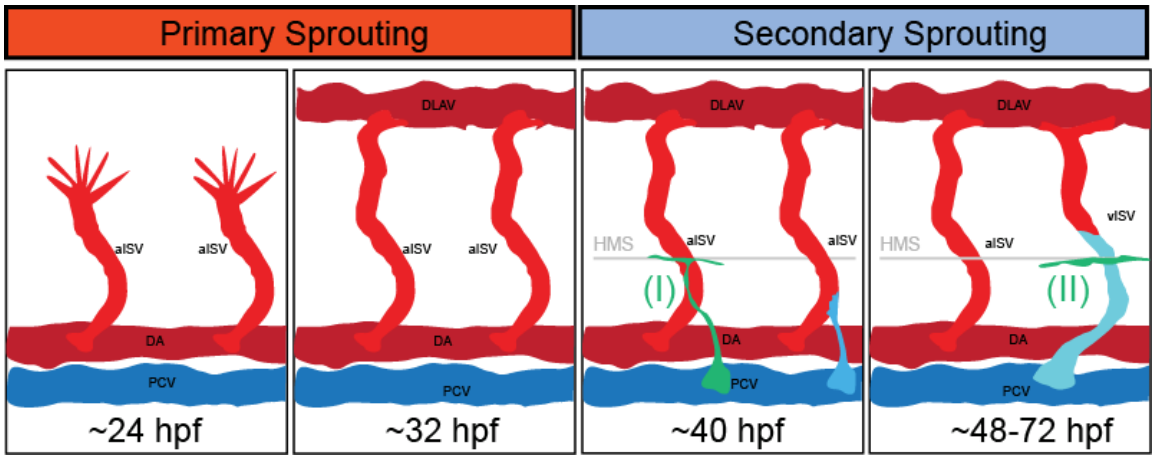

Figure 3-4. Primary and secondary sprouting in the zebrafish trunk

Primary arterial sprouts emanate from the DA and anastomose with each other at the dorsal border of the trunk to form the DLAV. Secondary sprouts appear later and originate from the PCV. 50% of the secondary sprouts connect to aISVs, which are remodeled into vISVs (light blue sprout). The other 50% of secondary sprouts form a T-shape at the level of the HMS and differentiate into parachordal lymphangioblasts (green sprout depicted with (I)). Parachordal lymphangioblasts (PLs) originate also from the vISVs at the level of the HMS building a second pool of PLs, depicted with (II). DA, dorsal aorta; PCV, posterior cardinal vein; DLAV, dorsal longitudinal vessel; aISV, arterial intersegmental vessel; vISV, venous intersegmental vessel; HMS, horizontal myoseptum.

3.7.2 Decision making – becoming vein or lymphatic?

It is debated why 50% of venous sprouts connect with aISVs and the other 50% become lymphatic ECs (Isogai et al. 2003; Koltowska et al. 2015). There are at least three possible scenarios. The lymphatic specification is programmed in the PCV (I), aISVs decide which venous sprouts connect and which form lymphatics (II) or a mixed scenario would be possible (III). Accordingly, one hypothesis is that the onset of flow in aISVs adjacent to vISVs inhibits anastomosis formation with venous sprouts activating lymphatic differentiation in these cells (Isogai et al. 2003). Interestingly, loss of *dll4* leads to the formation of increased vISV numbers (Leslie et al. 2007). In these mutants almost all aISVs are remodeled into vISVs, suggesting that Notch signaling could be involved in venous sprout anastomosis inhibition and could thus regulate venous remodeling (Leslie et al. 2007).

Since Dll4/Notch signaling is restricted to the arterial domain, this scenario suggests that aISVs cell-autonomously decide which secondary sprouts connect and which do not. Contradictory, recent findings suggest that venous PCV cells already adopt a lymphatic fate

prior to secondary sprout formation by *prox1* upregulation (Koltowska et al. 2015). This suggests that Prox1, by an unknown mechanism, prevents lymphatic cells from anastomosis and vISV formation (Koltowska et al. 2015). However, there is no known mechanism that could randomly assign every other sprout lymphatic or venous fate. Therefore the regulation of arteriovenous ISV-remodeling by flow remains tempting.

By 48 hpf, the major trunk vessels carry flow and supply the somites and neurons with nutrients (Isogai et al. 2001). At 3dpf the vertebral artery forms between the floor plate and the notochord, just below the neural tube, interconnecting the ISVs with the hindbrain vasculature (Kimura et al. 2015).

3.7.3 Bmp signaling drives caudal vein plexus formation

The caudal vein plexus (CVP), which is formed from 32 hpf onwards at the posterioventral part of the zebrafish tail, is a honeycomb-like network of vessels, composed of a dorsal and a ventral vein interconnected by vessels (Isogai et al. 2001; Wiley et al. 2011). Strikingly, the CVP is formed in a Vegfaa- and Vegfc- independent manner and is rather regulated by Bmp signaling (Wiley et al. 2011). Mechanistically, *bmp2b* is expressed in the posterioventral tail region and is sensed by venous ECs of the PCV with the Bmpr2a/b and Alk2/Alk3 receptors activating ventral venous sprouting angiogenesis and CVP formation. This is in contrast to all other sprouting processes in the zebrafish being either Vegfaa-Kdrl or Vegfc-Flt4 dependent (L. D. Covassin et al. 2006; Hogan et al. 2009; B. Hogan et al. 2009).

In conclusion, the simple zebrafish trunk vasculature composed of DA, PCV, CVP, ISVs and DLAV is formed by at least three signaling pathways unequivocally demonstrating EC-heterogeneity during development. It will be interesting in the future to investigate other organ-specific vasculatures to presumably identify other signaling pathways involved in their maturation. The EC heterogeneity clearly shows that there will be no single concept or targeting mechanism for the clinics instead depending on the origin of tumors or the tumor bed many different pathways have to be targeted. On the other hand pro-angiogenic therapies could be fine-tuned for ECs of a specific organ's vasculature preventing side effects in other organs.

3.7.4 Directional migration of angiogenic sprouts

After selection of endothelial tip cells they extend filopodia to sense their environment for guidance cues (Gerhardt et al. 2003; De Smet et al. 2009). Tip cells are thought to migrate against a growth factor gradient in the direction of the highest growth factor concentration, extending and retracting filopodia in a saltatory manner (Carmeliet & Tessier-Lavigne 2005). Interestingly, Phng and coworkers recently showed that certain zebrafish ECs can sprout even in the absence of filopodia, albeit at a lower speed, implicating that filopodia increase the guidance efficacy and speed but are in principle dispensable for guided sprouting (Phng et al. 2013). The source of guidance cues such as VEGF can be developmental structures or oxygen-deprived tissue such as wounds, ischemic tissues or tumors (Ferrara 2005; Haigh 2008). VEGF is thought to be upregulated in these tissues to recruit vessels until supply meets demand (Carmeliet 2003).

However, it has never been physically shown that VEGFs form a gradient or that different VEGF isoforms form different gradients, which combine then into a comprehensive gradient. It was recently shown that blood flow is necessary for the formation of some but not all sprouts in zebrafish (Watson et al. 2013). These sprouting events are most likely activated by two factors, namely Vegfa and blood flow. Similarly sprouting could also be induced by shear stress using *in vitro* systems (Galie et al. 2014). Thus, sprout elongation seems to be in most cases blood flow and growth factor dependent. Apart from Vegfa sources and gradients, blood flow could also provide sprouts with some degree of directionality perpendicular to the direction of flow of the parent vessel. Whether the presumed Vegfa gradient directs or only activates and maintains sprouting angiogenesis remains elusive.

3.7.4.1 Common guidance factors of vessels and nerves – same patterns same cues?

Recent evidence suggests that well-known nerve repellents and attractants can also be utilized by vessels to prevent invasion into certain tissue regions, such as somites during development (Torres-Vázquez et al. 2004; Zygmunt et al. 2011). Semaphorins and their Neuropilin and Plexin receptors are known as nerve repellents but are also expressed in endothelial cells. Sema3a (the mouse and human Sema3E homolog) is expressed in the somites of the developing zebrafish embryo, whereas the Sema3a receptor Plxnd1 is expressed in primary arteries, sprouting dorsally in between the somites at the somite

boundaries. In *plxnd1*^{um7} mutants or in *sema3a* knockdown scenarios primary sprouts are not restricted anymore to the region close to the somite boundaries as observed in wild type embryos but sprout in a chaotic fashion at all levels of the trunk (Torres-Vázquez et al. 2004). It has been suggested that Sema3a-Plxnd1-mediated upregulation of *sflt1* in ECs prevents sprouting at the level of the somites in a cell-autonomous manner and allows only sprouting close to the somite boundaries (Gay et al. 2011; Torres-Vázquez et al. 2004). Thus, it was concluded that the Sema3a-PlxnD1 signaling pathway has similar repellent functions in the vasculature and in neurons (Winberg et al. 1998).

Another example are the Ephrins and the Eph receptors, which can be negative or positive nerve guidance cues (Kania & Klein 2016). In ECs, EphrinB2 and EphB4 were the first markers found to be specifically expressed in arteries or veins, respectively (Wang et al. 1998). They are critical for artery-venous differentiation early in development and are important for VEGFR-2 internalization and signaling capacity in angiogenesis (Wang et al. 1998; Wang et al. 2010; Sawamiphak et al. 2010). Hence, Ephrins and their receptors have different functions in endothelial cells acting as repellents similar to their nerve function, but also as coreceptors enhancing angiogenesis. The connection between these controversial functions is poorly understood.

In summary, sprouting angiogenesis is typically non-stereotyped and is activated according to demand, which is regulated by growth factors such as VEGF. In contrast to axon guidance, angiogenesis can only span short distances, which are normally guided by growth factor gradients. This is very similar to axonal terminal arborization in terms of guidance and survival of only physiologically relevant connections (Carmeliet 2005). Recent evidence suggests that tissues under some circumstances may utilize well-known neuronal guidance factors to determine vascular patterning, but the relevance for development or guidance of sprouting angiogenesis during wound healing or disease remains elusive (Adams & Eichmann 2010). Of note, several of the neurovascular factors described to be relevant for vascular guidance were investigated or substantiated using morpholino-mediated knockdown experiments in zebrafish (Carmeliet & Tessier-Lavigne 2005). Morpholinos are known to be good agents for gene silencing in zebrafish but can induce unspecific side effects limiting their use to situations where a reference such as a mutant is available (Kok et al. 2014).

These early investigations on neurovascular guidance cues were performed solely with morpholinos and may thus be misleading. Guidance cues utilized from the nervous system could have been evolutionarily evolved to prevent sprout penetration and tissue or cell differentiation damage during embryonic development. For non-developmental sprouting angiogenesis sprout penetration could also be harmful and could for instance oxygenize and hence damage hypoxic stem cell niches (Eliasson & Jönsson 2010).

3.8 The zebrafish spinal cord – development and function

Upon specification of the neuroectoderm the neural plate is formed. In zebrafish the neural plate does not fold into the neural tube (NT) as observed in other vertebrates, but rather forms a rod-like structure, which is only secondarily infiltrated to form the NT (Nyholm et al. 2009). The final structure of the zebrafish NT is comparable with that of other vertebrates (Lewis & Eisen 2003; Nyholm et al. 2009; Goulding 2009; Schmidt et al. 2013).

The neuroepithelium in the NT is divided into three zones, namely the ventricular zone (source of neurons and glia), which is in contact with the cerebrospinal fluid, the intermediate zone and the marginal zone (Goulding 2009). The neuroepithelium is polarized with an apical (luminal side) and a basal side. Proliferating progenitors move from the apical side to the basal side to differentiate (Lewis & Eisen 2003; Goulding 2009). This process is known as interkinetic nuclear migration (Del Bene 2011; Spear & Erickson 2012; Strzyz et al. 2015). Thus, neuroepithelial cells (stem cells) are connected to the apical and the basal side forming a neuroepithelium. These cells asymmetrically divide, whereby one daughter cells remains attached to the apical surface whereas the other detaches and differentiates at the basal side into a mature neuron (Strzyz et al. 2015). As the neural tube matures, stem cells differentiate into radial glia cells (RGCs) (Goulding 2009).

RGCs have a similar orientation as neuroepithelial cells (radial from apical to basal) and give rise to mature neurons (stained by the *xla.tubb* promoter), oligodendrocytes and astrocytes and are the main source of neurons during development (Noctor et al. 2001; Götz & Huttner 2005). Neurons further differentiate into motor neurons (mnx promoter domain), sensory neurons, interneurons or other types of neurons. The xenopus beta-tubulin promoter (*xla.tubb*) is specifically active in mature neurons, whereas the *huc* promoter (also known as

elavl3) is considered to be a pan-neuronal promoter in zebrafish (Park et al. 2000; Peri & Nüsslein-Volhard 2008). Motor neurons are formed at the ventrolateral margin of the NT whereas sensory neurons and interneurons are located dorsally (Eisen 1991; Goulding 2009). Mechanistically, Shh, which is secreted from the notochord and floorplate, drives motor neuron differentiation, whereas Bmps secreted from the dorsal ectoderm drive sensory and interneuron differentiation resulting in a distinct dorsoventral neuronal pattern (Nguyen et al. 2000; Wilson & Maden 2005).

3.9 A late friendship – neurovascular development

In contrast to other organs the central nervous system does not produce vascular progenitors and therefore blood vessel ingression into the developing nervous system has to occur continuously from adjacent tissues (Ruhrberg & Bautch 2013). Vascularization of the CNS is one of the most studied and therefore one of the best-understood vascular processes.

During development, angioblasts migrate to the CNS to form a PNVP (Bautch & James 2009). The brain and the spinal cord are vascularized from the surrounding PNVP by angiogenic sprouting. Noteworthy, the delicate neuronal architecture is not perturbed upon vascularization by penetrating angiogenic sprouts showing the remarkable communication between ECs and their target tissue (Ruhrberg & Bautch 2013; Tata et al. 2015).

In the mouse embryonic skin, nerves guide the patterning of vascular remodeling resulting in neurovascular congruence (Mukouyama et al. 2002). Mechanistically, VEGF provided by nerves was shown to promote artery marker expression but to be not necessary for alignment and arteriogenesis (Mukouyama et al. 2005). Mutant mice lacking nerves show defective patterning of vascular remodeling. However, the underlying mechanism is still unknown (Mukouyama et al. 2002; Mukouyama et al. 2005). The most tempting assumption is the secretion of guidance factors by nerves to direct vessel migration, however the somewhat less spectacular guidance along morphological structures such as nerves themselves should not be disregarded. In other cases, neurovascular congruence could be the result of empty tissue space similarly utilized for growth by vessels and nerves.

Vice versa, blood vessels guiding motoneurons have also been reported (Kwon et al. 2013). The zebrafish DA was shown to guide motorneuron development and alignment with the DA in a Vegfc-Flt4 dependent manner (Kwon et al. 2013). Another example is the external carotid artery, which acts as an intermediate target for sympathetic nerves to find their final target, such as salivary glands. In this guidance process, Endothelin secreted by the carotid artery guides the axons towards their final target, serving as a gateway (Makita et al. 2008).

In these examples nerves or vessels secrete factors to support growth and alignment of the other. However, in many instances nerve and vessel development proceed independently. For instance, dorsal root ganglia development in zebrafish as well as hindbrain development proceed normally in the absence of vessels in *cloche* mutants (a vessel-depleted zebrafish mutant), suggesting that blood vessels are dispensable for some early CNS developmental processes and necessary for others (Miller et al. 2010; Ulrich et al. 2011). Another tempting explanation for close anatomical positioning of vessels and nerves is that nerves and vessels share the same guidance cues and are thus guided to the same tracks (Carmeliet & Tessier-Lavigne 2005).

In summary, nerve and blood vessel alignment can be a phenomenon of mutual or common guidance or proceed altogether independently. However, if and how modulation of neurovascular guidance cues can be used as new therapeutic target remains to be shown. Due to their dual functions in vessels and nerves it remains unclear whether they could be used as therapeutic targets without affecting neuronal integrity (Piper et al. 2002; Furne et al. 2008; Ben-Zvi et al. 2008).

3.9.1 VEGF receptors

3.10 The master regulators of angiogenesis – VEGF receptors

The class of VEGF receptors (VEGFRs) belongs to the RTK superfamily consisting of three VEGFRs. The VEGFR-1 (Flt1), VEGFR-2 (Kdr/Kdrl) and VEGFR3 (Flt4) have been described (Olsson et al. 2006). VEGFRs are single pass transmembrane proteins with characteristic

seven immunoglobulin (Ig) domains in the extracellular part together with a split-kinase and a C-terminal domain in the intracellular part of the receptors (Herbert & Stainier 2011). The 5th Ig domain of the VEGFR3 is replaced with a disulfide bridge. Ig domains 2 and 3 bind to the VEGF ligands whereas the function of the domains 4 to 7 is poorly understood (Brozzo et al. 2012).

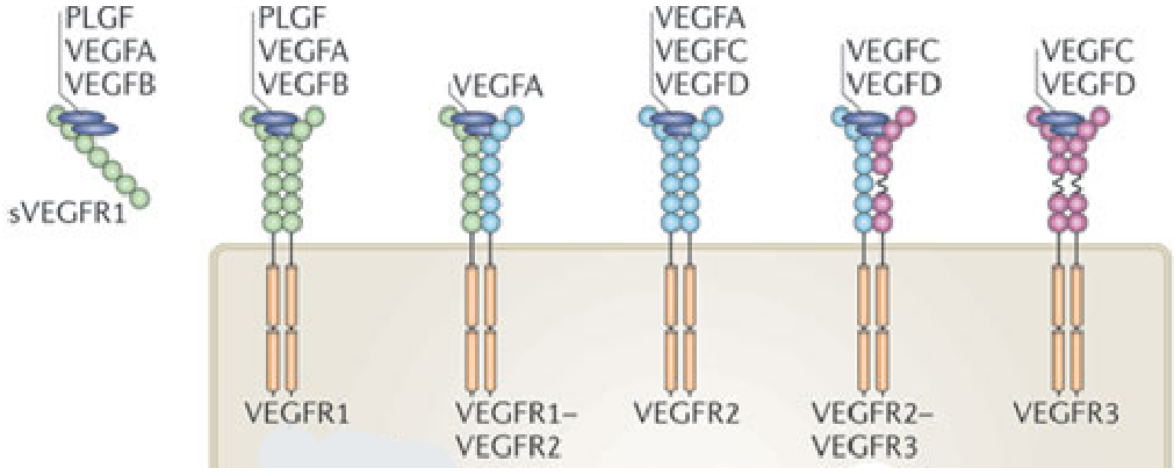

Figure 3-6. VEGFRs and their ligands

Vascular endothelial growth factors (VEGFs) bind homo- and heterodimers of three VEGF receptors. VEGFR1 (FLT1) has at least two isoforms (depending on the organism), a soluble (sVEGFR1/sFlt1) and a membrane bound (VEGFR1/mFlt1) binding three ligands, PLGF, VEGFA and VEGFB. VEGFR2 binds to VEGFA, processed VEGFC and VEGFD. The lymphatic VEGFR3 binds to VEGFC and VEGFD. Modified from (Herbert & Stainier 2011).

Ligand-induced VEGFR homo- or heterodimerization leads to conformational changes inducing receptor-kinase activity and autophosphorylation of defined tyrosine residues of the receptors (Olsson et al. 2006). Interacting proteins are recruited to the phosphorylated receptors activating downstream signaling (Olsson et al. 2006; Herbert & Stainier 2011). VEGFR-1 (Flt1) is thought to act mainly as a VEGF-A decoy receptor limiting VEGFR-2 signaling and thus functions as a negative regulator of angiogenesis. VEGFR-1 binds to its ligands VEGF-A, PlGF and VEGF-B. The VEGFR-2 is the key regulator in vascular biology and regulates EC functions as diverse as EC survival, proliferation, vessel permeability, vasculogenesis and angiogenesis. VEGFR-2 (Kdr/Kdrl) binds to VEGF-A and the processed forms of VEGF-C and VEGF-D (Joukov et al. 1997; Leppänen et al. 2013). The third VEGFR, VEGFR-3 (Flt4) binds to VEGF-C and VEGF-D and regulates lymphangiogenesis and early vein formation (Küchler et al. 2006; Adams & Alitalo 2007)

3.10.1 Expression and Regulation of VEGFRs

The VEGFRs were originally identified in the vascular domain (Fong et al. 1995; Shalaby et al. 1995; Dumont et al. 1998). Notably, recent findings showed that VEGFR-1, VEGFR-2 and VEGFR-3 are also expressed in some neuronal populations (Kwon et al. 2013; Okabe et al. 2014; Selvaraj et al. 2015).

VEGFR-2 is expressed both in blood endothelial cells and in the lymphatic system in mice, but is restricted to the blood endothelial cells in zebrafish (Adams & Alitalo 2007). Flt1 is known as an arterial marker and is expressed at higher levels in arteries compared to veins (Cui et al. 2015; Krueger et al. 2011; Hogan et al. 2009). In zebrafish *flt1* is even barely detectable in the venous domain (Hogan et al. 2009; Bussmann et al. 2010). VEGFR-1 is also expressed in myeloid cells and trophoblasts of the placenta (Stefater et al. 2011). During early development, Vegfr-3 (Flt4) is expressed in arterial and venous ECs and may be enriched in the tip cells of angiogenic sprouts (Siekmann & Lawson 2007; Hogan et al. 2009). By 26 hpf, *flt4* expression is restricted to venous ECs and LECs (Bussmann et al. 2007). At later developmental stages and in adults, VEGFR-3 is restricted to the lymphatic system and is mostly downregulated in venous endothelium (Adams & Alitalo 2007). The only mature blood vessels expressing *flt4* are fenestrated capillaries and angiogenic vessels (Saharinen et al. 2004).

3.10.2 VEGFR-1 (FLT1, Flt1) function and signaling

The VEGFR-1 (FLT1/Flt1) is a high affinity receptor for VEGF, PlGF and VEGF-B (Autiero et al. 2003; Olsson et al. 2006). As the VEGFR-2 is the focal point in EC biology, its signaling capacity has to be tightly controlled. Flt1 mainly acts as a decoy receptor scavenging VEGF-A and thereby limiting VEGFR-2 signaling (Fong et al. 1995; Carmeliet 2003; Krueger et al. 2011).

3.10.2.1 Flt1 is alternatively spliced

The *Flt1* gene (mouse *Flt1,* human *FLT1*, zebrafish *flt1*) of all vertebrates so far investigated

codes for at least two alternative isoforms, a membrane-bound receptor (mFlt1) and a shorter secreted, soluble receptor (sFlt1) produced by alternative splicing (Sela et al. 2008; Krueger et al. 2011). In humans, at least three soluble isoforms exist, which are formed by alternative splicing or alternative 3'UTR processing. In zebrafish, only one membrane-bound and one soluble isoform have been described, which are produced by alternative splicing (Krueger et al. 2011). The zebrafish *sflt1* is spliced further upstream compared to the human sFlt1 isoforms and contains only Ig1-5 (Krueger et al. 2011).

Alternative splicing may be regulated by the protein hydroxylase Jumonji domain-containing protein 6 (jmjd6) (Boeckel et al. 2011). Jmjd6 is thought to hydroxylate U2AF65 at normoxic conditions, thereby shifting the alternative splicing equilibrium towards mFlt1. Under hypoxic conditions this regulation is relieved and sFlt1 production is favored (Webby et al. 2009; Boeckel et al. 2011). This regulation is in contrast to the expectations since hypoxia is a condition under which vessel recruitment is normally favored, thus the upregulation of the highly anti-angiogenic factor sFlt1 is elusive. Accordingly, another research group identified that in contrast to HUVECs that were used by Boeckel and colleagues, microvascular ECs downregulate *sFlt1* under hypoxic conditions to induce vascularization (Ikeda et al. 2011). In conclusion, reports on the regulation of Flt1 splicing and the correlation with hypoxia appear inconsistent, but could be the result of differing regulatory mechanisms depending on the subtype of endothelia. Moreover, *Flt1* splicing was only investigated in ECs, but may be different in other cell types such as neurons.

3.10.2.2 Flt1 protein structure

Flt1 is a receptor tyrosine kinase and shares structural similarities with the fms family and was therefore originally described as fms-like tyrosine kinase 1 (Shibuya et al. 1990). Structurally the VEGFR-1 is organized into seven extracellular immunoglobulin-like domains followed by a transmembrane domain. The intracellular part is composed of a juxtamembrane domain, a split tyrosine-kinase domain and a C-terminal tail. The kinase insert domain has ~70 amino acids with unknown function (Olsson et al. 2006), a typical feature of the VEGFR class of receptors. Crystal structures and deletion analyses have revealed that the Ig2 domain is most relevant for VEGF binding (Wiesmann et al. 1997; Christinger et al. 2004).

3.10.2.3 Is Flt1 a negative or a positive regulator of angiogenesis?

Flt1 has been conversely described as a positive and negative regulator of angiogenesis and has been implicated in the regulation of monocyte and macrophage migration (Clauss et al. 1996; Tchaikovski et al. 2008; Hiratsuka et al. 1998; Chappell et al. 2009). Flt1 loss-of-function scenarios can lead to vascular overgrowth with unproductive angiogenesis or vessel fusion and thus decreased perfusion. These findings prompted some investigators to define Flt1 as a positive modulator of angiogenesis (Kearney et al. 2004; Chappell et al. 2016). Most other studies classify Flt1 as a negative regulator of angiogenesis which will be discussed in the next chapters (Fong et al. 1995; Chappell et al. 2009).

3.10.2.4 Flt1 and its tyrosine kinase domain function in angioblast differentiation

In monocytes and macrophages Flt1 may act as a signaling receptor, activating downstream signaling pathways such as MAPK and PI3K/Akt (Stefater et al. 2011). Apart from this, Flt1 is thought to act mainly as a VEGF decoy receptor limiting VEGFR-2 signaling (Fong et al. 1995; Krueger et al. 2011). In Flt1 knock-out mice ($Flt1^{-/-}$) increased hemangioblast commitment can be observed, which results in the formation of a disorganized vascular plexus and early embryonic lethality (Fong et al. 1995; Fong et al. 1999). Interestingly, the intracellular domain and thus Flt1 signaling capacity seems to be dispensable and its depletion is compatible with life (Hiratsuka et al. 2001). Protein domain deletion experiments show that mice lacking the entire Flt1 intracellular domain are phenotypically normal (Hiratsuka et al. 2001). Only if the transmembrane domain is deleted, causing mFlt1 conversion into a soluble Flt1 form, mice show decreased EC numbers and survival (Hiratsuka et al. 2001; Hiratsuka et al. 2005).

In summary, Flt1 tyrosine kinase activity seems to be dispensable but mFlt1 membrane fixation is important to ensure proper sFlt1 levels. It is unknown whether the additional decoy capacity of mFlt1 is required for normal development, as mFlt1 splicing deficient mice were so far not published.

3.10.2.5 Is FLT1 function compatible with its prominent role in the tip cell concept?

Conducting morula transplantation experiments, Fong and colleagues could show that FLT1 is necessary to restrict hemangioblast commitment, but is not required for vascular growth in general (Fong et al. 1999). *Flt1*-depleted, transplanted endothelial cells were able to form normal vascular networks, suggesting that after the completion of vasculogenesis FLT1 may have only minor functions in vascular growth in mice (Fong et al. 1996). However, from this experiment it cannot be concluded to what extent non-vascular FLT1 regulates murine angiogenesis. Moreover, inducible FLT1 depletion experiments in the mouse retinal plexus or ubiquitously in postnatal mice induce only mild phenotypes with increased filopodial numbers, suggesting a minor role for FLT1 in angiogenesis (Chappell et al. 2009; Ho et al. 2012). Chappell and Ho are claiming an important function of FLT1 in retinal sprouting angiogenesis as well as in other vascular beds, however the observed effects appear mild compared to the extremely potent function of the FLT1 protein (Yamaguchi et al. 2002). Additionally, the differences in tip cell numbers reported by Ho and coworkers in postnatal mice with inducibly depleted *Flt1* are very subtle. It is remarkable that up to now the inducible $Flt1^{flox/flox}$ mouse used by Chappell and Ho has not been published in combination with a vascular Cre driver line. One could speculate that postnatal vascular *Flt1* loss-of-function phenotypes observed after angioblast differentiation and plexus formation are even milder than ubiquitous *Flt1* depletion, questioning its important role in angiogenic processes such as tip cell formation. Another possibility is that embryonically produced vascular Flt1 is sufficient to prevent hypersprouting in postnatal *Flt1*-depleted mice. Therefore, in order to understand the diverse functions of FLT1 it is important to study neuronal or vascular tissue-specific *Flt1* loss-of-function models after angioblast differentiation.

Contradictory to these findings, which imply a collateral role of vascular FLT1 in angiogenesis, FLT1 is widely seen as an important component of the “tip cell concept” (Herbert & Stainier 2011; Siekmann et al. 2013). In this model DLL4-NOTCH signaling is considered to upregulate *Flt1* in stalk cells limiting VEGFR-2 signaling in the microenvironment of the stalk cells and thus preventing tip cell formation (Funahashi et al. 2010; Herbert & Stainier 2011). In addition, Chappell and coworkers hypothesized that FLT1 is necessary to prevent “backsprouting” of a newly forming vascular sprout and its

reconnection with the parent vessel (Chappell et al. 2009). In this model, sFLT1 was suggested to form a corridor guiding the nascent spout away from its origin (Chappell et al. 2009). Similarly, a recent publication conducted in zebrafish, suggests that sFlt1 acts in a cell-autonomous manner downstream of Sema3a-PlxnD1 signaling guiding the sprout away from *sema3a* expressing cells, such as zebrafish somites (Zygmunt et al. 2011).

Noteworthy, both concepts imply a cell-autonomous FLT1 function and are not compatible with the transplantation experiments performed by Fong and colleagues (Fong et al. 1996; Fong et al. 1999). In addition, the effects observed in *Flt1* inducible knockout scenarios appear extremely mild if compared with *Dll4* loss-of-function scenarios which are supposed to be upstream of *Flt1*, with FLT1 being one important effector of the DLL4/NOTCH pathway to prevent tip cell formation (Suchting et al. 2007; Hellström et al. 2007). Therefore, it is important to carefully analyze data and put the effects into relation to previous publications. This is extremely important since many authors claim small but statistically consistent results to be physiologically relevant but may be frequently misguided by the wish to publish their results. In doing so it may be easier to substantiate the current opinion than publishing against it.

3.10.2.6 Non-vascular flt1 – the overseen regulator?

Flt1 is mainly expressed in arterial endothelial cells, but it is also found in trophoblasts, myeloid cells, monocytes and hematopoietic stem cells and certain neuronal populations (Sawano et al. 2001; Stefater et al. 2011; Selvaraj et al. 2015). sFLT1 secreted by trophoblasts is known for its prominent role in pre-eclampsia, a disease associated with pregnancy, which manifests in widespread endothelial dysfunction (Hirashima et al. 2003; Sawano et al. 2001; Stefater et al. 2011). More recently, expression of Flt1 has been detected in various neuronal cell populations, such as motor neurons, sensory neurons and dorsal root ganglia (Poesen et al. 2008; Storkebaum et al. 2005; Selvaraj et al. 2015). In neuronal cells, Flt1 was found to have neuronal cell autonomous functions including induction of cancer pain in sensory neurons or neurodegenerative functions in motoneurons (Storkebaum et al. 2005; Selvaraj et al. 2015). Robciuc and colleagues recently showed that VEGF-B gain-of-function or *Flt1* knockdown prevents VEGFR-1/VEGFR-2 heterodimer

formation and thus favored VEGFR-2 homodimer formation, which have higher signaling capacity (Robciuc et al. 2016). This study shows that FLT1 cannot exclusively act as a decoy receptor but can also negatively modulate angiogenesis by heterodimer formation with VEGFR-2, which reduces angiogenic potential (Robciuc et al. 2016). Since mice with deleted Flt1 intracellular domain are phenotypically normal, this result suggests that the transmembrane, and the extracellular domain of FLT1 are sufficient for VEGFR-2 interaction.

In conclusion, loss of *Flt1* has tremendous effects on early vasculogenesis but its function in angiogenesis is less well understood. Remarkably, FLT1 is seen as a prominent regulator in sprouting models, disagreeing with its known *in vivo* functions. Recently, FLT1 has been shown to have cell-autonomous functions in neuronal cells, monocytes and macrophages. Whether non-vascular FLT1 can also act non-cell autonomously and affect vascular growth is currently unknown.

3.10.3 Clinical implications of angiogenesis and Flt1

VEGF levels are critical for various physiological processes, including vasculogenesis, angiogenesis, EC barrier formation, survival as well as glomeruli filter function (Senger et al. 1993; Carmeliet 2003; Lee et al. 2007). Increased vascular growth is involved in tumorigenesis and ocular disease and can be regulated by FLT1 (Carmeliet 2003; Lange, Storkebaum, et al. 2016). Moreover, *FLT1* is expressed in various tumors, such as breast, prostate and colon cancer, pulmonary adenocarcinoma, hepatocellular carcinoma, glioblastoma and lung cancer, albeit with unknown function (Yao et al. 2011). In healthy conditions, sFLT1 expression in the cornea of the eye maintains it avascular to safeguard optimal vision. Without *sFlt1* expression, VEGF expressed in the cornea recruits vessels from the directly adjacent vascularized tissues, which impairs vision (Ambati et al. 2006).

Flt1 was recently implicated in the phenomenon of cancer pain (Selvaraj et al. 2015). Here, Flt1 expressed by sensory neurons can be activated by its ligands VEGF-A, PlGF and VEGF-B, which are released by tumors. As a result, Flt1 signaling in sensory neurons alters them structurally and functionally. Mechanistically, activation of Flt1 downstream kinases PLCy, PI3K and Src kinase sensitizes sensory transducers such as TRPV1 and thereby produces cancer pain (Selvaraj et al. 2015).

Pre-eclampsia, a disorder of pregnancy is characterized by hypertension and proteinuria (Young et al. 2010). This disease is caused by endothelial dysfunction, which is induced by elevated circulating sFLT1 levels and other factors such as PLGF and soluble Endoglin (Young et al. 2010; Agarwal & Karumanchi 2011). It is speculated that pre-eclampsia is induced by abnormal placentation leading to hypoxia and sFLT1 release into the circulation by trophoblasts of the placenta. On the molecular level, sFLT1 could be shown to impair eNOS phosphorylation and thus nitric oxide (NO) production in ECs, thereby preventing vasodilation and blood pressure reduction (Burke et al. 2016). Proteinuria is most likely caused by a decreased bioavailability of VEGF in podocytes of the kidney glomeruli caused by elevated circulating sFLT1 levels evoking podocyte and fenestrated-EC dysfunction (Eremina et al. 2003).

3.10.4 VEGFR-2 (Kdr/Kdrl) – the focal point of vascular biology

The VEGFR-2 is implicated in all facets of endothelial cell biology and has a critical role during development (Shalaby et al. 1995; Carmeliet 2003; Olsson et al. 2006). The prominent role of VEGFR-2 has been highlighted in Vegfr-2 KO mice, which do not show any signs of blood islands or blood vessel formation (Shalaby et al. 1995). In addition, haploinsufficiency of the VEGFR-2 ligand VEGF and the absence of blood vessels in these mice substantiates the crucial role of VEGFR-2 during development (Ferrara et al. 1996; Carmeliet et al. 1996).

In the zebrafish two VEGFR-2 homologs exist, Kdr (Kdrb) and Kdrl (Kdra). Kdr is orthologous to mammalian KDR, whereas kdrl is a fourth VEGFR, which was secondarily lost in the eutherian lineage (Bussmann et al. 2008). In zebrafish Kdrl, although not orthologous to the mammalian KDR, is the major Vegf receptor as substantiated by loss-of-function experiments. On the other hand, Kdr is dispensable for normal vascular development but retained some residual function in genetically sensitized backgrounds (Bussmann et al. 2008; L. D. Covassin et al. 2006; Covassin et al. 2009).

Ephrin-B2 mediated VEGFR-2 internalization was shown to be important for full VEGFR-2 signaling capacity (Wang et al. 2010; Sawamiphak et al. 2010). However, whether all VEGFR-2 signaling modes are affected by VEGFR-2 internalization and whether VEGFR-2

internalization is needed for signal integration with other parallel signaling pathways, remains to be determined.

Complex signaling cascades activated by VEGFR-2 and modulated at various levels facilitate the tight coordination of a vast diversity of cellular responses activated by VEGFR-2 signaling.

3.10.4.1 VEGFR-2 mediated EC-migration

Migration of ECs is a complex process, since ECs are organized in tight association and covered with a basement membrane (Adams & Alitalo 2007; Herbert & Stainier 2011). Thus, ECs have to dissociate from the EC monolayer and to degrade the basement membrane, without compromising the integrity of the vessel. VEGF-VEGFR-2 activation leads to autophosphorylation of several VEGFR-2 tyrosine residues involved in the regulation of migration (Olsson et al. 2006). VEGF induced phosphorylation of Y951, Y1175 and Y1214 activates downstream signaling resulting in actin polymerization at the leading tip and focal adhesion turnover (Koch & Claesson-Welsh 2012).

In order for sprout induction to be initiated, the basement membrane surrounding the vessel has to be degraded (Adams & Alitalo 2007). Subsequently, actin is polymerized at the leading edge to push the tip forward, thereby forming a protrusion. PI3K activation and production of phosphatidylinositol (3,4,5)-trisphosphate (PIP3) at the leading edge of the cell leads to Rho activation and actin polymerization (Holmqvist et al. 2003). Low levels of phosphatase and tensin homolog (PTEN) at the cellular front and high levels at the rear of the cell are considered to substantiate the concentrated actin polymerization at the tip of the cell (Iijima et al. 2002). In zebrafish *ptena*$^{-/-}$*;ptenb*$^{-/-}$ double mutants show a strong vascular phenotype with hypersprouting occurring at the level of the spinal cord, emphasizing the importance of PI3K signaling for EC function (Choorapoikayil et al. 2013). Notably, polarization in the *ptena*$^{-/-}$*;ptenb*$^{-/-}$ depleted migrating ECs is not affected suggesting that at least in zebrafish, Pten function is not necessary for proper migration (Choorapoikayil et al. 2013). Moreover, the hypersprouting phenotype in *ptena*$^{-/-}$*;ptenb*$^{-/-}$ mutants is not induced by relief of RTK signaling blockade but rather through upregulation of *vegfaa*.

As a consequence of PIP3 accumulation at the leading edge, small GTPases of the Rho family become activated and induce actin polymerization. The small GTPase CDC42 is an important regulator of polarization regulating lamellipodia formation as well as Golgi and microtubule organizing center (MTOC) positioning in front of the nucleus (Gundersen & Worman 2013). Thus, all organelles are oriented towards the side of migration. Although it is clear that nuclear positioning is important for cell migration, its function is poorly understood (Gundersen & Worman 2013). As many proteins and membrane lipids have to be transported to the leading migrational edge it seems reasonable to orient the entire cellular machinery such as nucleus, ER and Golgi in the direction of migration to enable fast and efficient migrational behavior. However, how this is achieved mechanistically remains elusive.

Besides EC-migration, VEGF also regulates EC-proliferation, survival and vascular permeability. How one receptor can regulate such a remarkable diversity of functions is poorly understood. Mice specifically lacking vascular VEGF expression show endothelial degeneration and sudden death. Since paracrine VEGF cannot compensate for autocrine VEGF, endothelial VEGF is thought to be necessary for EC survival (Lee et al. 2007).

In order to make a sprout the entire repertoire of VEGF-induced functions have to be activated in a coordinated manner. ECs have to migrate, proliferate and increase their permeability to dissociate from the tight endothelial cell sheet. Thus, it appears reasonable that one factor, namely VEGF can activate such a wealth of cellular functions. However, how such a factor can activate the spatially and timely coordinated activation of all these processes resulting in sprout formation and eventually perfusion is an impressive miracle of nature.

3.10.5 VEGFR-3 (FLT4,Flt4) function in vascular biology

VEGFR-3 (FLT4, Flt4) is indispensible for venous angiogenesis and lymphangiogenesis during early development, and blockade of FLT4 or its ligand VEGF-C inhibits vein and lymphatic vessel formation (Dumont et al. 1998; Küchler et al. 2006; Hogan et al. 2009). Adults express Flt4 in angiogenic blood vessels, in some fenestrated endothelia and in the lymphatic system

where it is required for lymphangiogenesis and lymphatic maintenance. (Zarkada et al. 2015). Similar to VEGFR-2, FLT4 receptor internalization and signaling is regulated by EphrinB2, DAB2 and PAR-3 (Nakayama et al. 2013; Wang et al. 2010). Interestingly, in zebrafish *efnb2* and *dab2* are almost exclusively expressed in arteries and veins, respectively. Thus, the regulation of Flt4 internalization in zebrafish does possibly not require Ephrin-B2 (L. Covassin et al. 2006; Wang et al. 1998).

Flt4 is expressed in arteries and veins during early development. It has been speculated that Vegfc responsiveness of arteries is inhibited by Dll4 (Hogan et al. 2009). Hogan and colleagues reported that depletion of Flt4 rescues the hypersprouting phenotype in dll4 morphants and concluded that Dll4 represses Flt4 function in aISVs (Hogan et al. 2009). However, this interpretation does not take into account that in *dll4* morphants, aISVs are almost completely absent and thus the hypersprouting observed in these morphants most likely occurs from the venous domain. Furthermore, *flt4* depletion does not only prevent signaling in ISVs but also prevents vISV formation, which could influence the results of this experiment.

Benedito and colleagues showed that VEGFR-2 function in postnatal angiogenesis can be completely sustained by FLT4 and that FLT4 not VEGFR-2 is upregulated by NOTCH signaling, which is contradictory to the tip cell concept (Benedito et al. 2012). In contrast, Zarkada et al. recently published that VEGFR-2 has non-redundant functions, which could not be compensated by FLT4 in postnatal retinal angiogenesis (Zarkada et al. 2015).

Remarkably, primary sprouting in zebrafish is sustained in *flt4*^{hu4602} mutants, whereas secondary sprouting and venous remodeling is blocked. These findings substantiate that Flt4 is not generally required for sprout formation but most likely of particular importance in venous angiogenesis.

3.10.6 VEGF ligands

In mammals, the VEGF family consists of five VEGF ligands: VEGF-A, VEGF-B, VEGF-C, VEGF-D and the placental growth factor PlGF. In snake venoms and in parapoxviruses, structurally

related proteins named VEGF-E and VEGF-F have been identified (Olsson et al. 2006; Suto et al. 2005; Takahashi & Shibuya 2005). In zebrafish more *vegf* isoforms exist due to the teleost genome duplication, namely *vegfaa, vegfab, vegfba, vegfbb, vegfc, vegfd* and *plgf* (Liang et al. 2001; Glasauer & Neuhauss 2014; Jensen et al. 2015). VEGFs are secreted, disulfide-linked, homodimeric glycoproteins of approximately 40 kDa and dimerization occurs in a head-to-tail fashion (Muller et al. 1997; Shibuya 2001).

3.10.6.1 VEGF function and gradient formation

Alternative splicing generates multiple isoforms of VEGF-A, with decreasing diffusibility. VEGFA189 (VEGFA188 in mice) contains two heparin-binding domains, VEGFA165 (VEGFA 164 in mice) only one and VEGFA121 (VEGFA164 in mice) lacks both heparin-binding domains (Ruhrberg et al. 2002). VEGFs and other growth factors are thought to bind heparane sulfate proteoglycans (HSPGs) in the ECM and thereby forming a gradient (Cohen et al. 1995; Ruhrberg et al. 2002; Zhao et al. 2012). This gradient is thought to be formed by secretion and extracellular degradation but to be also dependent on the differing diffusibility of the various VEGF isoforms (Ruhrberg et al. 2002; Ruiz de Almodovar et al. 2009). VEGF189 generates very steep and short gradients, whereas VEGFA165 forms intermediate and VEGFA121 long shallow gradients. However, under which conditions these different gradients are needed is still discussed. Interestingly, VEGF164/164 knock-in mice expressing only the intermediate form and VEGF120/188 expressing the short and the long distance isoform show no phenotype (Ruhrberg et al. 2002). Thus, there seems to be no strict necessity for neither of the VEGF isoforms (Ruhrberg et al. 2002).

ECM-bound VEGF can be released by matrix metalloproteinases (MMPs), which can potentially alter the gradient. In addition, it has been put forward that cleaved VEGF may have different VEGFR-2-signaling outcomes (Lee et al. 2005). VEGF gradients are believed not only to activate angiogenic processes but also to guide them (Gerhardt et al. 2003). However, the mechanism of guidance and which VEGF isoforms are involved remains elusive (Ruhrberg et al. 2002). Recent evidence suggests that not only VEGF gradients but also other signaling pathways such as NETRIN-UNC, SLIT-ROBO and SEMA3-NRP1/PLXND1 are involved in sprout guidance, analogous to the growth cone in migrating axons (Carmeliet 2005;

Adams & Eichmann 2010). Interestingly, in contrast to all other VEGF isoforms, the splice isoform VEGF165b has been proposed to negatively regulate VEGFR function (Woolard et al. 2004).

3.10.7 Expression and regulation of VEGFs

During early development, *vegfaa* is expressed in the somites of developing zebrafish and in a bilateral fashion in the hindbrain at the origin of central arteries (Bussmann et al. 2011; Stahlhut et al. 2012). *Vegfab* is expressed in the axial vessels of zebrafish larvae and in the midline of the developing hindbrain driving hindbrain vascularization (Bussmann et al. 2011). Vegfaa and Vegfab activate ISV formation, since *vegfaa* loss-of-function completely abolishes ISV formation (L. D. Covassin et al. 2006). Strikingly, *vegfaa* gain-of-function in miRNA-1 and miRNA-6 morphants does not change ISV patterning (Stahlhut et al. 2012), thus primary sprouting appears to be rather resilient to changes in *vegfaa* expression.

In the early zebrafish embryo, *vegfc* is expressed in the hypochord and becomes restricted to the DA and ISVs at ~24 hpf (L. D. Covassin et al. 2006; Gore et al. 2011). Vegfc activates secondary sprouting in the venous ECs of the PCV which are needed for venous ISV remodeling (Isogai et al. 2003). The expression patterns of *vegfb*, *vegfd* and *plgf* and their function in zebrafish are poorly understood. Mutants such as vhl^{hu2117} and $ptena^{-/-};ptenb^{-/-}$ were shown to globally upregulate *vegfaa* in zebrafish larvae by 3 dpf, which results in a hypervascularization phenotype at the level of the spinal cord (Choorapoikayil et al. 2013; van Rooijen et al. 2011).

In mice, VEGF is expressed in various tissues. The nerves in the skin produce VEGF to regulate arterial differentiation (Mukouyama et al. 2002; Mukouyama et al. 2005) and VEGF secreted by retinal astrocytes has been shown to activate postnatal retinal vascularization (Ruhrberg et al. 2002; Gerhardt et al. 2003). Non-developmentally expressed VEGF is considered to be activated by HIF1α in an oxygen-dependent manner (Pugh & Ratcliffe 2003). HIF1α is constantly hydroxylated by prolyl hydroxylase domain-containing enzymes (PHDs) under normoxic conditions, and the E3 ubiquitin ligase pVHL binds to hydroxylated HIF1α, ubiquitinylates it and thereby targets it for degradation (Carmeliet et al. 1998;

Weidemann & Johnson 2008). Under hypoxic conditions, Hif1α cannot be hydroxylated and is therefore stabilized. Stabilized HIF1α translocates to the nucleus and activates transcription of genes bearing a hypoxia response element (HRE) in their regulatory sequences (Carmeliet et al. 1998; Kimura et al. 2000). The major HIF1α target gene is VEGF, which is dramatically upregulated upon oxygen depletion (Liu et al. 1995; Carmeliet et al. 1998). The exact role of the hypoxia-HIF1α -VEGF pathway is debated, since mice lacking the HREs in the VEGF gene (*Vegf*$^{\partial/\partial}$) suffer from motor neuron degeneration, but remarkably lack major vascular defects (Oosthuyse et al. 2001). Chronic hypoperfusion and resulting ischemia in the spinal cord was suggested to be the reason for the motorneuron degradation in the (*Vegf*$^{\partial/\partial}$) mice (Oosthuyse et al. 2001). Other authors suggest a HIF1α-independent VEGF regulation by PGC-1α and ERR-α under hypoxic conditions (Arany et al. 2008). This would explain the rather subtle phenotype in the (*Vegf*$^{\partial/\partial}$) mice

Taken together, it is clear that hypoxia can regulate VEGF, but how this is accomplished is not fully understood yet.

3.11 Dll4-Notch signaling

The Dll4-Notch pathway is of ample importance for both, AVD and angiogenesis (Lawson et al. 2001; Siekmann & Lawson 2007; Suchting et al. 2007; Herbert & Stainier 2011). *Notch1* and its ligand *dll4* are predominantly expressed in arterial ECs in the developing zebrafish and Notch signaling is strictly restricted to the arterial domain (Siekmann & Lawson 2007; Quillien et al. 2014; Lawson et al. 2001; Leslie et al. 2007).

3.11.1 Notch signaling in AVD

The arterial Notch restriction is highlighted by the observation that following venous remodeling in zebrafish, where *notch1a*-expressing aISVs are converted into vISVs, *notch1a* expression and signaling in remodeled segments is rapidly lost (Quillien et al. 2014). Moreover, NOTCH signaling was recently shown to be dependent on mechanical force, e.g. blood flow, which could be an explanation for the rapid loss of signaling under decreased force conditions with less shear stress in veins (Gordon et al. 2015). Other authors indicate that *Notch* is expressed in a pan-endothelial manner and becomes only restricted to arteries

after the onset of flow (Jahnsen et al. 2015). After activation of Notch in arterial ECs, *efnb2, hey/hes* and other arterial markers are activated (Siekmann & Lawson 2007). Of note, in *dll4* depleted zebrafish, venous remodeling is greatly favored suggesting that Notch signaling inhibits venous remodeling in zebrafish (Leslie et al. 2007).

In summary, Notch is an arterial marker, which activates arterial differentiation in ECs. *Notch* expression can be genetically hardwired or reprogrammed in response to hemodynamic forces.

3.11.2 The role of Notch in angiogenesis

Besides determining arterial fate, NOTCH is widely seen as an important regulator of angiogenesis with mainly anti-angiogenic functions (Suchting et al. 2007; Herbert & Stainier 2011; Siekmann et al. 2013). This is illustrated since loss of *Notch* or *Dll4* leads to a massive increase in tip cell and sprout formation (Suchting et al. 2007; Thurston et al. 2007; Noguera-Troise et al. 2006). NOTCH anti-angiogenic function is attributed to *Flt1* upregulation and/or blockade of VEGFR-2 signaling (Krueger et al. 2011; Funahashi et al. 2010; Chappell et al. 2013; Bentley et al. 2014). FLT1 is thought to limit VEGFR-2 signaling by decreasing the VEGF bioavailability in the immediate microenvironment of stalk cells (Funahashi et al. 2010). Blockade of VEGFR-2 signaling via FLT1 or directly via NICD was also suggested to prevent EC dissociation from the endothelial sheet and thus formation of angiogenic sprouts and shuffling (Bentley et al. 2014). Furthermore, it is known for more than a decade that Notch depletion leads to more tip cells and non-productive angiogenesis and therefore paradoxically to less tumor growth (Noguera-Troise et al. 2006; Thurston et al. 2007). Interestingly, in contrast to all other tissues, in bone ECs NOTCH has pro-angiogenic functions and supports sprouting angiogenesis (Ramasamy et al. 2014).

The functions of NOTCH in AVD and angiogenesis are regarded as separate processes. NOTCH activates arterial fate and restricts angiogenesis. Possibly, both processes are linked or can be converged into one common NOTCH function.

3.12 Anastomosis and lumen formation

In order to form a patent vessel an angiogenic sprout has to connect to another sprout or to an already lumenized vessel, establishing a functional loop (Herwig et al. 2011; Lenard et al. 2013). A vascular anastomosis is the connection of two sprouts that form a lumenized continuum. Tissue macrophages may support vascular anastomosis formation acting as chaperons by bringing two angiogenic sprouts into close physical contact (Fantin et al. 2010). How macrophages mechanistically detect nascent sprouts and bring them together is poorly understood (Fantin et al. 2010).

3.12.1 Vascular lumen formation

There are mainly two models for vascular lumen formation currently debated. Lumen formation was first suggested to proceed by pinocytosis and vacuole formation. These vacuoles were reported to eventually fuse and form an intracellular and then intercellular lumen (Folkman & Haudenschild 1980; Davis & Camarillo 1996; Kamei et al. 2006; Sigurbjörnsdóttir et al. 2014). Recently, Gebala and colleagues reported that lumen formation in zebrafish primary sprouts involves inverse membrane blebbing (Gebala et al. 2016). It may be that different vessels have varying mechanisms for lumen formation, for instance depending on whether the lumen is de novo formed or expanded from a pre-existing lumen.

Taken together, sprouting angiogenesis is completed by anastomosis formation with adjacent sprouts or lumenized vessels and subsequent lumen formation by inverse membrane blebbing or vacuole formation and fusion mechanisms. After the lumen is formed the vessel is perfused and becomes stabilized.

3.13 Endothelial cell junctions

The endothelial cell monolayer lining the inner vessel wall is interconnected by adherens junctions, tight junctions and gap junctions (Bazzoni & Dejana 2004; Dejana 2004). These junctions are important for vascular integrity, vascular permeability, sprouting angiogenesis

and extravasation of leucocytes (Dejana et al. 2009). Junctions are constituted of adhesion proteins that are linked to the intracellular cytoskeletal network and signaling molecules. The junctions are not only rigid structures maintaining vascular integrity, but they are necessary to sense cell position and to form tubular structures (Wallez & Huber 2008). Post-capillary venules have less complex adherens and tight junctions and are therefore the major extravasation sites for leukocytes (Wallez & Huber 2008; Dejana 2004; Dejana et al. 2009). Similarly, tumor vascularization arises from capillaries and post-capillary venules which are vessels with weak cell junctions (Bergers & Benjamin 2003). During sprouting angiogenesis, junctions have to be loosened to allow cell rearrangements. A recent publication suggests that this is achieved via differential VE-cadherin endocytosis in a NOTCH-dependent manner (Bentley et al. 2014).

In summary these findings suggest that cell junctions do not only connect ECs but also constitute a major determinator of the angiogenic potential of ECs, possibly regulated by NOTCH signaling.

3.14 Morpholinos – friend or foe?

Morpholinos are known to be great tools for gene silencing in zebrafish if used carefully (Eisen & Smith 2008). They can either be used to sterically block the start codon and thus the translation of an mRNA or to block an splice site of the pre-mRNA to prevent splicing (Bill et al. 2009). Depending on the morpholino, the knockdown achieved can be almost complete and therefore constitutes a very robust and fast tool to examine gene function. The downside of morpholino use is the subjectiveness of the approach. Morpholinos need to be titrated for optimal usage. Depending on their RNA binding characteristics and equilibrium binding constant they need distinct injection amounts for optimal effects. This poses the risk that dosages are increased until the expected/desired phenotype is observed. This phenotype can be correct or the result of side effects which cannot be clearly distinguished. Researchers normally do various controls to safeguard the specificity of the knockdown. Rescue experiments, where the mRNA of the morpholino-knockdowned gene is injected into morphants to verify complementation and rescue of the phenotype. This approach again is subjective and therefore error-prone. With the use of CRISPR/Cas and TALENs many

morpholino results were questioned because the generated mutants did not display the expected morpholino phenotype or no phenotype at all (Schulte-Merker & Stainier 2014; Kok et al. 2014). Therefore, the generation of CRISPR/Cas mutants to verify the specific morpholino dosage was suggested as a gold standard (Kok et al. 2014; Stainier et al. 2015). This is controversially discussed, since mutant generation is time-consuming and comes along with higher space requirements for fish tanks or can even ban certain organisms from developmental biology research for lack of alternatives (Blum et al. 2015).

In conclusion, the usage of morpholinos is safe if a reference mutant is available for comparison and would also be safe if controls would be used stringently, which is not always the case as revealed by the numerous bad examples in the past.

3.15 Aim of the work

VEGFR-1 (Flt1) has been reported to limit tip cell formation as well as being a critical player in shaping Vegf microgradients to direct sprout migration. Despite two decades of intensive research on Flt1, its function in forming vascular networks and the role of neuronal Flt1 and other cellular sources is still controversially discussed. Flt1 is a Vegf scavenger limiting Vegf bioavailability and Kdrl signaling. Vegf has been shown to influence neurodegenerative processes since adequate vascular supply is critical for neuronal function and survival. The role of the soluble and membrane bound Flt1 in neurons and their function in endothelial cells remains elusive.

The aim of this study is therefore to dissect the distinct physiological functions of neuronal and vascular Flt1 and its different isoforms sFlt1 and mFlt1. In order to elucidate the cell-autonomous and non-cell autonomous functions of Flt1 in vessels and nerves, an extensive set of isoform-specific, and tissue-specific zebrafish mutants, cell transplantation experiments as well as a variety of sFlt1 and Vegfaa gain-of-function transgenic zebrafish were generated and analyzed. FACS analysis, real-time PCR evaluation and RNA sequencing experiments supplemented these data.

4 Results

4.1 Loss of Flt1 induces massive hypervascularization of the spinal cord

To study the role of Flt1 in neurovascular development, we used the zebrafish model since vascular development can be dynamically tracked in various vascular and neuronal reporter lines (Isogai et al. 2003; Kamei & Weinstein 2005). In addition, owing to recent advances in genomic engineering, the genome can be easily modified using CRISPR/Cas or TALENs (Hwang et al. 2013; Auer & Bene 2014). Two *flt1* mutants were generated utilizing the novel CRISPR/Cas technique. The zebrafish *flt1* gene consists of 34 exons encoding membrane-bound mFlt1 and at least one soluble form, which are formed by alternative splicing at the exon 10-intron 10 boundary (Krueger et al. 2011). In order to dissect the roles of membrane-bound and soluble Flt1, a mutant targeting both isoforms (full mutant) and an mFlt1-specific mutant were generated.

4.1.1 Generation of *flt1* full mutants

To obtain *flt1* full mutants, *flt1* exon 3 was targeted with a small guide RNA (sgRNA), designed to target exon 3 (Figure 4-1). As exon 3 codes for the first Ig1 domain, all frameshift mutants obtained generate an early premature stop codon that produces a truncated protein lacking the Ig2 domain that is essential for VEGF-binding (Figure. 4-1a) (Herley et al. 1999). Four independent full *flt1* mutant founder fish were recovered and outcrossed. The lines were annotated according to the ZFIN zebrafish nomenclature using the Karlsruhe (KIT) lab designation 'ka' (Figure 4-1d). Mutant lines $flt1^{ka601}$ (-1nt), $flt1^{ka602}$ (-5nt), $flt1^{ka603}$ (+5nt) and $flt1^{ka604}$ (-14nt) were crossed to the reporter lines $Tg(Xla.Tubb:DsRed)^{zf148}$, $Tg(kdrl:EGFP)^{s843}$, $Tg(kdrl:hsa.-HRAS-mcherry)^{s916}$ and $Tg(fli1a:nGFP)^{y7}$ to allow phenotypic analysis of the mutants. To evaluate if the *flt1* mRNA is degraded by non-sense mediated decay (NMD), the reads of an RNAseq experiment performed with $flt1^{ka601}$ mutants and WT siblings were mapped to the *flt1* mRNA depicted in a Sashimi-plot. Comparison of read numbers covering the exons revealed that *flt1* mRNA levels are unchanged in $flt1^{ka601}$, demonstrating that *flt1* NMD does not occur in $flt1^{ka601}$ mutants (Figure 4-2a).

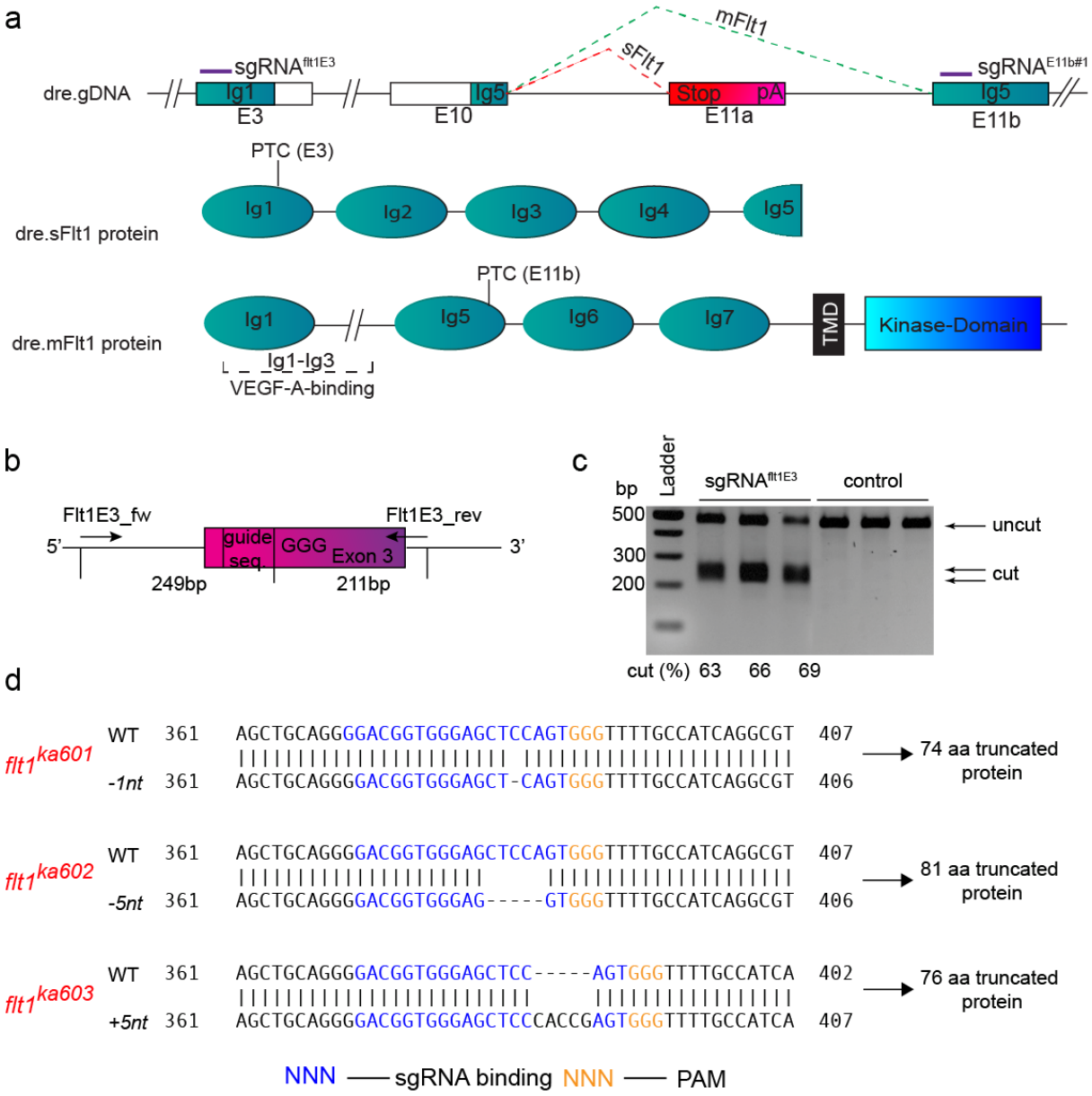

Figure 4-1. CRISPR/Cas approach for generating *flt1* mutants and *mflt1* mutants.

(**a**) Flt1 exon structure and splice sites for zebrafish *sflt1* and *mflt1*. Schematic protein structure and IgG domains of sFlt1 and mFlt1 for comparison. Domains targeted by sgRNA in exon 3 (*full flt1 mutants flt1* $^{ka601\text{-}604}$, targeting both *sflt1*, *mflt1*) and exon 11b (targeting only *mflt1, flt1* $^{ka605\text{-}608}$) are indicated. (**b**). Position of guide sequence, Flt1 exon 3 forward and reverse primers and expected PCR band size after T7EI cleavage. (**c**) T7EI assay and quantification of sgRNA^{flt1E3} (targeting exon 3) efficiency (**d**) Structure and DNA sequence of *flt1*^{ka601} (-1nt), *flt1*^{ka602} (-5nt), *flt1*^{ka603} (+5nt) mutant alleles. PTC, premature termination codon; PAM, protospacer adjacent motif; sgRNA, small guide RNA.

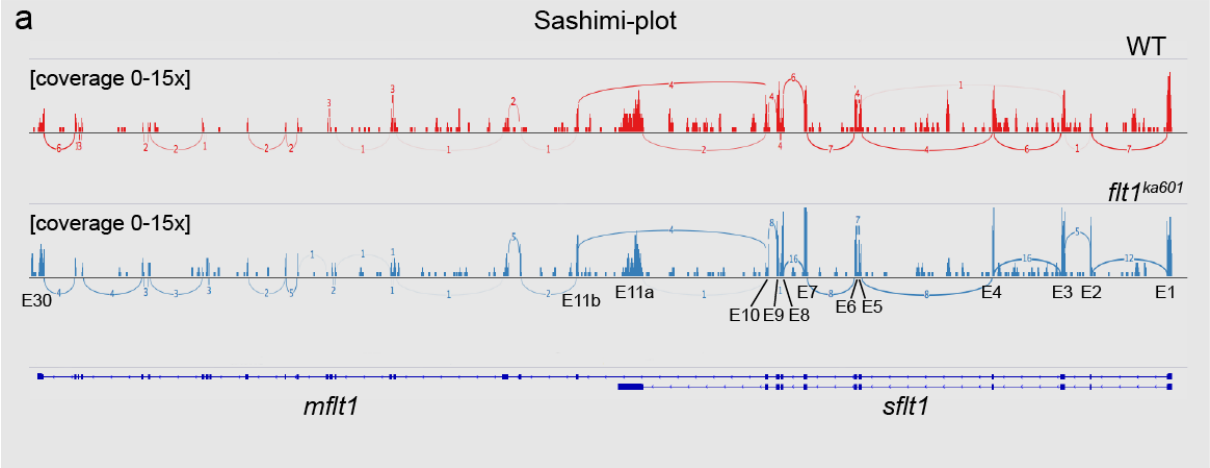

Figure 4-2. *flt1* mRNA NMD does not occur in *flt1*^{ka601} mutants.

(**a**) Sashimi-plot showing number of reads mapped to the *flt1* genomic locus in WT and *flt1*^{ka601} mutants. Note that the number of reads in shared exons (1-10), sFlt1 unique exons (11a) and in mflt1 unique exons (11b-30) are comparable.

Flt1 KO mice exhibit a severe angioblast over-commitment phenotype resulting in a disorganized vascular plexus and early lethality (Fong et al. 1995; Fong et al. 1999). Accordingly, an early phenotype affecting the first angiogenic processes was also expected in zebrafish deficient for *flt1*. Surprisingly, primary sprouting and secondary sprouting in the zebrafish trunk was normal in *flt1*^{ka601} mutants (Figure 4-3).

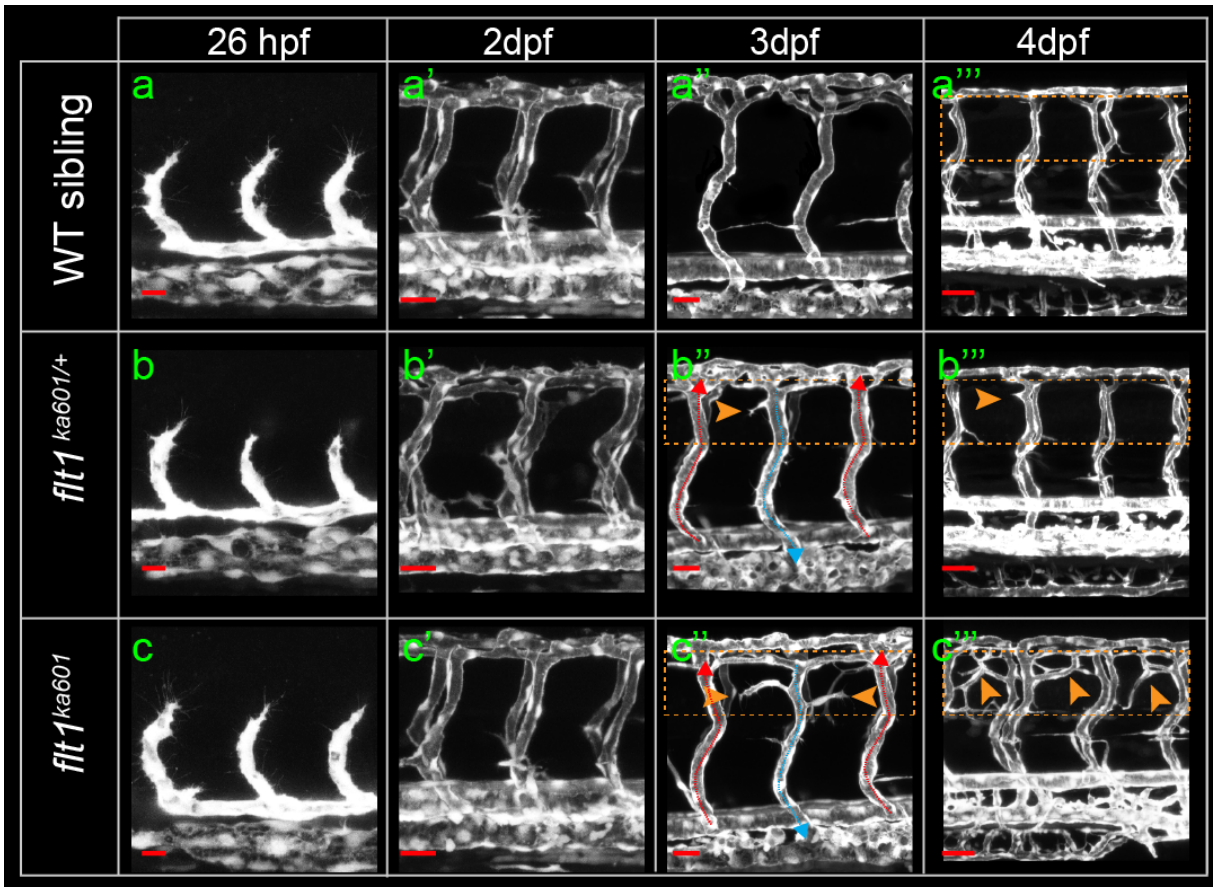

Figure 4-3. Primary and secondary sprouting are not affected in flt1ka601 mutants.

(**a-a'''**) Trunk vascular network in WT embryos at indicated time points. (**b-b'''**) Trunk vasculature in *flt1*$^{ka601/+}$ embryos at indicated time points. (**c-c'''**) Trunk vasculature in *flt1*^{ka601} embryos at indicated time points. Arrowheads indicate ectopic branches. dpf, days post fertilization. Scale bar, 50µm in a'-c', a'''-c'''; 25µm in a-c, a''-c''.

At slightly later stages, *flt1*^{ka601} mutants displayed severe hyperbranching at the level of the neural tube starting at ~2.5dpf (Figure 4-3 and 4-4). *flt1*^{ka601} (-1nt), *flt1*^{ka602} (-5nt), *flt1*^{ka603} (+5nt) and *flt1*^{ka604} (-14nt) mutant lines were phenotypically undistinguishable, therefore only the *flt1*^{ka601} line was used for further investigations (see Figure 4-4d-f).

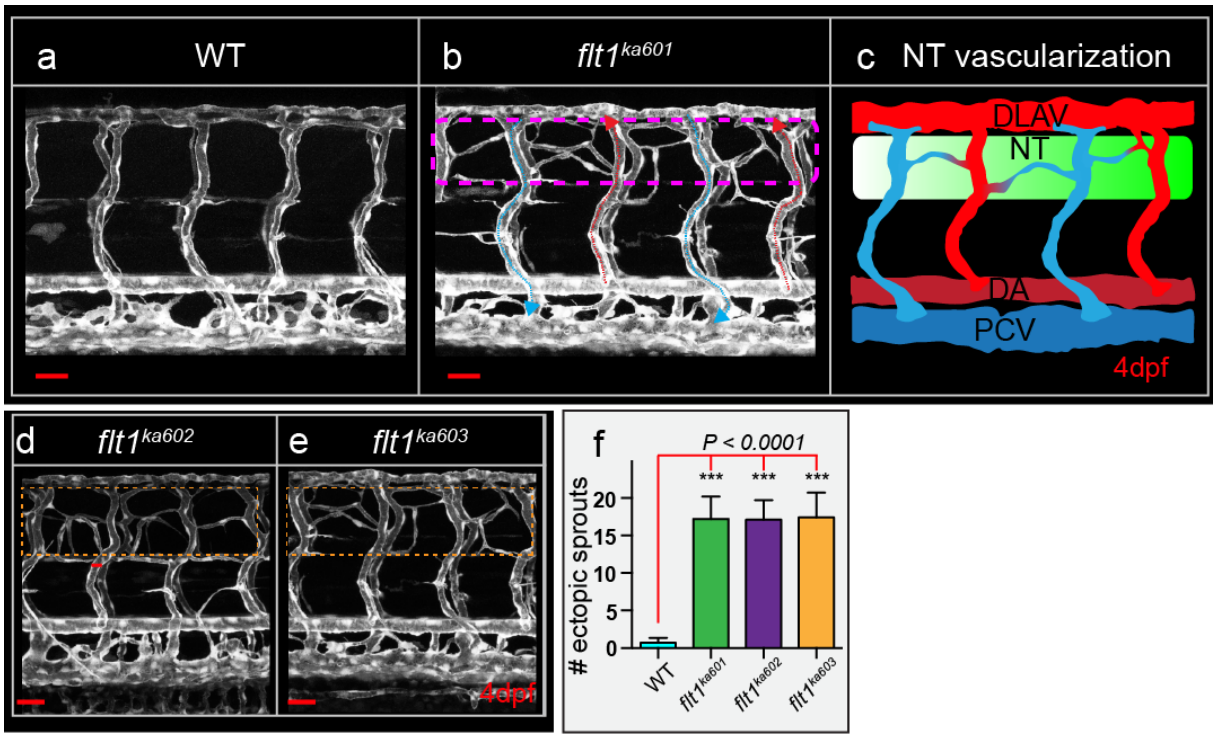

Figure 4-4. *Flt1* mutants develop hyperbranched vascular networks at the level of the neural tube.

(**a**) Trunk vasculature in 4dpf WT sibling, (**b**) trunk vasculature in 4dpf *flt1*^{ka601} mutant, in *Tg(kdrl:EGFP)*^{s843} background. Perfused aISVs with red arrow, veins with blue arrow. Note the extensive amount of hyperbranching (dotted box) at the level of the neural tube. (**c**) Schematic representation of hyperbranching phenotype along the neural tube; ectopic vessels make anastomosis between vISV (blue) with aISVs (red). (**d**) Hyperbranching (dotted box) is also observed in *flt1*^{ka602} and (**e**) *flt1*^{ka603} mutants. (**f**) Quantification of hyperbranching for indicated mutant alleles. Mean ± s.e.m, *n=10*. DA, dorsal aorta; PCV, posterior cardinal vein; DLAV, dorsal longitudinal anastomotic vessel; NT, neural tube; hpf, hours post fertilization; dpf, days post fertilization. Scale bar, 50µm.

To substantiate the specificity of the *flt1*^{ka601} mutants and to exclude that residual Flt1 protein is produced in the *flt1*^{ka601} mutant, the phenotype was compared with morpholino-mediated knockdown. At low *flt1*-ATG morpholino dosages (1ng) ectopic sprouting at the level of the neural tube starting at 2.5dpf as observed in *flt1*^{ka601} mutants could be exactly phenocopied (Figure 4-5).

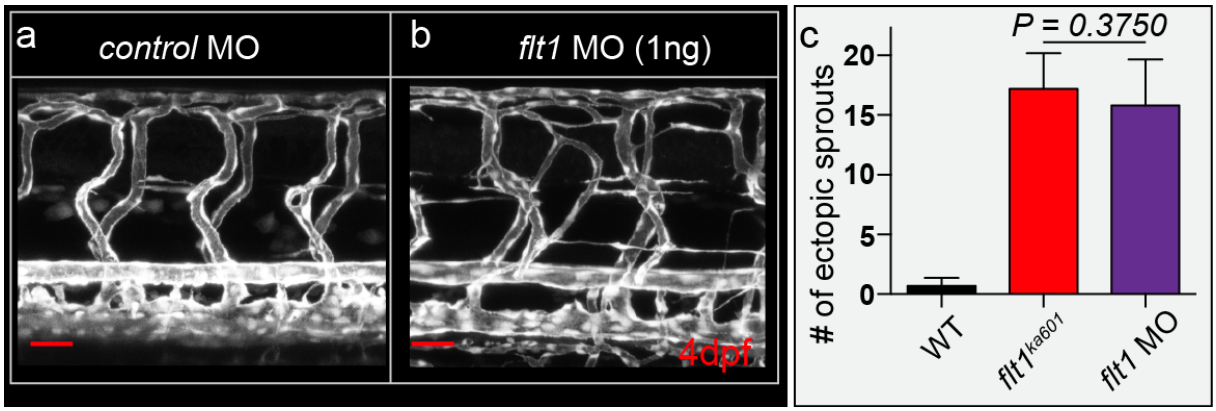

Figure 4-5. Low dosage morpholino injection phenocopies *flt1*^{ka601} mutants.

(**a**,**b**) Vascular pattern in *Tg(kdrl:EGFP)*^{s843} embryos injected with control MO (a), and 1ng *flt1* targeting MO (b). (**c**) Quantification of a,b; mean ± s.e.m, n=10. Note hyperbranching equal to *flt1*^{ka601}. MO, morpholino. Scale bar, 50µm.

Nevertheless, high morpholino dosages (3ng) induced excessive primary sprouting and increased tip cell numbers as previously reported (Krueger et al. 2011). Morpholino injection into a *flt1*^{ka601} mutant background did also result in hypersprouting suggesting that unspecific morpholino effects and not molecular compensations induce this early arterial hypersprouting phenotype (Figure 4-6) (Rossi et al. 2015). Strikingly, all *flt1*^{ka601} mutants shown in this manuscript are maternal zygotic *flt1*^{ka601} mutants (*flt1*^{ka601} X *flt1*^{ka601} breeding), which are phenotypically identical to homozygous *flt1*^{ka601} mutants from heterozygous parents (not shown). Hence, contribution of maternally deposited Flt1 protein or *flt1* mRNA can be excluded.

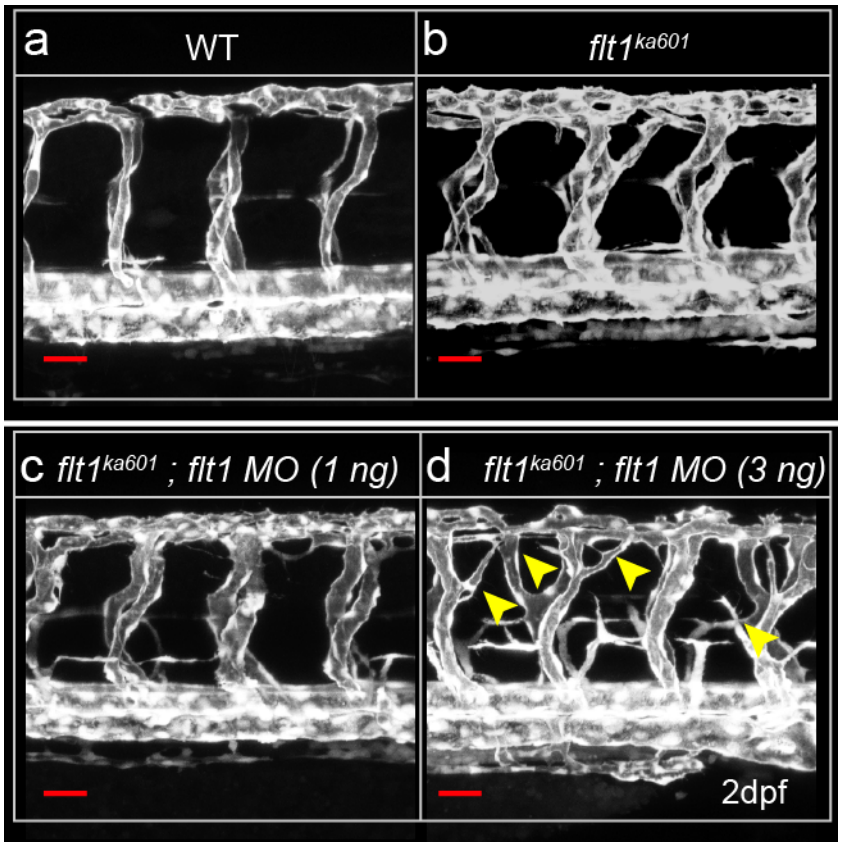

Figure 4-6. High dosage morpholino injections induce unspecific early vascular phenotypes.

(**a-d**) *flt1*^{ka601} with 1ng (c) and 3ng (d) *flt1* targeting MO injected.

Note: the 3ng dosage causes arterial branching defects (arrowheads) not observed *in* *flt1*^{ka601} mutants. MO, morpholino. Scale bar, 50µm.

During zebrafish vascular development, secondary sprouts emanating from the PCV connect in roughly ~50 % of the cases to aISV forming a vISV (venous remodeling) and the other ~50% of the secondary sprout migrate along the aISV and split at the level of the horizontal myoseptum (HMS) to form the parachrodal lymphangioblasts (PL cells) and eventually the lymphatic system (Isogai et al. 2003). Careful inspection of the *flt1* mutants revealed that the lymphatic secondary sprouts migrated along the aISV as observed in WT but rather connected to the aISV at the level of the HMS forming an arteriovenous shunt (Figure 4-7b).

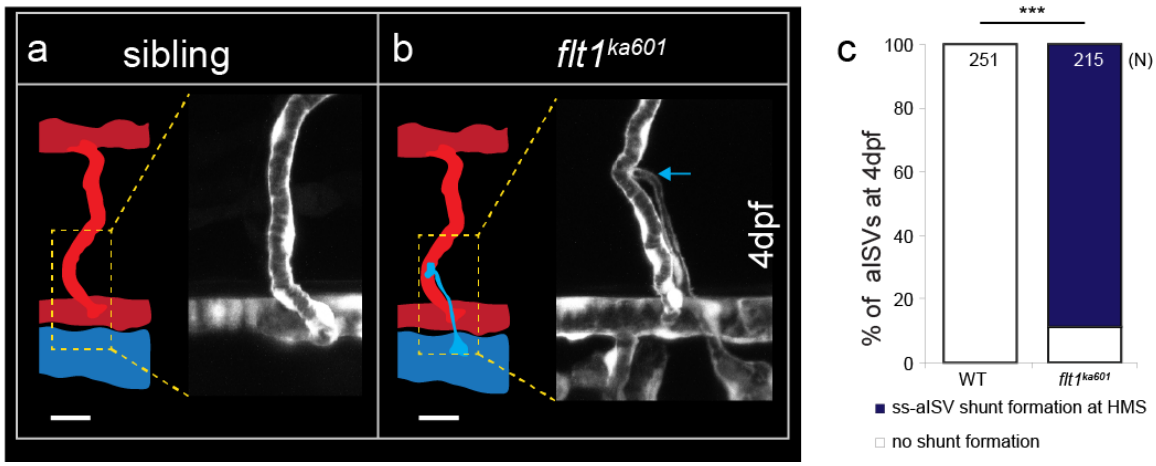

Figure 4-7. Arteriovenous shunt formation in *flt1*^{ka601} mutants.

(**a**) Representative image of the ventral aspect of aISV in WT zebrafish at 4dpf. Note that secondary sprouts differentiated into lymphatic ECs and downregulated *kdrl* and are therefore not visible in these images. (**b**) Ventral aspect of the aISV of a *flt1*^{ka601} mutant. Note that the secondary sprout connected to the aISV forming an arteriovenous shunt, blue arrow. (**c**) Quantification of shunt formation in *flt1*^{ka601} mutants. ss, secondary sprout. Scale bar, 10µm.

This pathological behavior remained unobtrusive, most likely because parachordal lymphangioblasts are also formed from vISVs at the level of the HMS. These cells can possibly compensate for the loss of direct secondary sprout contribution to the lymphatic system. Analysis of other vascular beds in *flt1*^{ka601} mutants revealed that vascular density is also affected in other tissues. For instance *flt1*^{ka601} mutants display a hypersprouting phenotype in the hyaloid vascular plexus of the retina (see Figure 4-8).

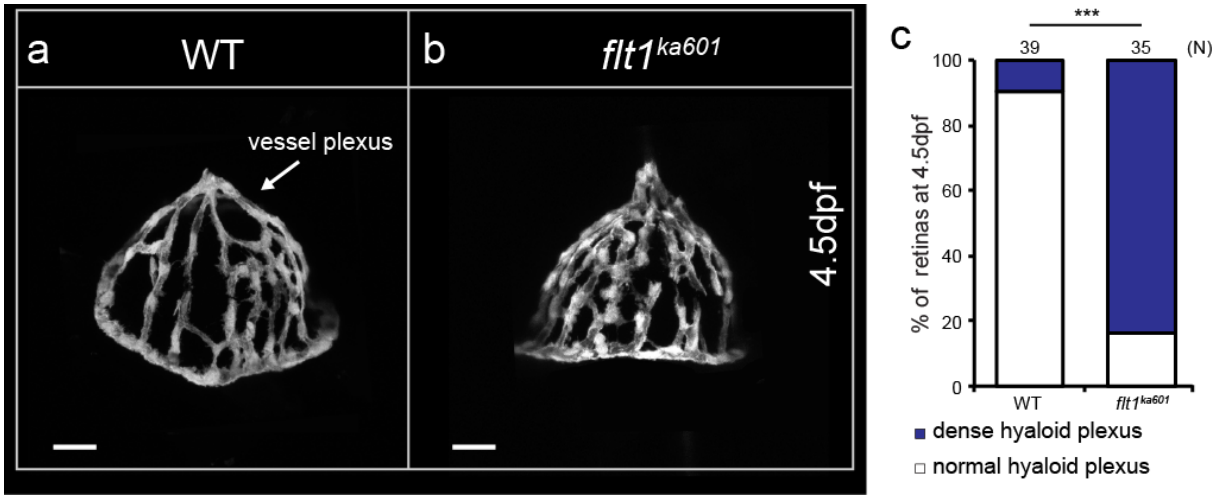

Figure 4-8. *flt1*^{ka601} mutants display increased vascular hyaloid plexus density in the eye.

(**a**) Representative image of the vascular hyaloid plexus in the eye of a WT sibling (**b**) and a *flt1*^{ka601} mutant at 4.5dpf. (**c**) Quantification of vascular plexus density in the eye. Dense was defined as more than 50% of the retina area covered by ECs. Scale bar, 15µm.

Flt1 KO mice display a serve angioblast over-commitment phenotype resulting in early lethality. Surprisingly, *flt1*^{ka601} mutants display no early vascular defects. To ascertain whether angioblast commitment and proliferation are affected in *flt1*^{ka601} mutants EC numbers were counted using *Tg(Fli1a:nGFP)*^{y7} reporter fish staining the nuclei of ECs. Interestingly angioblast formation and proliferation appeared normal in *flt1*^{ka601} zebrafish mutants (Figure 4-9).

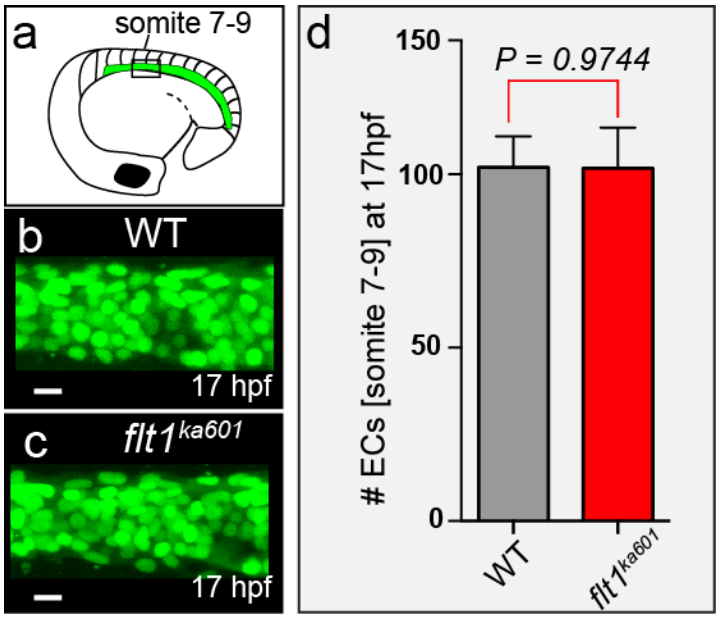

Figure 4-9. Angioblast numbers are not affected in *flt1*^{ka601} mutants.

(**a**) Graphical illustration of angioblast localization and quantification area in zebrafish embryos. (**b,c**) Imaging of endothelial nuclei in 17hpf WT and *flt1*^{ka601} embryos. EC numbers were counted between somite 7-9 (a). (**d**) Quantification of angioblasts at 17hpf shows no difference in angioblast numbers. Angioblasts were counted using ImageJ plugin 3D object counter, mean ± s.e.m, *n=4*. Scale bar, 10µm.

Similarly, primary sprouting and venous remodeling were not altered in *flt1*^{ka601} mutants (Figure 4-10). Rottbauer and colleagues reported that VEGF controls cardiac contractility in mice and rats via Flt1 receptor signaling. As opposed to this, in *flt1*^{ka601} mutants we could not find changes in contractility as depicted in Figure 4-11 (Rottbauer et al. 2005).

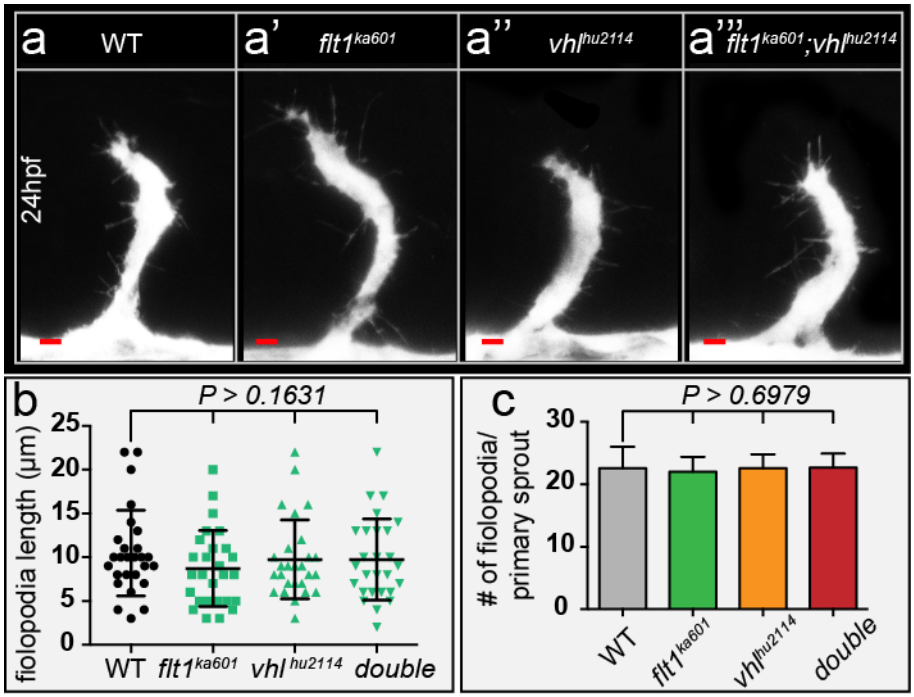

Figure 4-10. Primary arterial sprouting is not affected in *flt1*^{ka601} mutants and other Vegfaa gain-of-function scenarios.

(**a-a'''**) Confocal images of primary arterial segmental vessel sprouting in WT (a), *flt1*^{ka601} (a'), *vhl*^{hu2114} (a''), and *flt1*^{ka601};*vhl*^{hu2114} double mutants (a'''). (**b,c**) Quantification of filopodia characteristics for indicated genotypes. Note that there are no differences in sprouting or filopodia between indicated mutants and WT, mean ± s.e.m, *n=27* (b), mean ± s.e.m, *n=9* (c). Double, *flt1*^{ka601};*vhl*^{hu2114} double mutants; hpf, hours post fertilization. Scale bar, 10µm.

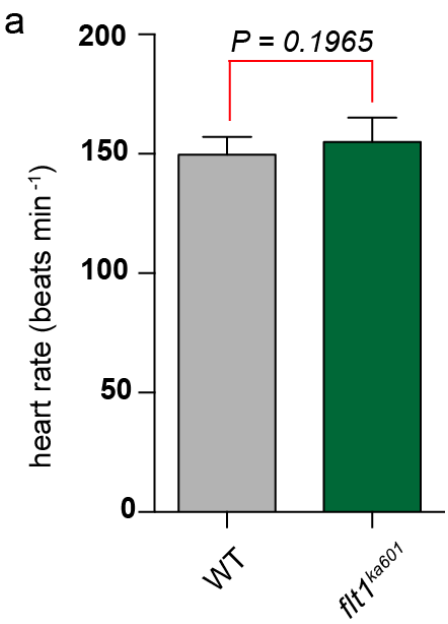

Figure 4-11. The heart rate in *flt1*^{ka601} mutants is normal.

(**a**) Heart rate in WT and *flt1*^{ka601} mutants, mean ± s.e.m, *n=10*.

Strikingly, the brain and hindbrain vasculature, which are – similar to the ISVs – in close contact to CNS neurons, are not affected in *flt1*^{ka601} mutants, although sprouting in *vhl*^{hu2117} mutants, a well-known *vegfaa* gain-of-function zebrafish line, is significantly augmented (Figure 4-12). This indicates that either the brain vessels do not express *flt1* and therefore do not respond in *flt1* loss-of-function scenarios or the brain does not produce Vegfaa in sufficient amounts to induce sprouting in *flt1*^{ka601} mutants.

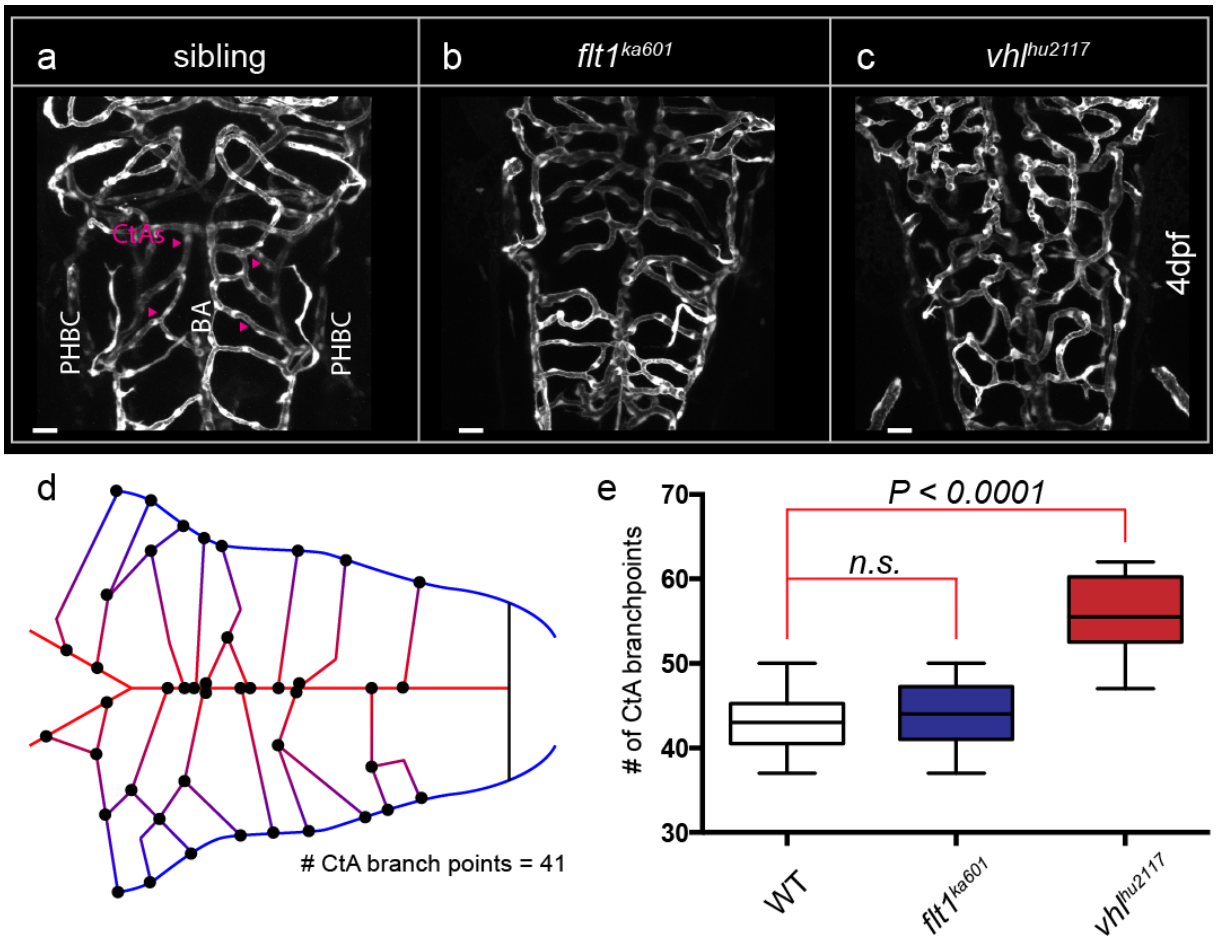

Figure 4-12. Formation of the hindbrain vasculature is not affected in *flt1*^{ka601} mutants.

(**a-c**) Representative images of the hindbrain vasculature at 4dpf in (a) WT, (b) *flt1*^{ka601} mutants, and (c) *vhl*^{hu2117} mutants. CtAs are indicated with red arrowheads. (**d**) Graphical illustration of a stereotypical hindbrain vasculature with indicated branch points as quantified in (e). (**e**) Quantification of branch points in WT siblings, *flt1*^{ka601} and *vhl*^{hu2117} mutants, mean ± s.e.m, *n=8*. PHBC, primordial hindbrain channel; BA, basilar artery; CtA, central artery; dpf, days post fertilization. Scale bar, 10µm.

Noteworthy, despite of their numerous vascular phenotypes *flt1*^{ka601} mutants were viable as adults and did not show any signs of abnormality. Careful analysis of the literature revealed that *ptena*$^{-/-}$*;ptenb*$^{-/-}$ double mutants and *vhl*^{hu2117} mutants exhibit a comparable spinal cord hypersprouting phenotype as *flt1*^{ka601} mutants (Rooijen et al. 2009; Choorapoikayil et al. 2013). Notably, in these mutants, *vegfaa* was reported to be ubiquitously upregulated at 3 or 6dpf, respectively.

4.1.2 Generation of *mflt1*-specific mutants

To obtain *mflt1*-specific mutants, the first *mflt1*-specific exon (exon 11b) was targeted using a CRISPR/Cas approach. Analysis of four independently generated mutant lines (*flt1*$^{ka605-608}$) did not show any obvious vascular malformations or prominent defects during early development (Figure 4-13). These observations are compatible with the lack of obvious vascular malformations found in murine mFlt1$^{TK-/-}$ mutants, which are mFlt1 signaling deficient (Takahashi & Shibuya 2005). These results indicate that sFlt1, but not mFlt1 regulates vascular patterning in zebrafish.

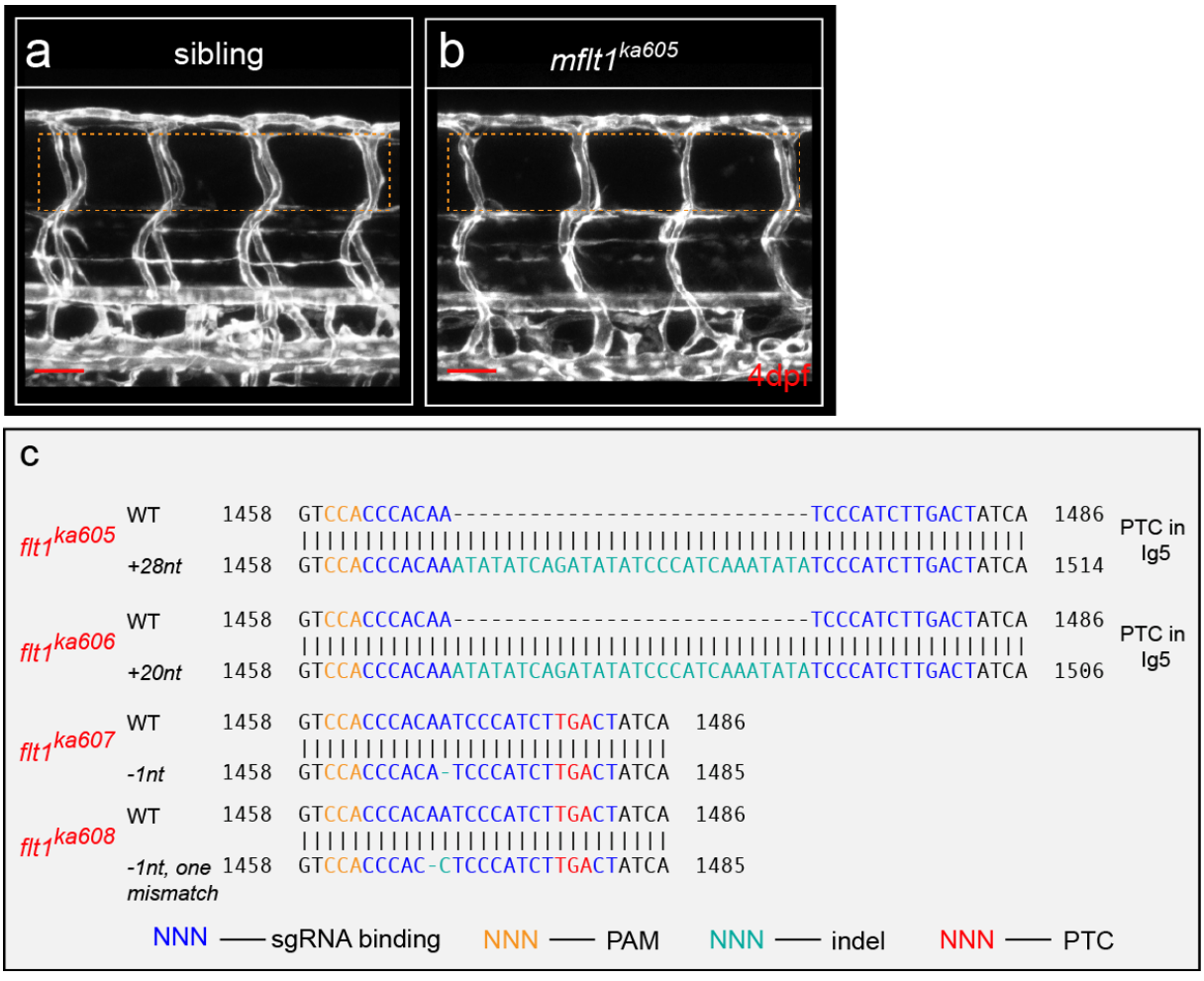

Figure 4-13. Generation of mflt1 mutants using CRISPR/Cas.

(**a,b**) Membrane-bound *flt1* mutant (*flt1*^{ka605}) without vascular phenotype (compare dotted box in b, with control in (a). (**c**) Structure and DNA sequence of *mflt1* mutants, *flt1*^{ka605} (+28nt), *flt1*^{ka606} (+20nt), *flt1*^{ka607} (-1nt) and *flt1*^{ka608} (-1nt,1MM). MM, mismatch; PTC, premature termination codon; PAM, protospacer adjacent motif; sgRNA, small guide RNA; Indel, insertion/deletion, dpf, days post fertilization. Scale bar, 50µm. Design of the sgRNA and cloning and injection of Cas9 mRNA and *mflt1* sgRNA was performed by Anna Klaus.

4.2 Spinal cord neurons express Flt1 and Vegfaa

The severe hyperbranching phenotype at the level of the neural tube was the most prominent phenotype in *flt1*^{ka601} mutants and therefore this work is focused on the analysis of the trunk hypervascularization phenotype. Interestingly, the ectopic vascular network was formed in close proximity to the trunk spinal cord. In addition, *flt1* is expressed in aISVs, the dorsal part of vISVs and some neuronal subpopulations of the zebrafish trunk (Figure 4-14). This suggests that neuronal Flt1 may contribute to the formation of the *flt1* loss-of-function phenotype.

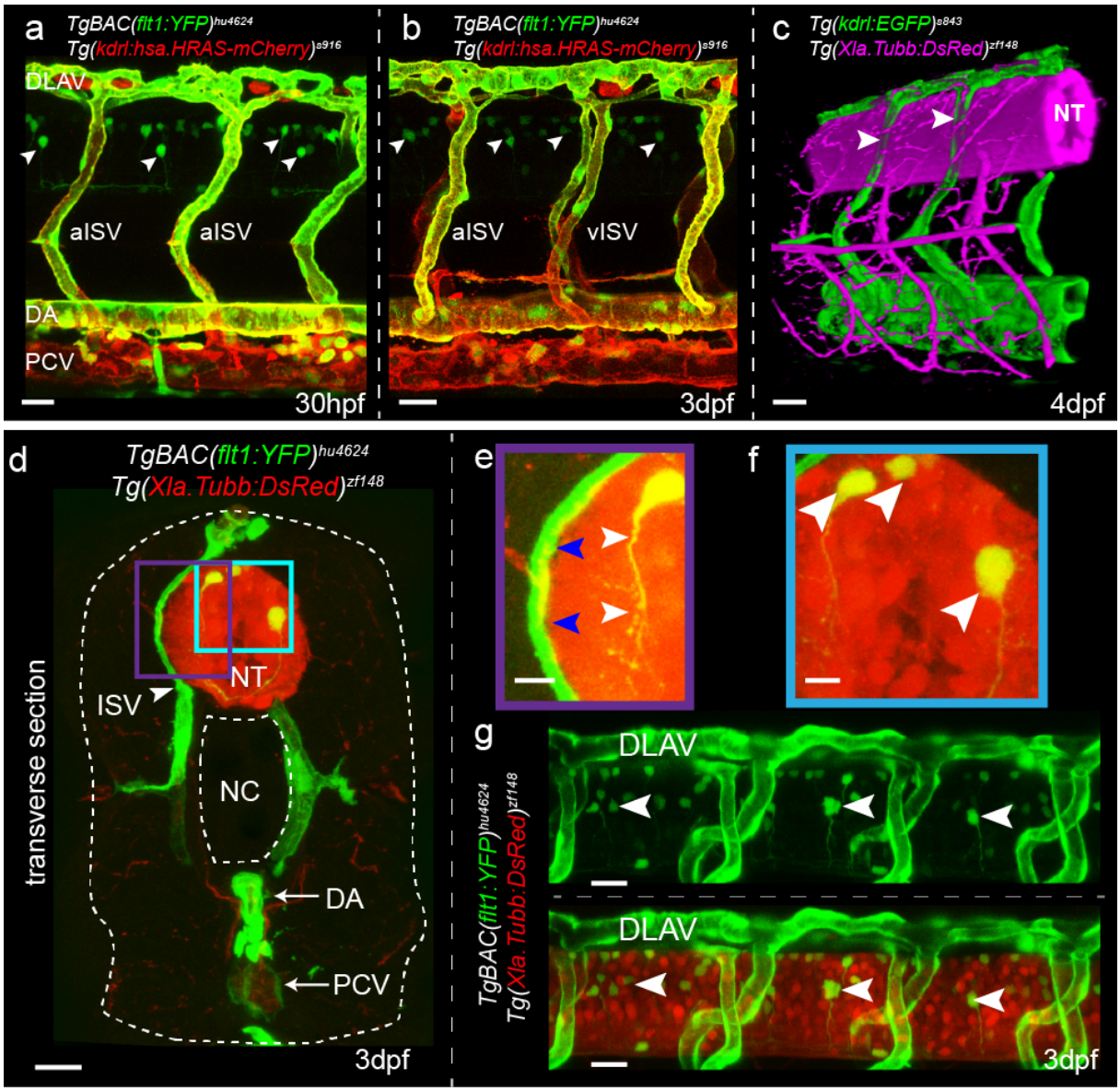

Figure 4-14. Expression of Vegf receptors and ligands at the neurovascular interface.

(**a,b**) Double transgenic embryos *TgBAC(flt1:YFP)*^{hu4624}*; Tg(kdrl:hsa.HRAS-mcherry)*^{916} at 30hpf and 3dpf shows *flt1* expression (green) in dorsal aorta, arterial ISV and dorsal aspect of venous ISV (3dpf), and neurons

(arrowheads). (**c**) 3D-rendered view of vessels (green), and nerves (purple) in *Tg(kdrl:EGFP)*^{s843}*;Tg(XIa.Tubb:DsRed)*^{zf148} embryos highlighting dorsal aspect of ISVs (arrowheads) in close contact to the neural tube (NT). (**d**) Transverse section of the trunk of *TgBAC(flt1:YFP)*^{hu4624}*;Tg(XIa.Tubb:DsRed)*^{zf148} embryos shows that ISVs (green, arrowhead) and neural tube (NT, red) are in close contact. The white dotted line demarcates the embryo boundaries, dorsal is up. (**e**) Magnified view of purple-boxed area in (d), showing direct contact of vessels with nerves at the neurovascular interface (blue arrowheads) and *flt1* expressing neurons with long axonal extensions in the neural tube (white arrowheads). (**f**) Magnified view of blue-boxed area in (d) showing *flt1* expressing neurons (arrowheads) and their axons inside neural tube (red). (**g**) Lateral view of *TgBAC(flt1:YFP)*^{hu4624}*; Tg(XIa.Tubb:DsRed)*^{zf148} at the level of the neural tube showing *flt1* expressing neurons (arrowheads) in neural tube. ISV, intersegmental vessel; DA, dorsal aorta; PCV, posterior cardinal vein; DLAV, dorsal longitudinal anastomotic vessel; NC, notochord; NT, neural tube; hpf, hours post fertilization; dpf, days post fertilization. Scale bar, 30µm in a, b, c, d, g; 10µm in e, f.

Careful analysis of the spinal cord neurons using an imageJ count algorithm revealed that 6-8% of the neurons are *TgBAC(flt1:YFP)* positive (not shown). As neurons extend long axons and dendritic branches, the entire spinal cord appeared penetrated by neuronal extensions presumably secreting sFlt1 (Figure 4-14d-f). *sflt1* production in neurons could also be shown using real-time PCR expression analysis (data not shown). Analysis of 3D-projections showed that ISVs are indenting the neural tube, indicating close contact and suggesting a tight neurovascular interface between the spinal cord neurons and ISVs with possible functional implications (Figure 4-14c). Real-time PCR analysis of FAC-sorted neuronal cells uncovered that not only *flt1* but also other vascular markers such as *kdr, kdrl* and *flt4* as well as their ligands *vegfaa*, *vegfab* and *plgf* are expressed in neurons at similar levels as known neuronal markers such as *sema3a* and *unc5b* indicative of a functional relevance for the genes in neurons (data not shown, experiments performed by Janna Krüger). As neuronal Flt4 was shown to have functional relevance in axonal guidance, the comparably high expression levels of *mflt1* and *sflt1* are highly suggestive of a functional relevance of neuronal Flt1 (data not shown, Janna Krüger). In zebrafish, two *vegfa* isoforms exist, namely *vegfaa* and *vegfab*. Real-time PCR analysis of isolated zebrafish trunks at various time points revealed that *vegfaa* is predominantly expressed in the trunk and that *vegfaa* upregulation in the zebrafish trunk occurs just prior to the appearance of the first ectopic *flt1*^{ka601} sprouts, starting at 2.5dpf (Figure 4-15a).

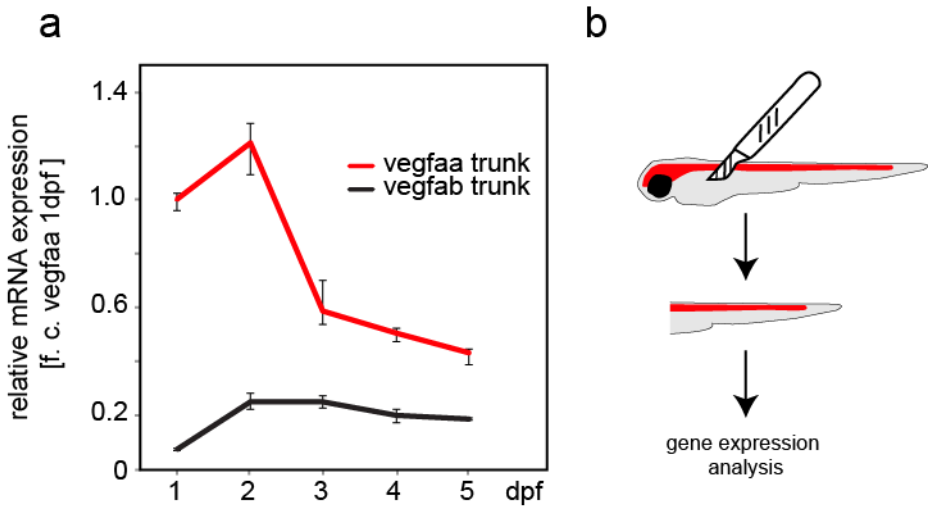

Figure 4-15. *vegfaa* is the major isoform expressed in the trunk and is upregulated just prior to *flt1*^{ka601} hypersprouting. (**a**) mRNA expression levels of *vegfaa* and *vegfab* in the trunks of zebrafish embryos at indicated time points. Note that *vegfaa* is upregulated at 2dpf, just prior to sprout emergence in *flt1*^{ka601} mutants. (**b**) RNA used in (a) was isolated from the trunks of embryos, severed behind the yolk sac.

Vegfab in contrast was only expressed at very low levels in the zebrafish trunk. To elucidate which cells in the trunk express *vegfaa*, real-time PCR analysis was performed on FAC-sorted neuronal cells of 3dpf old zebrafish larvae (schematic see Figure 4-16a). Real-time expression data conclusively show that *vegfaa* expression in neurons is more than 20x higher than in non-neuronal cells at 3dpf, substantiating that at 3dpf the major source of *vegfaa* are not the somites, as during early development, but indeed the spinal cord neurons (Liang et al. 2001). This clearly illustrates that hypersprouting is restricted to the spinal cord region since the spinal cord is the only source producing high amounts of Vegfa.

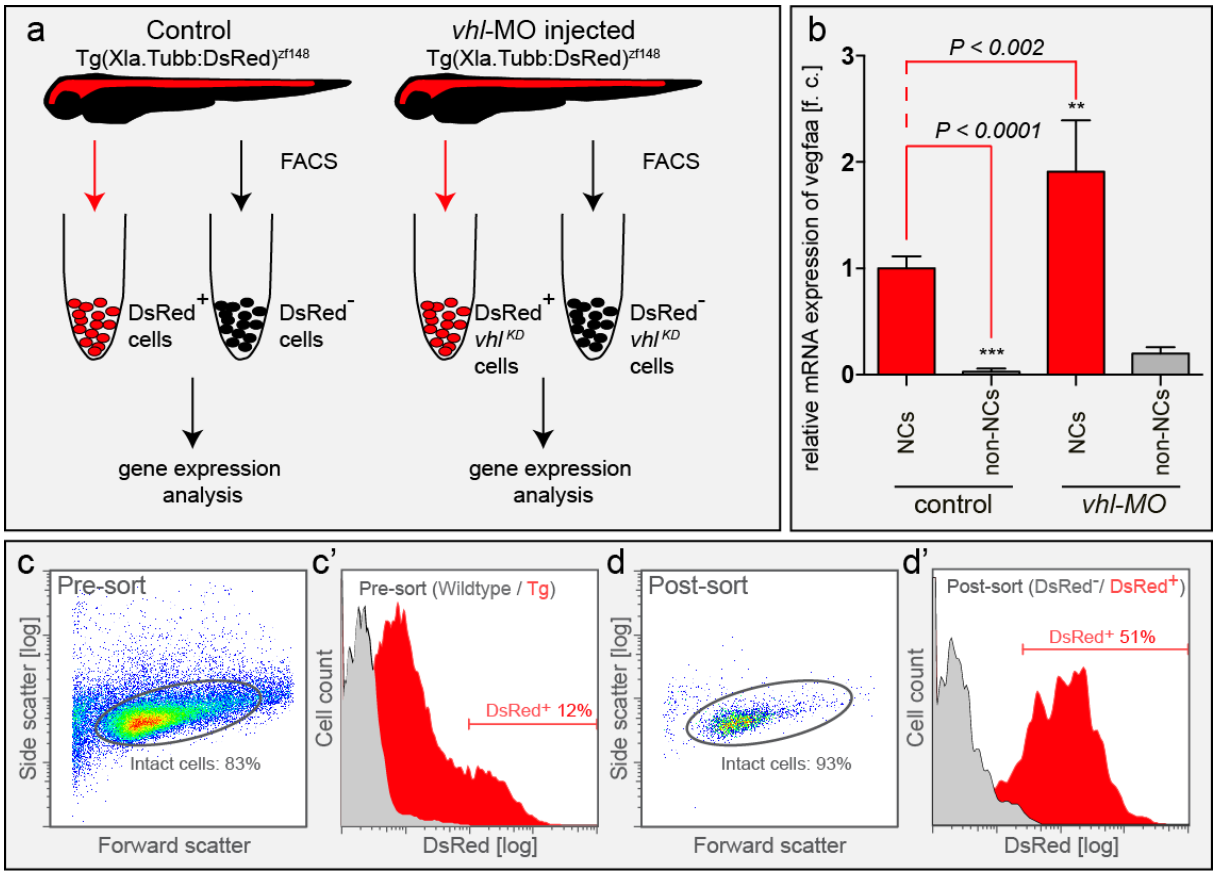

Figure 4-16. Neuronal cells are the major source of Vegfaa and vhl loss-of-function triggers predominantly neuronal Vegfaa upregulation.

(**a**) FACS procedure for obtaining neuronal cells in control and *vhl* morphants using *Tg(Xla.Tubb:DsRed)*^{zf148} neuronal reporter embryos at 3dpf. (**b**) Quantification of *vegfaa* expression using real-time qPCR in FACS-sorted cell populations. Note that neuronal cells expressed significantly more *vegfaa* than non-neuronal cells. Loss of *vhl* promoted neuronal *vegfaa* expression predominantly in neuronal cells. Mean ± s.e.m, *n=3* separate experiments in triplicate (two-way ANOVA). (**c,c'**) Neuronal cells were isolated from *Tg(Xla.Tubb:DsRed)*^{zf148} embryos at 3dpf by FACS with indicated gating settings. About 12% of all intact cells were DsRed+ neurons prior to sorting (Pre-sort) (c'). (**d,d'**) Post-sorting analysis showed that sorted neuronal cells are enriched to 51% neuronal DsRed^{+} cells. DsRed^{-} cells contained less than 1.7 % DsRed^{+} cells (d'). NC, neuronal cell; KD, knockdown; MO, morpholino. FACS sorting was performed in collaboration with Yuya Hayashi.

It is well-known that in *vhl*^{hu2117} mutants, *vegfaa* is upreglated due to stabilization of Hif1α (Rooijen et al. 2009; van Rooijen et al. 2010). However, the exact source of *vegfaa* remains elusive as in situ hybridizations only show a blurred staining with low resolution of expression (van Rooijen et al. 2011). To identify the cell population upregulating *vegfaa* in *vhl*^{hu2117} loss-of-function scenarios, *vhl* was knocked down using a morpholino approach. Subsequently, neuronal cells were FAC-sorted for further analysis. Real-time PCR analysis of *vegfaa* expression in *vhl* morphant-neuronal cells (NCs) showed that *vegfaa* is globally

upregulated in NCs and in non-NCs, but that the expression in NCs is almost 10x higher in *vhl* morphants (Figure 4-16b). These results suggest that (I) the spinal cord is a rich source of *vegfaa* and (II) neuronal *vegfaa* is the major driver of hypersprouting in *vhl* morphants.

4.2.1 Analysis of *flt1*^{ka601}; *vhl*^{hu2117} double mutants

Flt1 and pVhl are involved in different layers of VEGF biology. Whereas pVhl regulates Hif1α turnover and thus *vegfaa* transcriptional regulation, Flt1 regulates Vegfaa bioavailability of secreted Vegfaa protein (see schematic illustration in Figure 4-17a) (van Rooijen et al. 2011). Therefore, it can be assumed that loss of both tiers of regulation enhances the vascular phenotype. Indeed, in *flt1*^{ka601}; *vhl*^{hu2117} homozygous double mutants sprouting angiogenesis was dramatically augmented. Remarkably, hypersprouting was restricted to the dorsal region of the trunk at the level of the spinal cord similar to *flt1*^{ka601} mutants (Figure 4-17b). As expected, the observed ectopic vascular network in *flt1*^{ka601}; *vhl*^{hu2117} double mutants exhibited a higher vascular density than single *flt1*^{ka601}, *vhl*^{hu2117} or *ptena*$^{-/-}$;*ptenb*$^{-/-}$ mutants. Interestingly, using Y-Z projections it could be shown that ectopic sprouts did not only laterally vascularize the spinal cord, but also invaded into the spinal cord in *flt1*^{ka601}; *vhl*^{hu2117} double mutants (Figure 4-17d-e). This invasive sprouting behavior did not occur in any other single mutant investigated. The finding further substantiates that indeed the spinal cord is the source of Vegfaa and that the spinal cord neurons are the major source of Hif1α regulated Vegfaa.

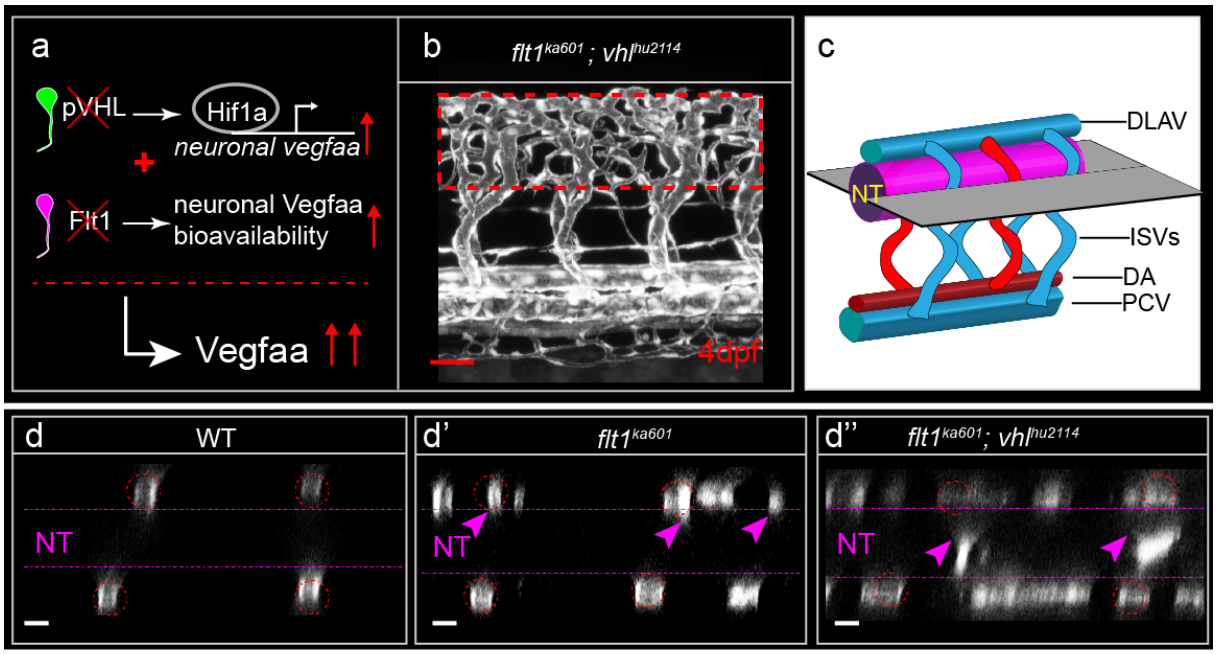

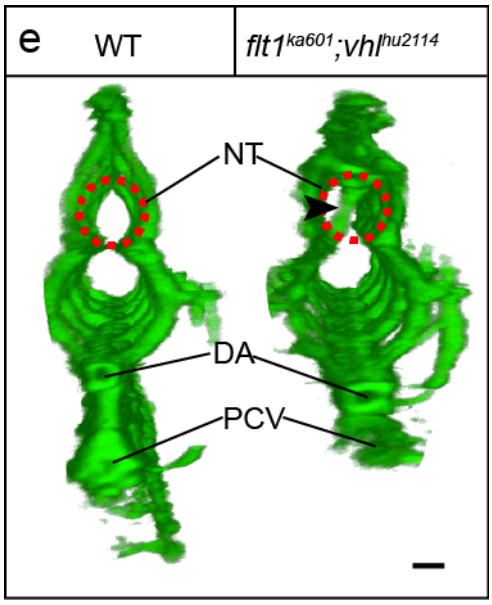

Figure 4-17. Massive *vegfaa* upregulation in *flt1*^{ka601};*vhl*^{hu2114} double mutants induces spinal cord sprout invasion.

(**a**) Schematic representation: loss of *vhl* augments *vegfaa* transcription, loss of *flt1* augments Vegfaa bioavailability; combining both mutants augments Vegfaa bioavailability above single mutant level. (**b**) Trunk vasculature in *flt1*^{ka601};*vhl*^{hu2114} double mutants at 4dpf. Note the severe hyperbranching at the level of the neural tube. (**c**) Schematic representation of optical section (shown in d'-d'') through the neural tube and associated trunk vasculature. (**d'-d''**) Dorsal view on optical section through WT (d), *flt1*^{ka601} (d'), and *flt1*^{ka601};*vhl*^{hu2114} double mutants (d''). Note invasion of sprouts into the neural tube in mutants (arrowheads in d', d''). Red circle indicates position of ISV, dotted line neural tube boundary. (**e**) Transverse 3D-rendered view of vasculature (green) through the trunk in WT (left panel) and *flt1*^{ka601};*vhl*^{hu2114} double mutants (right panel); note vessels penetrating the neural tube in mutant (compare vessel in dotted circle right panel, arrowhead; such vessels are absent in WT left panel). DA, dorsal aorta; PCV, posterior cardinal vein; NT, neural tube; f.c. fold change. Mutants are in *Tg(kdrl:EGFP)*^{s843} background. Scale bar, 50µm in b; 25µm in d-e.

4.3 Ectopic neurovascular networks in *flt1*^{ka601} and other Vegfaa gain-of-function scenarios originate from venous ISVs

The vascular spinal cord phenotype emerged around 2.5dpf with sprouts emanating exclusively from venous ISVs (Figure 4-18a,a'). Ectopic sprouts originating from arterial ISVs were never observed in *flt1*^{ka601} mutants (Figure 4-18a',b). Similarly, in *vhl*^{hu2117} and *ptena*$^{-/-}$*;ptenb*$^{-/-}$ mutants almost exclusively venous sprouts were observed (Figure 4-18a'',a'''). *PTEN* is a tumor suppressor gene acting as PI3K/AKT signaling attenuator and is linked to the progression of many tumors involving VEGF-A (Choorapoikayil et al. 2013).

To test if aISVs are generally responsive to Vegfaa, the trunk ISVs were exposed to high Vegfaa levels using either *flt1*^{ka601}; *vhl*^{hu2117} double mutants or inducible overexpression of *vegfaa* in neurons using a tamoxifen/endoxifen inducible Gal4ERt2/UAS system driven by the pan-neuronal promoter *huc* (also known as *elavl3*) (Figure 4-18b). The inducible system was used because early expression of sFlt1 or Vegfaa resulted in massive disturbance of vascular development and lethality. To make mosaic overexpression visible without disrupting Vegfaa function, the p2A peptide was used to co-express Vegfaa165 and eGFP. The expression was induced at 52 hpf, right after the vascular trunk network is formed. This time point was chosen to allow formation of an intersegmental network with venous ISV present and to recapitulate the endogenous *vegfaa* upregulation observed at a similar time point (see Figure 4-15a for endogenous expression of *vegfaa* and Figure 4-33a,e for schematic illustration of the Gal4ERt2/UAS system). Using neuronal *vegfaa* overexpression few arterial ectopic sprouts could be observed, although venous sprout numbers remained more than three fold higher (Figure 4-18b). These experiments illustrate that aISVs are generally responsive to Vegfaa but have a severely decreased angiogenic potential compared to venous ISVs.

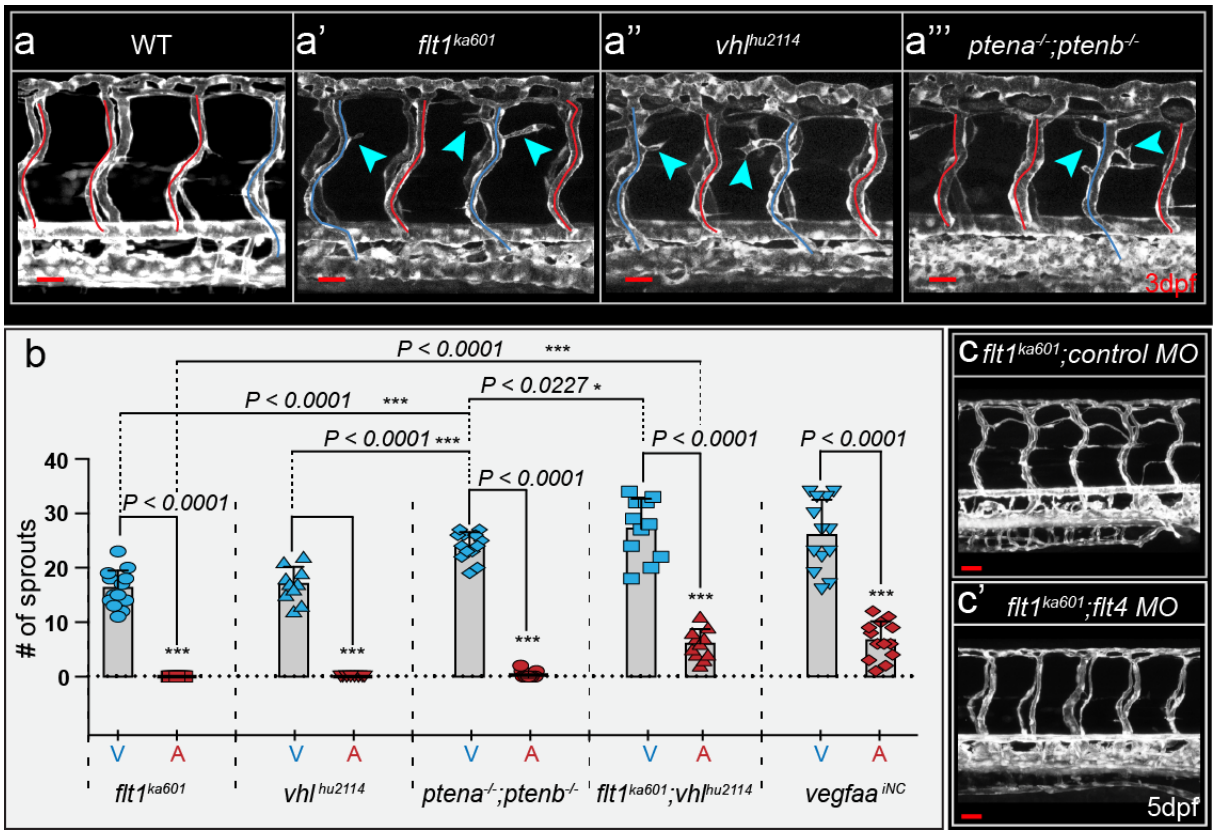

Figure 4-18. *flt1*^{ka601} mutants and *vegfaa* gain-of-function scenarios promote ectopic venous sprouting.

(**a-a'''**) Trunk vasculature at 3dpf in WT (a), *flt1*^{ka601} (a'), *vhl*^{hu2114} (a'') and *ptena*$^{-/-}$;*ptenb*$^{-/-}$ double mutants (a''') in *Tg(kdrl:EGFP)*^{s843} background. Note ectopic sprouts originate from vISVs (blue arrowheads) in mutants. aISVs indicated in red, vISVs in blue. (**b**) Quantification of ectopic sprouting in indicated mutants and inducible neuronal specific *vegfaa* gain-of-function. In all models ectopic sprouting preferentially occurs in veins, mean ± s.e.m, *n=13*. (**c-c'**) *flt1*^{ka601} mutants show hyperbranching and knockdown of *flt4* in *flt1*^{ka601} mutant rescues hyperbranching. MO, morpholino; vISV, intersegmental vein; aISV, intersegmental artery. Scale bar, 30µm in a-a''', 50µm in c-c'.

To verify if venous ISVs are necessary for hypersprouting in *flt1*^{ka601} mutants, venous ISV formation was blocked using a *flt4* morpholino knockdown approach. The Vegfc/Flt4 pathway drives venous sprouting and thus vISV formation is Vegfc/Flt4-dependent (Küchler et al. 2006; Hogan et al. 2009). Inhibiting either Vegfc or Flt4 leads to a phenotype displaying few or no vISVs, but with circulation mostly present up to 5dpf (Figure 4-19a). Depleting Flt4 in *flt1*^{ka601} mutants fully rescued the hypersprouting phenotype, stressing the imperative for the presence of veins to induce *flt1*^{ka601} sprouting (Figure 4-18c,c').

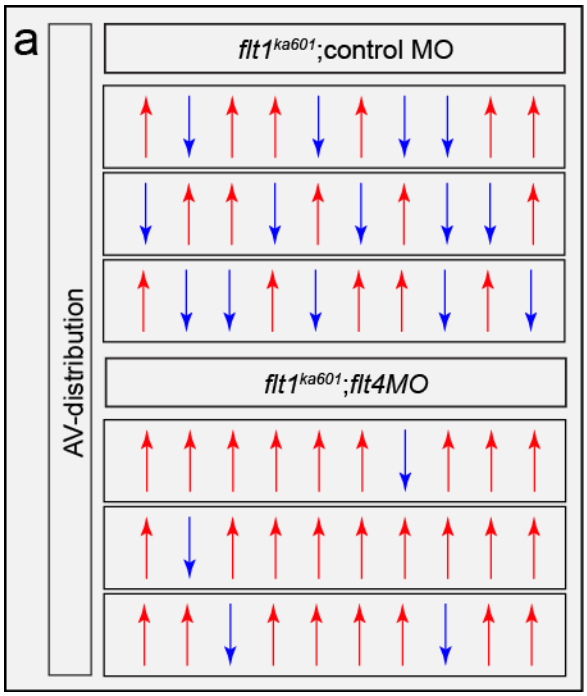

Figure 4-19. Venous ISV formation is required for *flt1*^{ka601} hypersprouting.

(**a**) Characterization of intersegmental blood flow characteristics in *flt1*^{ka601} (top panel) and *flt1*^{ka601} injected with *flt4* targeting morpholino (bottom panel). In *flt1*^{ka601} mutant ISVs carry both arterial (red arrow up) and venous (blue arrow down) flow and the artery/vein ratio is about 1. Upon loss of *flt4*, almost all investigated ISVs carry arterial flow consistent with *flt4* blocking remodeling of arteries into veins.

Accordingly, when the same experiment was repeated in *flt1*^{ka601}; *vhl*^{hu2117} double mutants *flt4MO*-mediated blockade of vein formation rescued only venous sprouting but not the few arterial sprouts present in *flt1*^{ka601}; *vhl*^{hu2117} double mutants (Figure 4-20a-c).

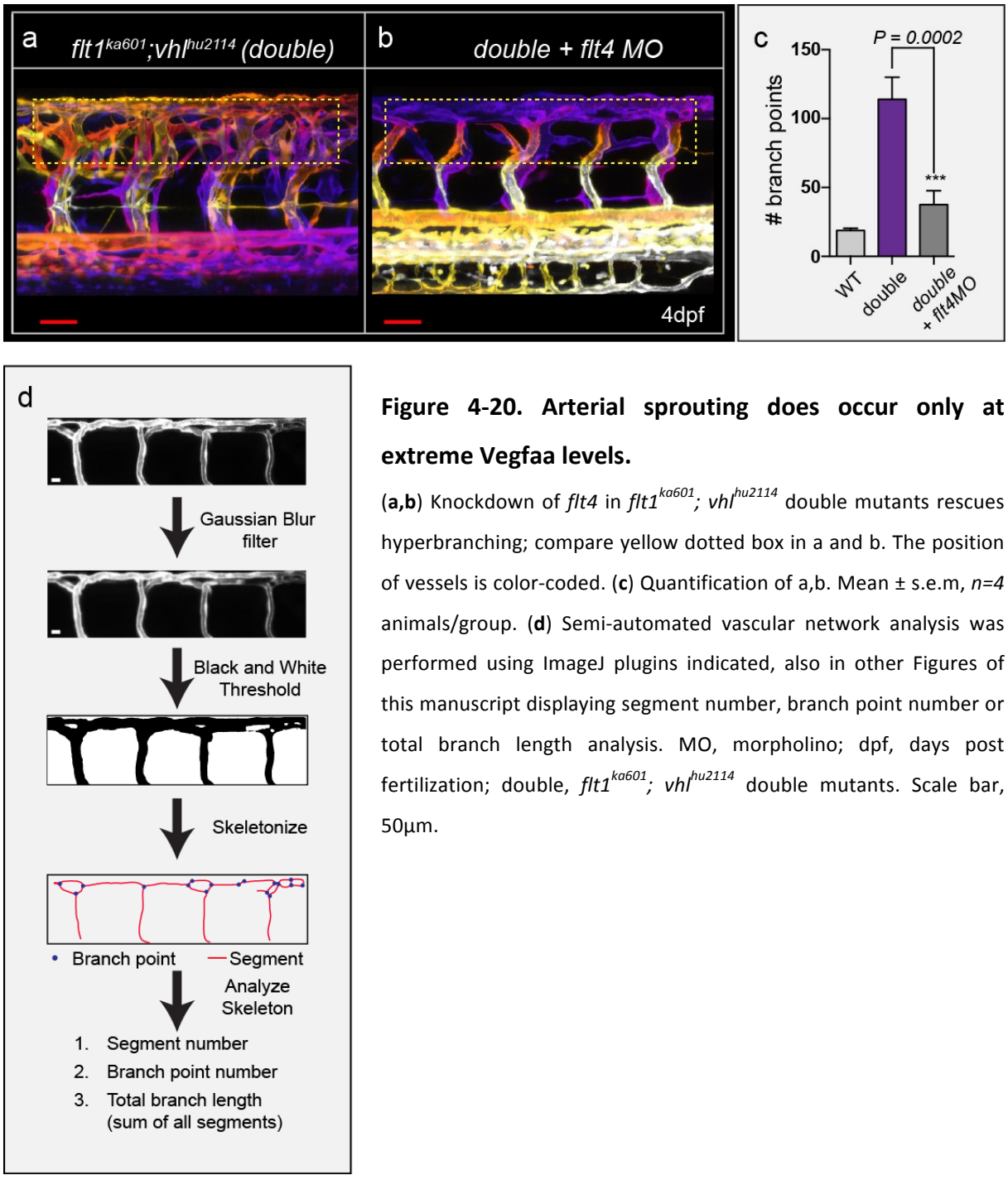

Figure 4-20. Arterial sprouting does occur only at extreme Vegfaa levels.

(**a,b**) Knockdown of *flt4* in *flt1*^{ka601}*; vhl*^{hu2114} double mutants rescues hyperbranching; compare yellow dotted box in a and b. The position of vessels is color-coded. (**c**) Quantification of a,b. Mean ± s.e.m, *n=4* animals/group. (**d**) Semi-automated vascular network analysis was performed using ImageJ plugins indicated, also in other Figures of this manuscript displaying segment number, branch point number or total branch length analysis. MO, morpholino; dpf, days post fertilization; double, *flt1*^{ka601}*; vhl*^{hu2114} double mutants. Scale bar, 50µm.

4.4 Ectopic sprouts in *flt1*^{ka601} mutants display distinctive angiogenic cell behaviors

Hyperactive ECs in the dorsal aspect of venous ISVs in *flt1*^{ka601} mutants extended sprouts, of which only ~55% generated patent connections whereas the remaining ~45% retracted (Figure 4-21c). From the population of patent ectopic venous sprouts ~95% formed an anastomosis with an aISV, whereas only ~5% made a connection with a vISV (Figure 4-21a-c).

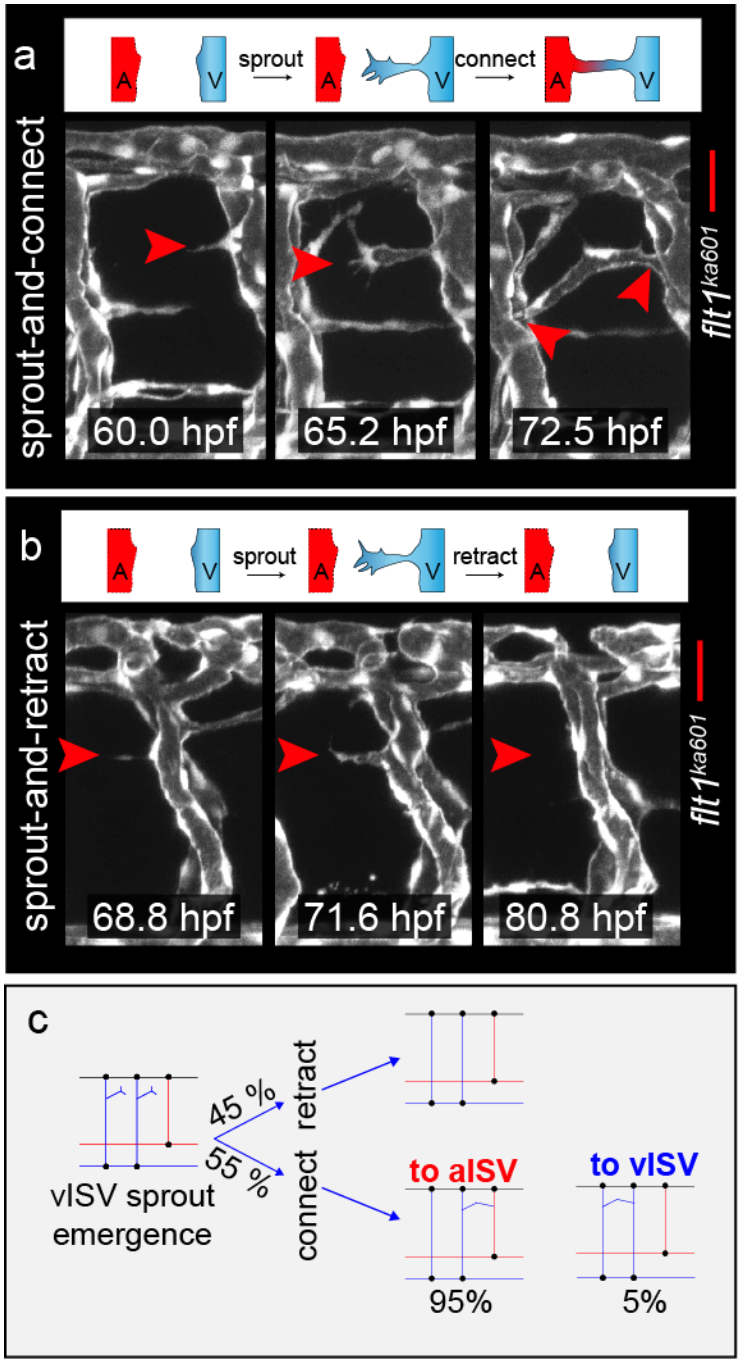

Figure 4-21. Sprouting kinetics in *flt1*^{ka601} hypersprouts.

(**a**) Time lapse imaging of sprout initiation and anastomosis formation in *flt1*^{ka601} mutant. Sprout initiation (60.0hpf), elongation (65.2hpf) and connection-anastomoses (72.5hpf) with adjacent aISV. (**b**) Time lapse imaging of sprout initiation and retraction in *flt1*^{ka601} mutant. ECs are hyperactive, produce filopodia (68.8hpf), extend a sprout (71.6hpf), which subsequently retracts (80.8hpf). (**c**) Quantification of data in a and b showing % of sprouts retracting (top part) or connecting (bottom part) to either aISV (red) or vISV (blue). In 45% of all sprouting events detected, filopodia formation and sprout initiation were followed by sprout retraction; in 55% of cases the sprout initiation was followed by sprout extension and connection with an adjacent ISV. From all these patent venous sprouts 95% made a connection with aISVs, whereas only 5% made a connection with vISVs. Sprouting behavior was analyzed in time-lapse confocal movies, *n=20* embryos. A, artery; V, vein; EC, endothelial cell. Scale bar, 30µm.

The clear preference for aISVs may have physiological relevance, since only connections with a blood pressure gradient promote blood flow perfusion. As the arteriovenous ratio in ISVs is roughly ~50% the likelihood that two veins are adjacent is ~25% thus the expected ratio would be ~25% venous anastomosis and ~75% arterial anastomosis (Isogai et al. 2003). In conclusion, venous anastomosis is greatly underrepresented suggesting a mechanism whereby angiogenic sprouts detect the pressure gradient, e.g. utilizing thin filopodia

interacting with adjacent vessels, enabling them to sense pressure gradients. The observed sprout filopodia-length ranged from 1-20µm and projected at an angle between 90°-120° with respect to the venous ISV, compatible with arterial anastomosis formation (Figure 4-22). Current models posit that sFlt1 secreted by sprouts forms a corridor to prevent back-sprouting and reconnection with their parent vessel (Chappell et al. 2009). Contradictory, *flt1* depleted sprouts retain their directionality and migrate away from their sprout initiation point (Figure 4-22c).

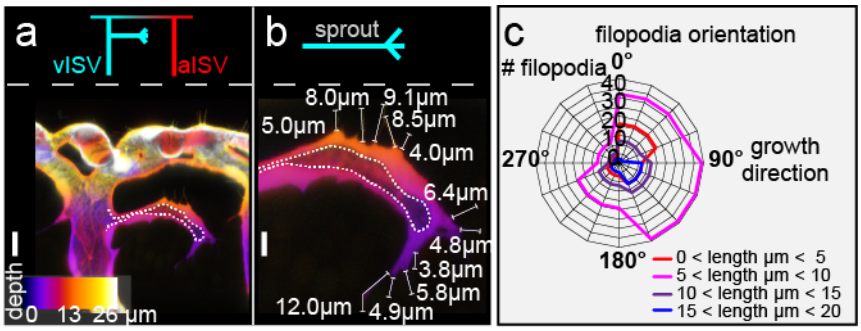

Figure 4-22. Flt1 is dispensable for sprout directionality.

(**a-c**) Filopodia directionality and length in *flt1*^{ka601} mutants (*n=10* embryos, *n=920* filopodia). Note that filopodia are oriented away from the sprout origin although Flt1 is absent (a,b). (**c**) Quantification of filopodia directionality. Note that the predominant direction is 120°, pointing to the ventral spinal cord which is rich in motor neurons and thus sFlt1 splicing in WT. aISV, intersegmental artery; vISV, intersegmental vein; Scale bar, 10µm (a) and 25µm (b).

4.4.1 Nuclear migration and positioning is linked to ectopic sprout initiation

Using the endothelial nuclear reporter line *Tg(fli1a:nGFP)*^{y7}, endothelial nuclear movements were carefully analyzed in *flt1*^{ka601} mutant ectopic sprouts. Remarkably, an association between nuclear positioning and sprout initiation was observed (Figure 4-23a-b). Nuclei migrated actively at velocities of up to 1µm·min^{-1} towards sprout initiation points (SIP) and in more than 80% of the sprout initiations studied, nuclear positioning was directly linked to sprout initiation (linkage was defined as nucleus-SIP distance of less than 5µm at sprout initiation) (Figure 4-23c,d). Nuclear migration is most studied in interkinetic nuclear migration behavior in neuroepithelia, but has never been described in endothelial cells nor was it linked to sprout formation (Del Bene 2011; Strzyz et al. 2015). Interestingly, these observations are in contrast to rearward nuclear positioning *in vitro* (Gundersen & Worman 2013) and were not described *in vivo* for primary or secondary sprouting events.

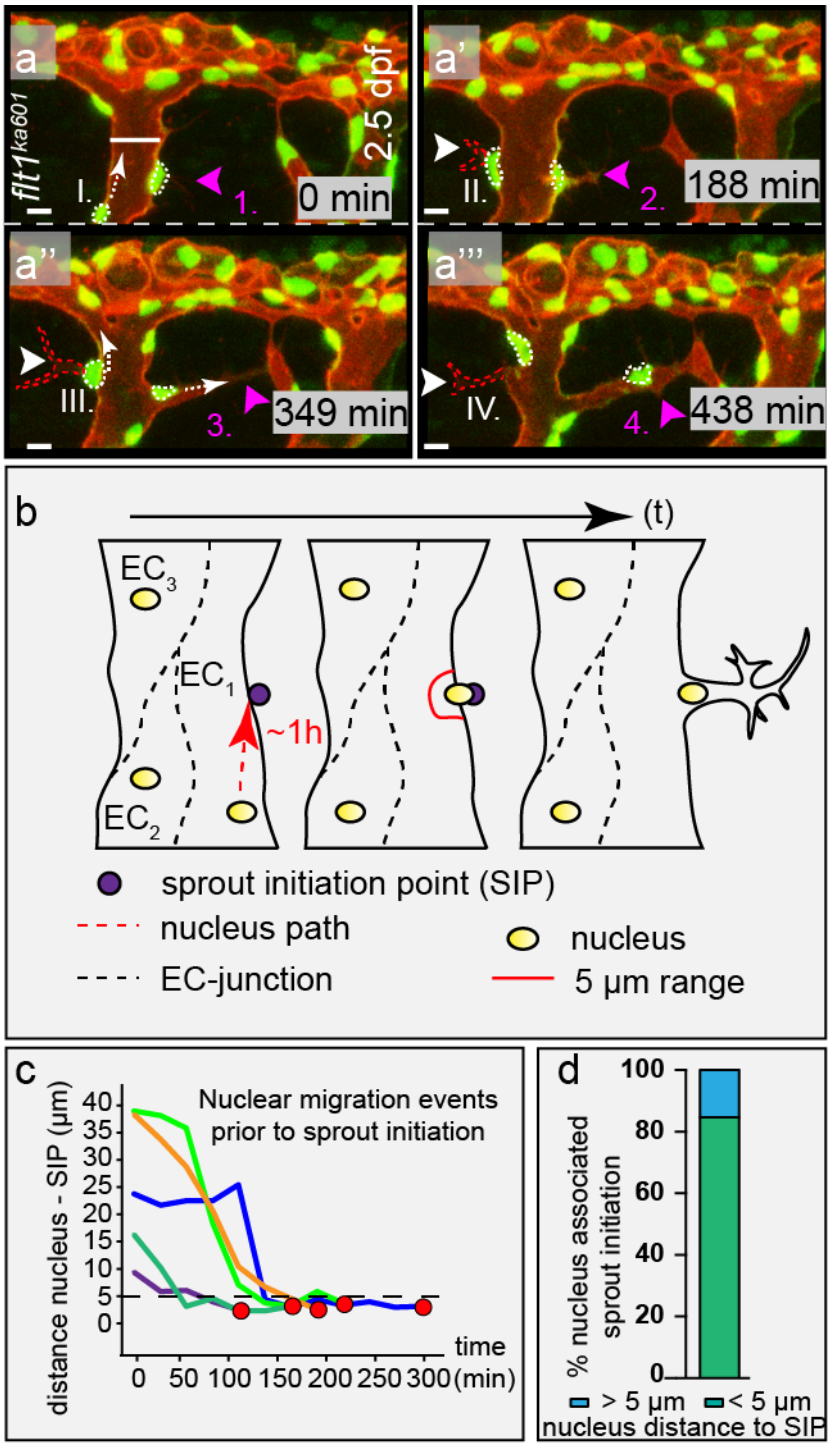

Figure 4-23. Nuclear positioning is associated with sprout initiation.

(**a'-a'''**) Time lapse imaging of endothelial nuclei in *Tg(fli1a:nGFP)*^{y7}*;Tg(kdrl:hsa.HRAS-mcherry)*^{s916} showing association between nuclear position and sprouting initiation point (SIP). Note that sprouts arise in close proximity to the position of the nucleus. Arrowheads indicate sprouts; nuclei at indicated time points (sprout initiation with actively migrating nucleus towards SIP I, II, III, IV, and nucleus already located at SIP 1,2,3,4). (**b**) Schematic representation of nuclear position with respect to SIP. (c,d) Quantification of observations in a-a'''. Red dot indicates sprout initiation time point. Note that sprouting preferentially occurs when endothelial nuclei are within less than 5µm from SIP. *n=5* (c) and *n=13* (d). SIP, sprout initiation point. Scale bar, 10µm.

Next, the proliferation rate in *flt1*^{ka601} mutants was evaluated. The cell numbers were markedly increased in *flt1*^{ka601} mutants, indicative of increased endothelial proliferation (Figure 4-24).

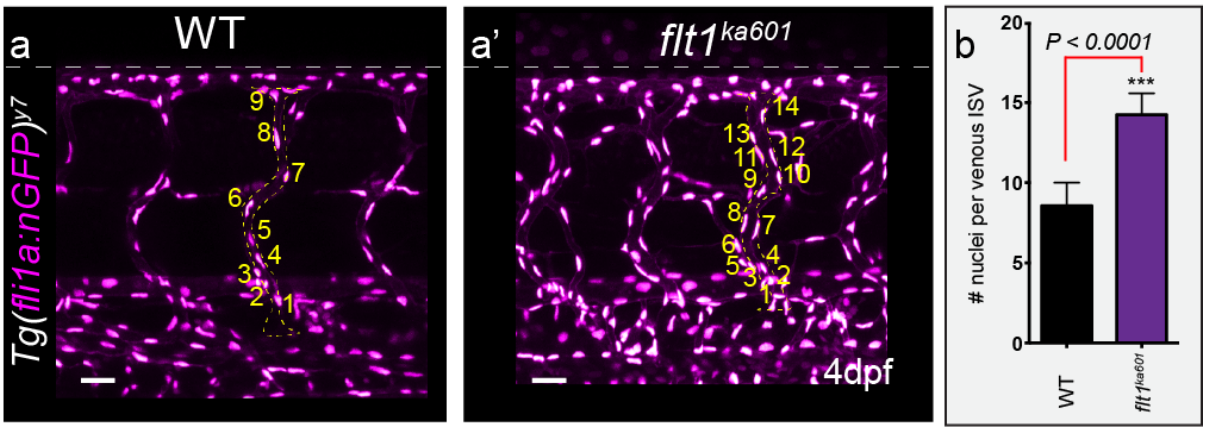

Figure 4-24. *Flt1*^{ka601} mutants display increased nuclear numbers.

(**a,a'**) Representative images of EC nuclei in vISVs of WT and *flt1*^{ka601} embryos at 4dpf. (**b**) Quantification of nuclei # in vISVs displayed as mean ±s.e.m, *n=21*. ISV, intersegmental vessel. Scale bar 50µm.

4.5 *flt1*^{ka601} ectopic sprouts are blood flow dependent

Primary sprouting is not dependent on blood flow, as blockade of heartbeat and blood flow does not prevent aISV formation (Watson et al. 2013). To test whether *flt1*^{ka601} sprouts are also resistant to loss of blood flow, the heartbeat was stopped using 2,3-Butanedione monoxime (BDM) or 2.5x Tricaine at 48hpf and sprout formation was analyzed at 4dpf. Surprisingly, depletion of blood flow using either approach completely prevented ectopic sprout formation in *flt1*^{ka601} mutants ((Figure 4-25).

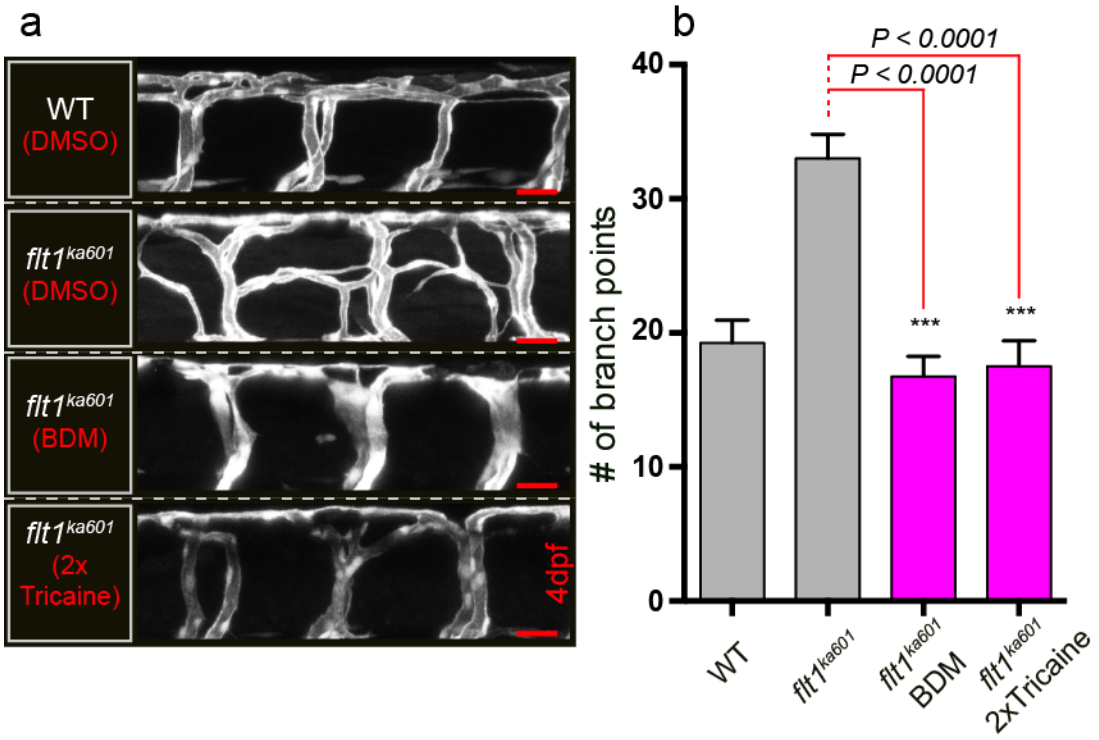

Figure 4-25. *Flt1*^{ka601} hypersprouting is blood flow dependent.

(**a**) Blood flow blockade using BDM or Tricaine prevents sprout formation at the level of the spinal cord in *flt1*^{ka601} mutants. Representative images of the dorsal part of ISVs at 4dpf (neural tube level). (**b**) Quantification of sprout formation under indicated conditions at 3dpf. Note that sprout formation is completely abolished under loss of flow (BDM) or deceleration of flow (Tricaine) conditions. ISV, intersegmental vessel; dpf, days post fertilization; BDM, 2,3-Butanedione monoxime. Scale bar, 20µm.

4.5.1 Ectopic *flt1*^{ka601} sprouts originate from remodeled arterial or purely venous ECs

To elucidate the endothelial identity of hyperactive, sprout initiating endothelial cells, *Tg(flt1*^{enh}*:tdTomato); Tg(flt4:mCitrine)*^{hu7135} double transgenics were analyzed. *Tg(flt1*^{enh}*:tdTomato)* is specifically expressed in arteries, whereas *Tg(flt4:mCitrine)*^{hu7135} is enriched in veins but is also expressed at somewhat lower levels in aISVs.

In the dorsal aspect of vISVs from *flt1* morphants, *Tg(flt1*^{enh}*:tdTomato)* positive as well as *Tg(flt1*^{enh}*:tdTomato)* negative hyperactive ECs were identified (Figure 4-26a-c). Thus, both venularized arterial ECs and purely venous ECs (originating from the PCV) can give rise to ectopic sprouts in *flt1* loss-of-function scenarios. This suggests, that not the EC origin but the position and exposure to factors differing between arteries and veins are critical to determine the angiogenic potential of ECs (Figure 4-26a-c).

The finding that sprouts typically originate at the dorsal aspect of vISVs in *flt1*^{ka601} mutants is in contrast to the current opinion of vISV formation in zebrafish (Bussmann et al. 2010). It is widely excepted, that secondary sprouts connect to aISV which are eventually remodeled into vISVs resulting in an hybrid vessel with ventral venous origin and dorsal arterial origin (Bussmann et al. 2010). To test this model, a photoswitchable *Tg(kdrl:nlskikGR)*^{hsc7} transgenic reporter line was utilized. Venous ECs were switched from green-kikGR to red-kikGR using UV light to allow cell tracking of venous ECs from the PCV. Time-lapse imaging identified that photoswitched red-kikGR venous ECs form secondary sprouts, anastomose with an aISV forming a vISV and subsequently migrate dorsally, proliferate and displace all, most or some of the venularized arterial ECs. This PCV-derived EC behavior explains that both *flt1*$^{+}$ (venularized arterial ECs) and *flt1*$^{-}$ (purely venous ECs from the PCV) sprouts can be observed (Figure 4-26d-e). Noteworthy, careful tracking of EC migration events revealed that vECs^{PCV} migrate against the flow direction dorsally into the vISVs whereas v_aECs^{ISV} never migrate ventrally into the PCV.

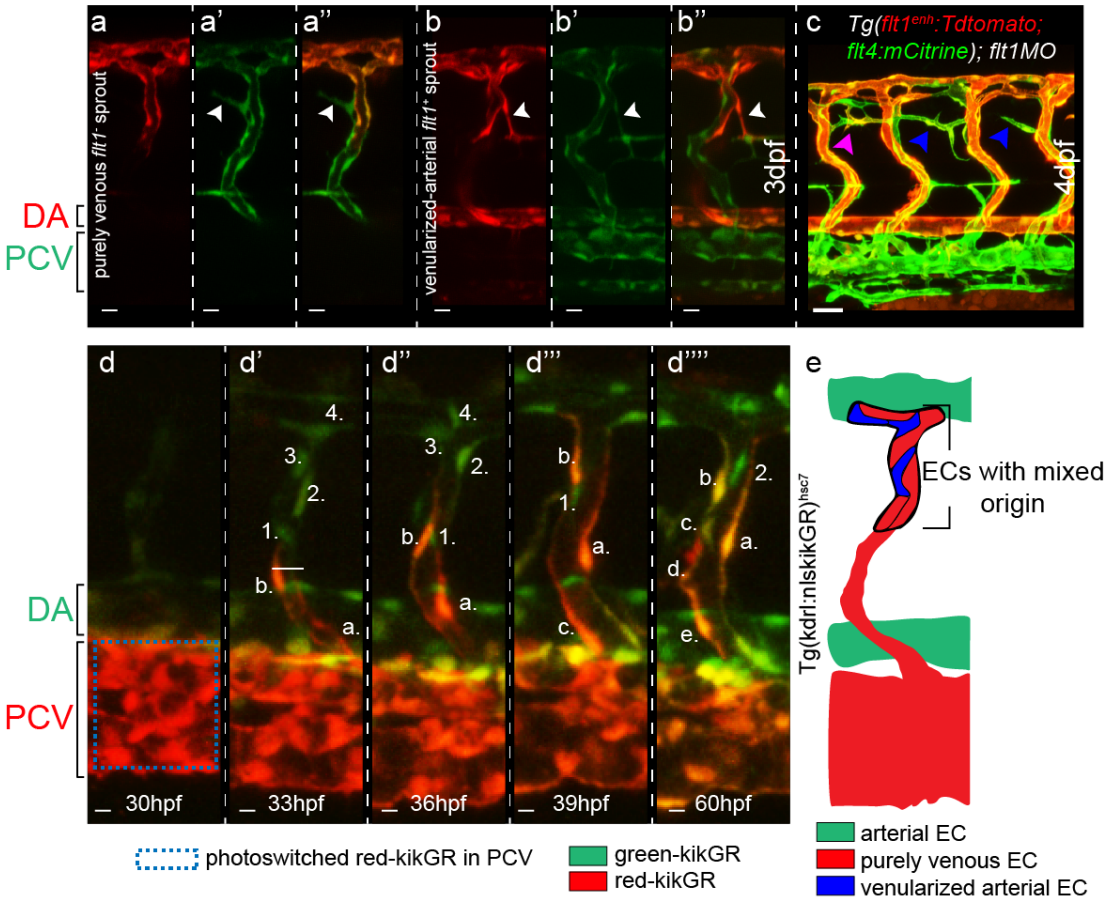

Figure 4-26. *Flt1*^{ka601} hypersprouts originate from both, venularized and purely venous ECs

(**a-a''''**) Time-lapse imaging of nuclear migration in *Tg(kdrl:nlskikGR)*^{hsc7} after photoswitching of venous ECs in the PCV. Venous ECs in the PCV were switched at 30 hpf just prior to secondary vein formation, and migration of purely venous PCV ECs was followed up to 60hpf. Note that ECs with PCV origin migrate up to the DLAV and that the dorsal venous ISV has mixed origin, consisting of purely venous ECs (marked with letters - red or yellow cells) and venularized arterial ECs (marked with numbers – green cells). (**b**) Schematic illustration of a venous ISV with mixed EC origin at the dorsal aspect. Venularized arterial EC in blue and purely venous ECs in red. (**c**) Time-lapse imaging of *Tg(flt1*^{enh}*:tdtomato);Tg(flt4:mCitrine)*^{hu7135} injected with *flt1MO* showing that both populations, venularized arterial ECs and purely venous ECs can give rise to ectopic sprouts. EC, endothelial cell; PCV, posterior cardinal vein; DA, dorsal aorta; hpf, hours post fertilization; dpf, days post fertilization. Scale bar a-a'''', 10µm, c.

4.5.2 Spinal cord vascularization in WT larvae involves venous sprouting

Spinal cord vascularization has been described only fragmentary in zebrafish (Okuda et al. 2012). Time-lapse imaging and careful counting of sprouts showed that normal vascularization occurs similarly in WT zebrafish larvae as in *flt1*^{ka601} mutants but at a

considerably later time point. From 12-15dpf sprouts originate mostly from venous ISVs (more than 90%) and laterally vascularize the spinal cord without invading it (Figure 4-27c). This vascularization is completed at 20dpf and is congruent with the *flt1*^{ka601} sprouting behavior at 2.5dpf (Figure 4-3c''). At later developmental stages the spinal cord is possibly also internally vascularized similar to spinal cord neurovascular development in mice (James et al. 2009).

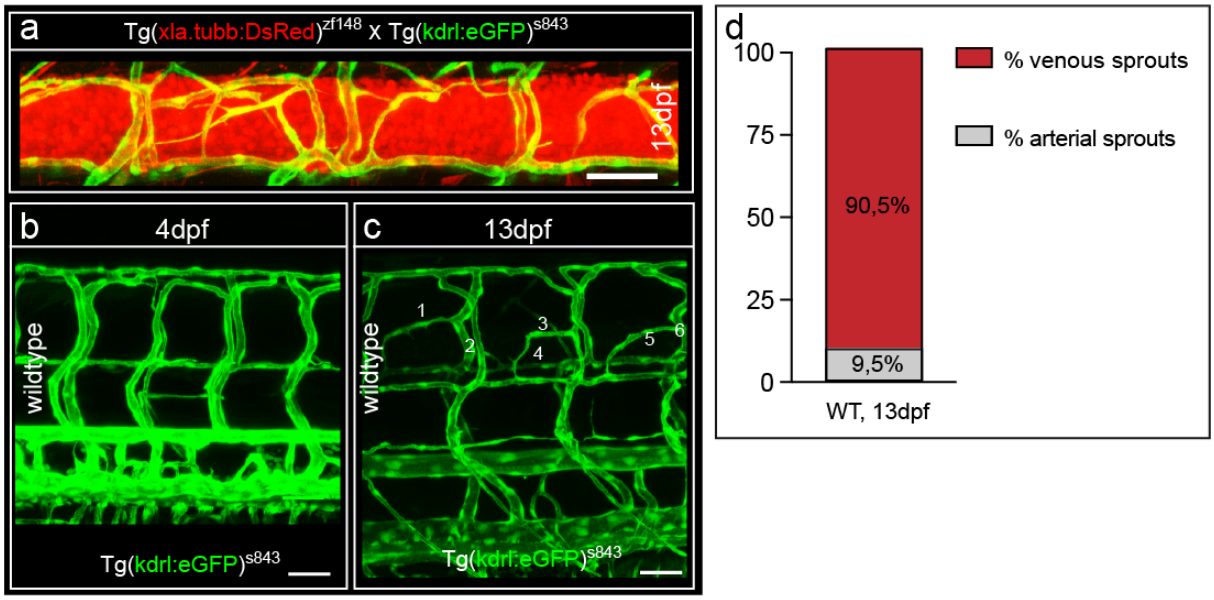

Figure 4-27. Spinal cord vascularization in WT larvae occurs from the venous side.

(**a**) The spinal cord is laterally vascularized between 11-15dpf from mostly venous ISVs. Spinal cord neurons in red, and ECs in green. (**b**) WT ECs lacking spinal cord vasculature at 4dpf. WT embryos do not show spinal cord vascularization prior to 11 dpf. (**c**) Representative image of the trunk vasculature with spinal cord vasculature marked with numbers. (**d**) Quantification of spinal cord vasculature sprout origin in WT at 13dpf. Note that most sprouts originate from venous ISVs. ISV, intersegmental vessel; dpf, days post fertilization. Scale bar 50µm. Sprout counting and imaging were performed by Alina Klems.

4.5.3 Notch related genes are not deregulated in *flt1*^{ka601} mutants

Various marker genes enriched in angiogenic tip cells have been described (Herbert & Stainier 2011). Genes downstream of Dll4/Notch1a signaling are strongly associated with tip- and stalk cell identity (Leslie et al. 2007; Herbert & Stainier 2011). Other markers such as *esm1*, which is known to increase VEGF bioavailability and *angpt2*, with poorly characterized tip cell function, are known tip-cell markers (del Toro et al. 2010; Rocha et al. 2014). To

transcriptionally profile sprout characteristics, the transcriptome of *flt1*^{ka601} mutants was analyzed using RNA sequencing and differentially regulated genes were identified. As expected, tip cell markers such as *angpt2a* and *esm1* were strongly upregulated (Figure 4-28a-c) whereas *notch* related genes such as *dll4*, *notch1a, nrarpa/b* and *hey/hes* were surprisingly not differentially regulated in *flt1*^{ka601} mutants (Figure 4-28b) (del Toro et al. 2010). This finding is in line with the observation that ectopic sprouts in *flt1*^{ka601} mutants originate from venous ECs, which were shown to have low or absent notch signaling (Quillien et al. 2014). The secreted Esm1 protein, according to its function in mice, would further increases Vegfaa levels (Rocha et al. 2014). This positive feedback loop would thus further increase Vegfaa bioavailability in *flt1*^{ka601} mutants.

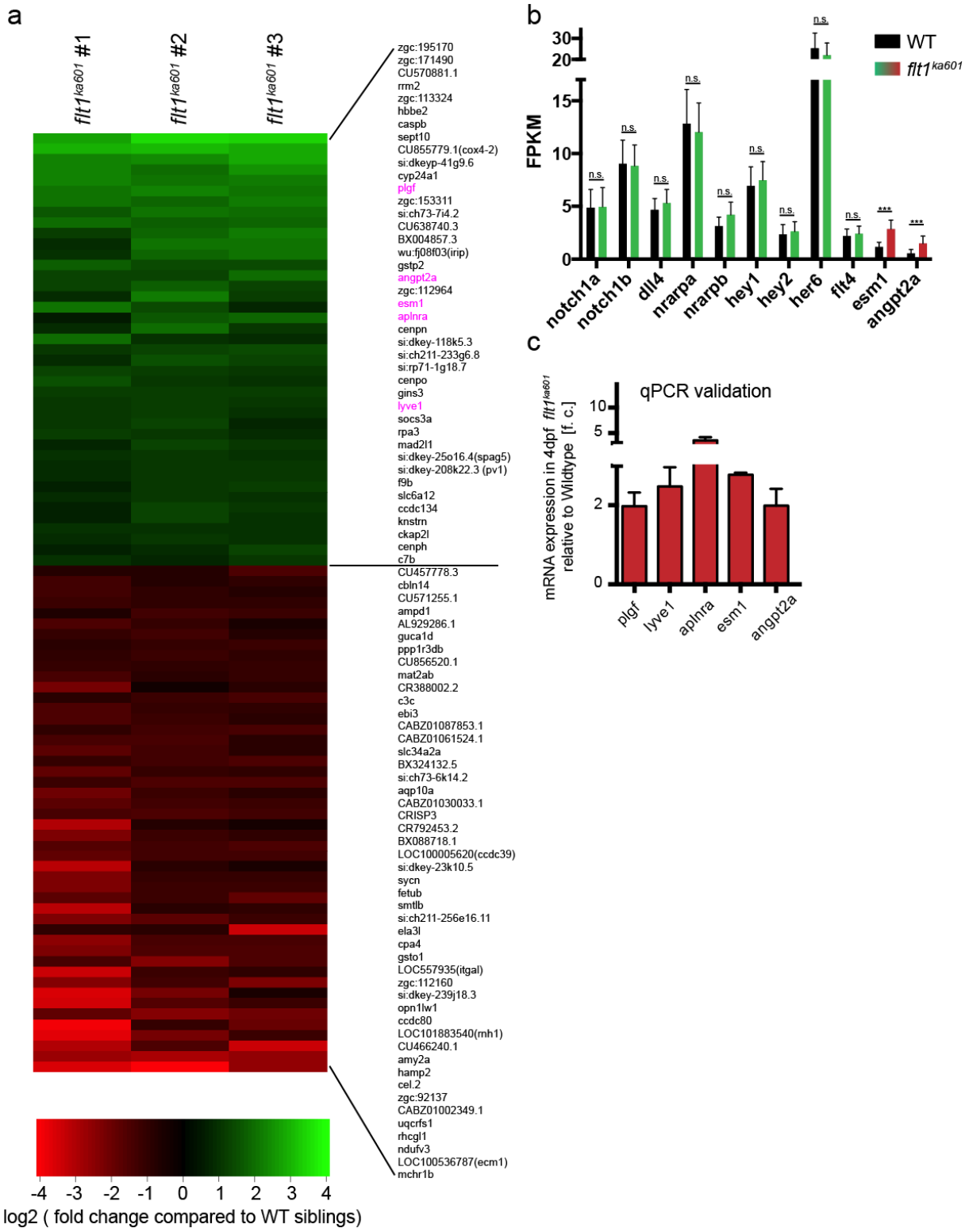

Figure 4-28. RNAseq analysis and qPCR validation of *flt1*^{ka601} mutants.

(**a**) Heat map showing deregulated genes defined as ≥ 2 fold significantly regulated *(P< 0.05)* with two independent methods (DEseq and Cuffdiff) from three independent biological replicates. Upregulated genes in green, downregulated genes in red. (**b**) qPCR validation of indicated genes identified as differentially expressed between WT and *flt1*^{ka601} mutants in RNAseq experiment at 4dpf. (**c**) Expression of known regulators of the tip-stalk cell identity. Note that expression of relevant genes, thought to be involved in tip cell formation are not altered in flt1ka601 mutants, although increased number of tip cells can be derived from elevated esm-1 and

angpt2a levels. F.c., fold change; dpf, days post fertilization; FPKM, Fragments Per Kilobase of exon per Million fragments mapped.

4.6 Artery-vein differences in Vegfaa responsiveness can be explained with notch

One major difference between arteries and veins is their Notch signaling status. NOTCH has been described as an activator or repressor of sprouting depending on the organ (Suchting et al. 2007; Ramasamy et al. 2014). The anti-angiogenic actions of NOTCH have been mostly attributed to FLT1, which is downstream of NOTCH signaling. To test if Notch signaling is anti-angiogenic in arterial ISVs, possibly explaining the discrepancy in angiogenic potential between aISVs and vISVs, Notch was inducibly depleted specifically in aISVs utilizing the dominant negative truncated fusion protein DN-Maml-GFP (Figure 4-29a-c) (Zhao et al. 2014). The inducible gal4ERt2 was driven using an arterial specific *flt1* enhancer promoter construct (Bussmann et al. 2010). Gal4ERt2 induction at 52hpf could be traced with the MAML-GFP signal in arterial ECs in *flt1*^{ka601} mutants. Remarkably, DN-Maml-GFP positive arterial ISVs, which have blocked notch signaling, emanated sprouts similar to vISVs in *flt1*^{ka601} mutants, albeit, at four fold decreased levels compared to venous ISVs (Figure 4-29a-c). This finding suggests that Notch is a strong negative regulator of sprout formation in arteries, independent of Flt1. Notably, in this experiment Notch signaling was inhibited in a mosaic fashion, hence incomplete Notch signaling deactivation cannot be excluded. Therefore, it is not surprising that sprouting levels in vISVs are higher than in aISVs even though their sprouting potential may be similar under *notch* loss-of-function conditions. It is known that NOTCH exhibits anti-angiogenic effects but that notch can be repressive even in the absence of its major effector FLT1 is novel (Suchting et al. 2007; Funahashi et al. 2010; Jakobsson et al. 2010). Moreover, ectopic venous sprout numbers did not differ between *flt1*^{ka601} mutants and arterial DN-Maml gain-of-function *flt1*^{ka601} mutants (Figure 4-29c), which is in line with Notch signaling being restricted to aISVs (Quillien et al. 2014).

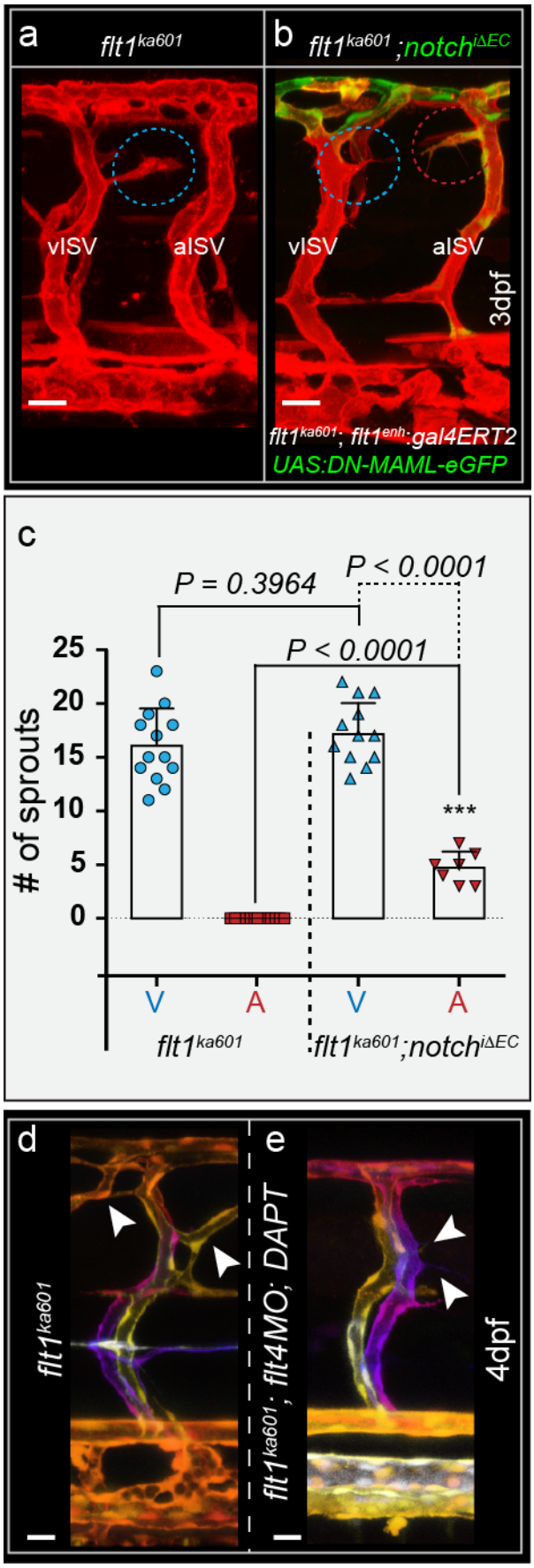

Figure 4-29. Inhibiting Notch partially restores arterial sprouting

(**a**) *flt1*^{ka601} mutants show ectopic venous sprouts (blue circles), but no arterial sprouts. (**b**) Inhibiting arterial Notch by endoxifen-induced arterial ISV specific expression of dominant negative *MAML* (Notch ^{iΔEC}) at 52hpf under control of the *flt1*^{enh} promoter in *flt1*^{ka601} mutant results in the emergence of ectopic arterial sprouts (red circles). (**c**) Quantification of experiments in (a,b), mean ± s.e.m, *n=7*. (**d,e**) Comparison of *flt1*^{ka601} mutant (d) with *flt1*^{ka601} mutant injected with *flt4* targeting morpholino and treated with notch inhibitor DAPT (e). Note that in *flt1*^{ka601}, *flt4* MO embryos, inhibition of notch with DAPT does not induce patent sprouts (only few filopodial extensions – arrowheads in (e), although *flt1* and Notch signaling are absent in arteries (e), *n=3* embryos. MO, morpholino; vISV, intersegmental vein; aISV, intersegmental artery; Notch ^{iΔEC}, inducible ISV specific loss of notch; A, artery; V, vein; dpf, days post fertilization. Scale bar 25µm.

To substantiate these data the gamma-secretase inhibitor DAPT was used to inhibit notch signaling in *flt1*^{ka601}; *Flt4MO* injected embryos (Figure 4-29d,e). These embryos have mostly aISVs and displayed even without arterial Notch signaling only mild filopodia and ectopic sprout induction with only few patent connections formed. These results substantiate that Notch negatively regulates the sprouting potential of aISVs.

4.7 Neuronal sFlt1 and Vegfaa determine angiogenic sprouting at the neurovascular interface

Flt1 and *vegfaa* are expressed in spinal cord neurons and not only *flt1*$^{+}$ venularized arterial ECs but also *flt1*$^{-}$ purely venous ECs contribute to the vascular hypersprouting (Figure 4-26). These *flt1*$^{-}$ ECs never expressed *flt1* during development but generate hypersprouts at the spinal cord in *flt1*^{ka601} mutants (Krueger et al. 2011). This strongly suggests a non-cell autonomous neuronal Flt1 function. To validate the possibility that indeed not the lack of vascular Flt1 but neuronal Flt1 is sufficient to explain the hypersprouting phenotype in *flt1*^{ka601} mutants, neuronal specific *flt1* mutants (*flt1*$^{\Delta NC}$) were generated using a CRISPR/Cas-mediated KO approach (Ablain et al. 2015). *Cas9* was expressed in neurons using the strong pan-neuronal promoter *xla.tubb* driving Gal4-VP16 to amplify the expression of UAS:Cas9-t2A-eGFP and allowing visualization of potential KO cells (Figure 4-30b). The same *flt1* specific sgRNA as used to generate *flt1*^{ka601} mutants targeting *flt1* exon 3, was expressed under the control of a ubiquitously expressed zebrafish U6 promoter (Ablain et al. 2015). To increase the likelihood of a biallelic KO, *flt1*$^{ka601/+}$ heterozygous mutants were used for the tissue-specific knockout experiment. In heterozygous *flt1*$^{ka601/+}$ mutants, rarely single ectopic sprouts can be observed, suggesting that Vegfaa levels in heterozygous mutants are close to the sprouting threshold (Figure 4-3b'''). Mosaic expression of *Cas9* and *sgRNA*^{flt1E3} resulted in massive induction of hypersprouting reaching almost comparable sprouting levels as in *flt1*^{ka601} mutants (compare Figure 4-30a and a''). This experiment strongly suggests, that neuronal Flt1 is necessary and sufficient to prevent spinal cord lateral hypervascularization.

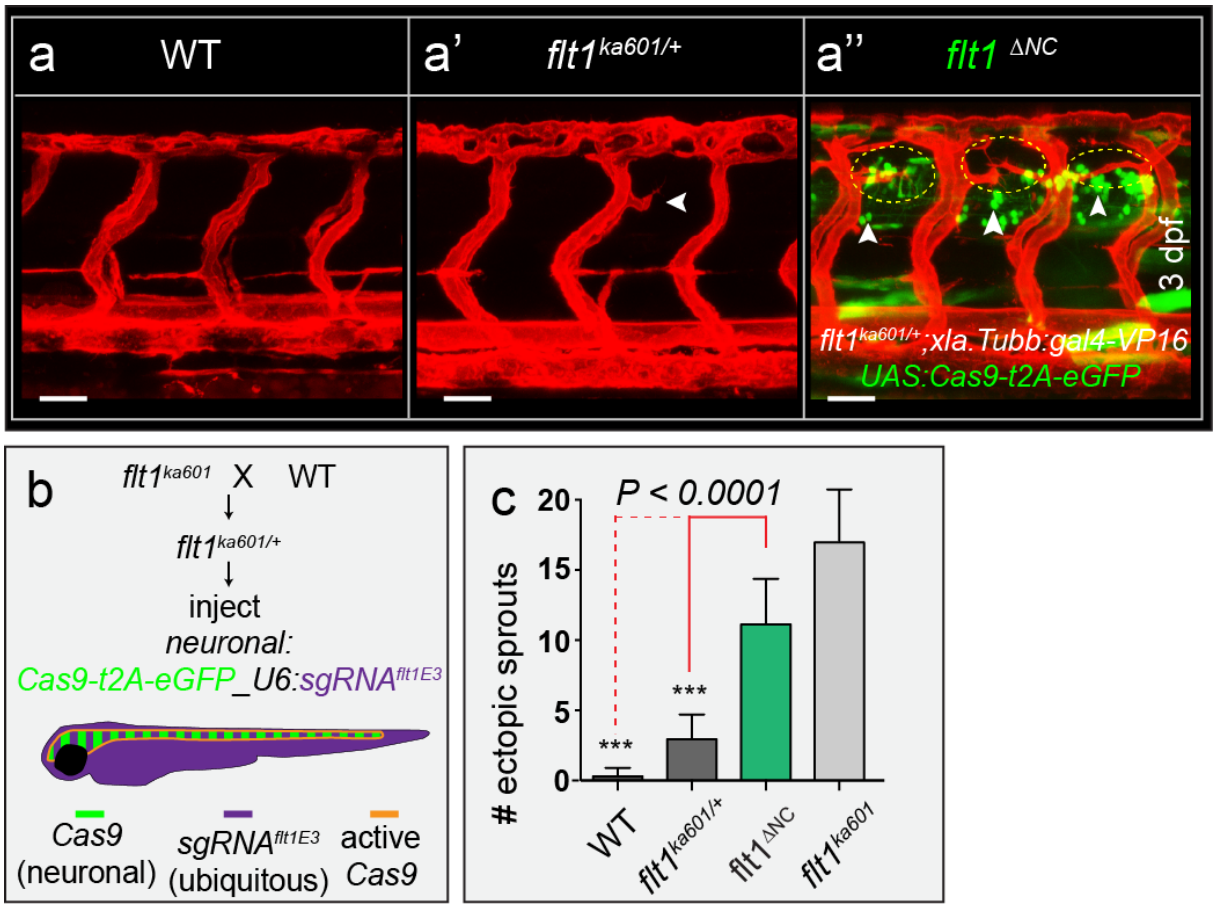

Figure 4-30. Loss of neuronal flt1 induces spinal cord vascularization.

(**a-a''**) Neuron-specific loss of *flt1* (*flt1*$^{\Delta NC}$) induces ectopic sprouting (e'', sprouts in yellow dotted ellipse), arrowheads indicate neuronal cells with Cas9 expression. (**b**) Approach for generating a neuron-specific *flt1* mutant. Cas9 was expressed under control of neuronal promoter *XIa.Tubb*; sgRNA was expressed ubiquitously, resulting in Cas9 activity in neuronal cells of *flt1*$^{ka601/+}$ only (domain marked by orange border). Heterozygous *flt1*$^{ka601/+}$ were used to facilitate biallelic knockout. (**c**) Quantification of ectopic sprouting for indicated genotypes. Note that neuron-specific loss of *flt1* significantly augments ectopic sprouting (green bar) mean ± s.e.m, *n=16* embryos. *flt1*$^{\Delta NC}$, neuron specific loss of *flt1*; dpf, days post fertilization. Scale bar, 50µm.

4.7.1 Transplanted *flt1*^{ka601} neurons but not ECs are competent to induce hypersprouting

To substantiate the results obtained from the tissue specific neuronal *flt1* knockout experiment, blastula cell transplantations were performed (Figure 4-31a) (Kemp et al. 2009). Undifferentiated cells from *flt1*^{ka601}; *Tg(kdrl:EGFP)*^{s843} donor blastulas were transplanted close to the margin into mesodermal regions (ECs) or in the middle between animal pole and margin into ectodermal regions (spinal cord neurons) of *Tg(kdrl:hsa.-HRAS-mcherry)*^{s916} wild type hosts (Figure 6-31a). Obtained mosaic zebrafish embryos were assayed for the emergence of ectopic sprouts as observed in *flt1*^{ka601} mutants at 4dpf. Remarkably,

transplantation of high numbers of *flt1*^{ka601} neuronal cells resulted in ectopic venous sprouting as observed in *flt1*^{ka601} mutants (Figure 6-33b). In contrast, transplantation of ECs did not result in ectopic sprout formation suggesting that *flt1* depletion in ECs is not sufficient to induce hypersprouting (Figure 6-33c). In summary, these data further substantiate that neuronal cells are the relevant source of Flt1 and that vascular Flt1 is dispensable for early sprouting angiogenesis in zebrafish.

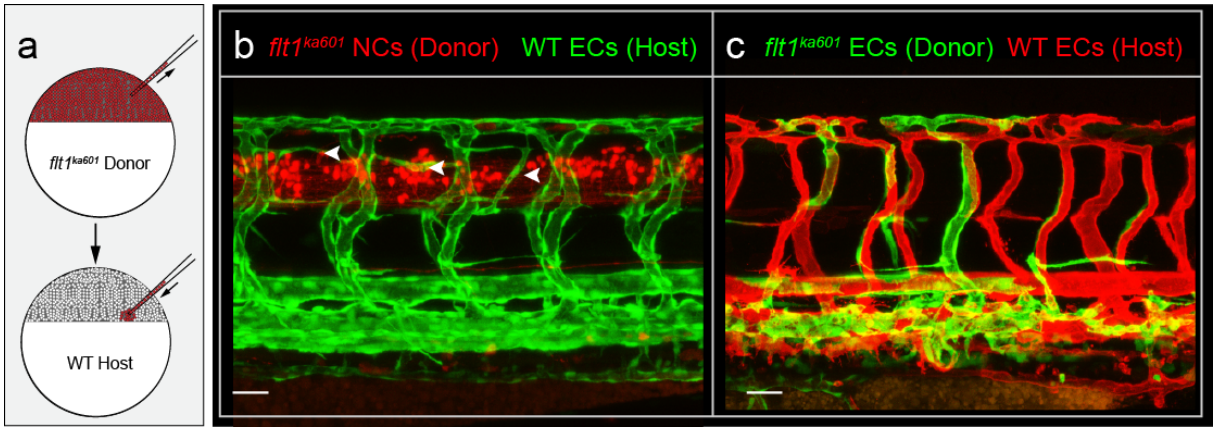

Figure 4-31. Transplantation of *flt1*^{ka601} NCs but not ECs induces ectopic sprouting.

(**a**) Schematic illustration of transplantation of 50-100 cells from a *flt1*^{ka601} Donor to a WT host. (**b**) Transplantation of NCs (red) from a *flt1*^{ka601} donor to a WT host (green ECs) induces ectopic hypersprouting at the level of the neural tube, white arrow heads. 4dpf. (**c**) Transplantation of ECs (green) from a *flt1*^{ka601} donor to a WT host (red ECs) does not induce ectopic sprouting, 4dpf. EC, endothelial cell; NC, neuronal cell. Scale bar, 20µm.

4.8 Neuronal soluble Flt1 controls spinal cord vascularization

mflt1^{ka605} and neuronal specific *flt1* KO analysis suggest that indeed neuronal sFlt1 and not mFlt1 is the major regulator of spinal cord vascularization in the zebrafish trunk. To examine if neuronal *sflt1* expression is sufficient to explain the venous spinal cord hypersprouting phenotype in *flt1*^{ka601} mutants, *sflt1* was overexpressed in spinal cord neurons using the pan-neuronal xenopus beta-tubulin promoter *xla.tubb*. Overexpression of even trace amounts of neuronal *sflt1* during early zebrafish development completely abolished ISV formation (Figure 4-32e). To circumvent impaired ISV-formation, an inducible approach using the Gal4ERt2/UAS system was utilized and activated after ISV remodeling at 52hpf (see Figure 4-32a for Gal4ERt2/UAS system and Figure 4-32e for experimental design). Strikingly, even few

sFlt1 expressing spinal cord neurons were sufficient to rescue *flt1*^{ka601} spinal cord hypervascularization (Figure 4-32b-c). This experiment demonstrates that even trace amounts of neuronal sFlt1 are sufficient to keep the neural tube avascular.

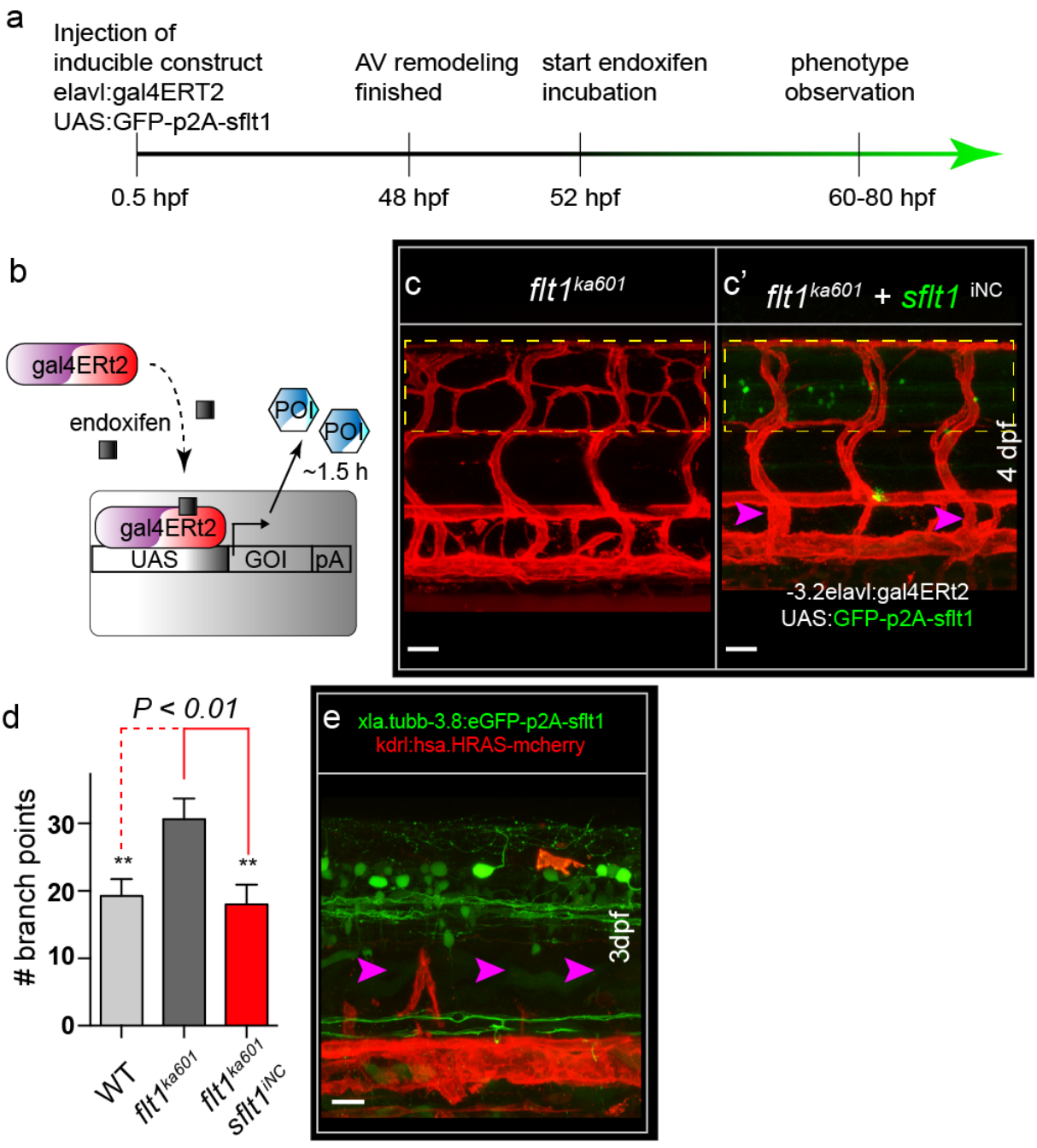

Figure 4-32. Neuronal sFlt1 gain-of-function rescues *flt1*^{ka601} hypersprouting.

(**a**) Schematic of injection, expression induction and observation. (**b**) Schematic representation of endoxifen inducible gain-of-function approach in zebrafish. In the present situation Gal4 is under the control of neuron-specific promoters *elavl* or *xla.tubb*. Expression can be observed within 1.5hrs upon endoxifen application. (**c**) Hyperbranching in *flt1*^{ka601} mutants (dotted box). (**c'**) Endoxifen inducible neuron specific *sflt1* gain-of-function rescues hyperbranching in *flt1*^{ka601} mutants; compare dotted box in b' and b. Purple arrowheads indicate vISVs;

endoxifen was applied at 52hpf. (**d**) Quantification of rescue in (c,c'), mean ± s.e.m, *n=5* embryos. (**e**) Non-inducible overexpression of sflt1 in neurons prevents ISV formation, rendering analysis impossible. GOI, gene of interest; POI, protein of interest; flt1iNC, inducible, neuronal cell specific gain-of-function; ΔNC; dpf, days post fertilization. Scale bar, 50µm.

4.9 Neuronal Vegfaa drives spinal cord vascularization in *flt1*^{ka601} mutants

To prove that neuronal Vegfaa promotes hyperbranching in *flt1*^{ka601} mutants, inducible neuronal *vegfaa*165 gain-of-function zebrafish were generated. Expression was initiated by adding endoxifen at 52hpf immediately after ISV remodeling is completed. Rapidly ectopic sprouts, resembling *flt1*^{ka601} mutant sprouts, appeared (compare Figure 4-33a and b). As the ectopic sprouts in *flt1*^{ka601} mutants evolved in part from purely venous ECs, endothelial responsiveness to Vegfc was evaluated in an analogous approach. Inducible expression of *vegfc* in the spinal cord did not in a single instance induce hypersprouting at the spinal cord level, suggesting that venous ECs after vISV incorporation lose their Vegfc responsiveness (Figure 4-33c).

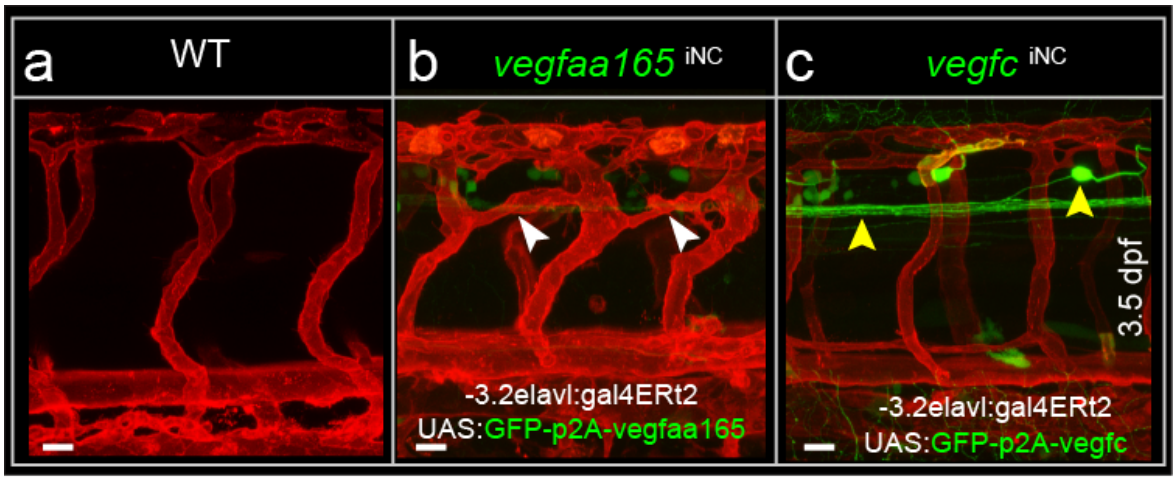

Figure 4-33. Vegfaa but not Vegfc induces hypersprouting in *flt1*^{ka601} mutants.

(**a, b**) Endoxifen inducible neuron specific *vegfaa165* gain-of-function induces hyperbranching (arrowheads in b) compared to WT (a). (**c**) Endoxifen inducible neuron specific *vegfc* gain-of-function (yellow arrowheads) does not induce ectopic sprouting at level of neural tube. iNC, inducible, neuronal cell specific gain-of-function. Scale bar 25µm.

On the other hand, reduction of Vegfaa levels using low dosage morpholino injections into *flt1*^{ka601} mutants resulted in complete rescue of the spinal cord hypervascularization

phenotype, confirming Vegfaa to be the driver of the *flt1*^{ka601} loss-of-function phenotype (Figure 4-34).

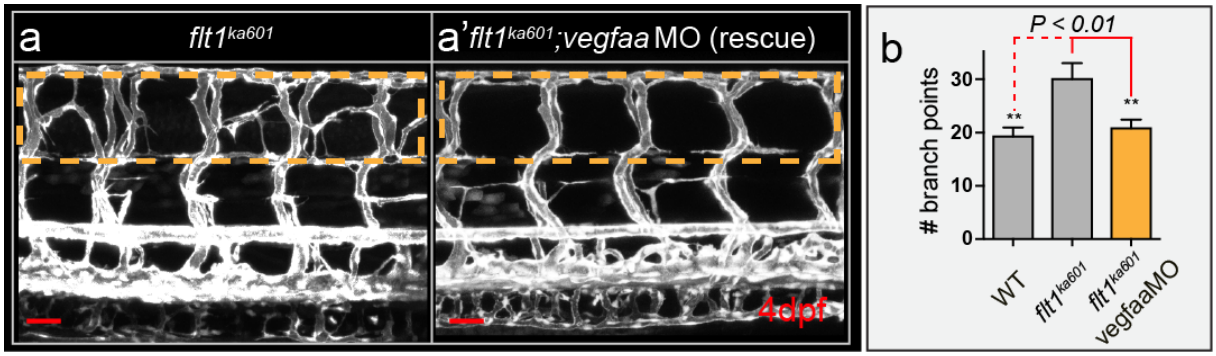

Figure 4-34. Vegfaa reduction rescues *flt1*^{ka601} hypersprouting.

(**a,a'**) Morpholino-mediated reduction of *vegfaa* expression in *flt1*^{ka601} mutants rescues sprouting defects; compare dotted box in a and a'. (**b**) Quantification of rescue in (a,a'), mean ± s.e.m, *n=5*. dpf, days post fertilization; MO, morpholino. Scale bar, 50 µm.

In line with the *vegfaa* MO rescue experiment, blockade of the cognate receptor Kdrl by application of the ki8751 Kdrl tyrosine kinase inhibitor to the media of *flt1*^{ka601} mutants annihilated the formation of the ectopic neovascular network. In contrast, the Flt4 specific tyrosine kinase inhibitor MAZ51 did not rescue hyperbranching in *flt1*^{ka601} mutants clearly showing that Vegfaa, but not Vegfc induces *flt1*^{ka601} hypersprouting (Figure 4-35).

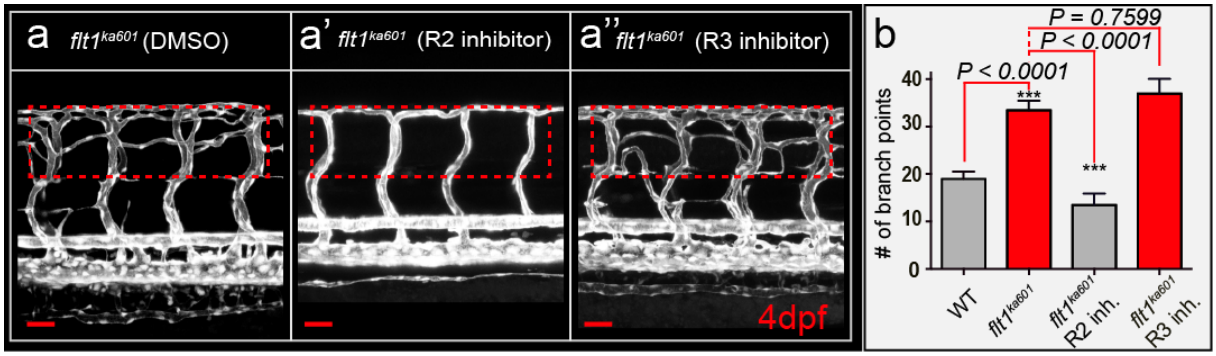

Figure 4-35. *Flt1*^{ka601} hypersprouting is Vegfaa-Kdrl-dependent.

(**a-a''**) *Flt1*^{ka601} mutant treated with DMSO (a); treated with Kdrl receptor signaling inhibitor ki8751 (R2 inhibitor, a'); treated with Flt4 tyrosine kinase inhibitor MAZ51 (a'', R3 inhibitor). (**b**) Quantification of a-a''. Mean ± s.e.m, n=11. R2, VEGF receptor 2; R3, VEGF receptor 3. Scale bar, 50µm. Imaging and quantification was performed together with Laetitia Preau.

5 Discussion

Angiogenesis is crucial for embryonic development, tissue regeneration upon ischemic tissue injury and tumor growth. Vegfa has been recognized as the principle driver of angiogenesis, involving signaling through Vegf receptor-2/Kdrl. Vegfa levels have to be well regulated as both loss- and gain of Vegfa result in profound angiogenesis defects. It has long been suggested that regulation of Vegfa levels involves Vegf receptor-1/Flt1, acting as a Vegfa scavenger limiting Vegfa bioavailability and Kdrl signaling. However, how Flt1 actions are coordinated and how this influences complex angiogenic cell behaviors culminating into the formation of perfused branched arterial-venous networks, is controversially discussed.

In the work presented in this dissertation the zebrafish model system was used to characterize the function of Flt1 in generating and shaping branched and perfused vascular networks. Additionally, the function of Flt1 at the neurovascular interface and how it affects formation of neurovascular units is poorly described. Using a combination of global and tissue-specific mutants, substantiated by cell transplantation and inducible gain-of-function experiments we find that neuronal Flt1, not vascular Flt1 controls vascular branching morphogenesis of the spinal cord vasculature. We furthermore provide evidence showing that sFlt1, not mFlt1 is the important mediator of spinal cord vascularization. Furthermore, loss of Flt1 or gain of neuronal Vegfaa induces a novel Kdrl-dependent venous sprouting form that based on cell kinetics and molecular signature differs from primary artery or secondary venous sprouting. In accordance with previous sprouting designations we termed this novel sprouting form, 'tertiary sprouting', and show that spinal cord neurons and the tertiary-sprout capillary network form a compact neurovascular unit that is regulated by tightly controlled neurovascular cross-talk. This novel sprouting-mode is also observed during normal development, and there also contributes to spinal cord vascularization. In contrast to previous reports, vascular Flt1 was found to be dispensable for tip cell selection and sprout guidance.

5.1 Distinctive angiogenic cell behaviors in *flt1*^{ka601} tertiary sprouts

The tertiary sprouts observed in *flt1*^{ka601} mutants are distinct from primary and secondary sprouting events in the trunk (Isogai et al. 2003; Ellertsdóttir et al. 2010). Primary sprouting

constitutes a special type of Vegfa-Kdrl-dependent arterial sprouting angiogenesis which is for instance insensitive to loss of flow whereas secondary sprouting is Flt4-Vegfc dependent. As opposed to this, tertiary sprouting is Vegfaa-Kdrl regulated and originates from the venular side. These characteristics closely resemble tumor angiogenesis and angiogenic processes during wound healing and therefore possibly constitute a better model for angiogenesis research than primary and secondary sprouting in zebrafish (Risau 1995; Bergers & Benjamin 2003).

Of note, primary and secondary sprouts are resistant to loss of blood flow shear stress (Watson et al. 2013; Lawson et al. 2003). *flt1*^{ka601}-tertiary sprouts in contrast are very sensitive to loss of blood flow and even decline if blood flow intensity is decreased. Moreover, *flt1*^{ka601}- tertiary sprouts from other *in vitro* sprouts as they rarely show shuffling behavior as described, rather most of the sprouts consist of only a single cell and sometimes sprouts even emanate from uni-cellular tubes (Jakobsson et al. 2010). Sprout characteristics and differences between the three types of sprouting observed in the zebrafish trunk during early development are depicted in Table 5-1.

Table 5-1 Zebrafish sprout-type-characteristics

Sprout type	Guidance cue	Impact of flow	Signaling pathway	EC origin	Features
Primary spouting (arterial or not specified)	Vegfa-Kdrl	Independent of flow	Plcy-Erk	DA	Very robust sprouts forming the DLAV. Unperfused network.
Secondary sprouting (venous)	Vegfc-Flt4	Independent of flow	PI3K-Akt	PCV	Purely venous sprouts remodeling aISVs and forming the lymphatic system
Tertiary sprouting (venous)	Vegfa-Kdrl	flow-dependent	PI3K-Akt	DA and PCV	Very similar to sprouting processes during wound healing/tumorangiogenesis. Venular sprouts anastomose with arterioles forming small capillaries.

It has been known for decades that nuclear positioning and nuclear migration are important for cell divisions in neuroepithelia, a process known as interkinetic nuclear migration (Del Bene 2011; Strzyz et al. 2015). However, nuclear positioning in endothelial biology has been so far only poorly characterized (Gundersen & Worman 2013). We could unambiguously show, that endothelial nuclei migrate at high velocities of up to 1µm·min^{-1} and position at future sprout initiation sites of tertiary sprouts. It has been described that migrating ECs and most other cell types position their nucleus rearwards *in vitro* and that this polarization seems to be critical for migration to proceed (Gundersen & Worman 2013). It can be speculated that the entire cellular machinery including MTOC, Golgi and ER has to be polarized to allow for efficient protein and lipid transport towards the side of migration. We found that nuclear positioning, within 5µm of the sprout initiation site, occurred prior to tertiary sprout elongation. Such far distance nuclear migration behavior has to our knowledge not been described before in migrating cells. One possible explanation could be that migration events in cell culture cells are normally very short, since ECs in culture have a spherical shape, and therefore nuclear migration could be difficult to detect (Gundersen & Worman 2013). In vivo endothelia in contrast, display large endothelial cells with lengths of sometimes more than 20µm in zebrafish. Future studies are important to untangle nuclear migration events in sprouting endothelial cells and if nuclear positioning is also observed in the vasculatures of other organs, different species if nuclear positioning in ECs is affected under pathological conditions. A tempting possibility would be the pharmacological inhibition of endothelial nuclear migration to block sprouting angiogenesis in disease.

Current models describe vISV remodeling as a process of secondary sprout connection and reprogramming of the dorsal arterial aspect into venous ECs after the onset of flow (Bussmann et al. 2010; Quillien et al. 2014). Utilizing time-lapse imaging of photoswitched vECs from the PCV (vECs^{PCV}), we could show that after connection of the secondary sprout to the aISV, venous ECs migrate dorsally along the vISV and actively proliferate and displace most arterial ECs (vECs^{ISV}), albeit few arterial ECs remain in the dorsal aspect of venous ISVs, which become venularized (v_aECs^{ISV}) and downregulate arterial markers such as Notch (Quillien et al. 2014) (Figure 5-2). Both venous EC-subpopulations vECs^{ISV} and v_aECs^{ISV} are capable to respond to Vegfaa and form tertiary sprouts. This shows that ECs in remodeled vISVs exhibit high heterogeneity in their origin but respond in a coherent manner. This type

of endothelium with mixed origin may be similar to endothelia in adults, which originate not only from one endothelial population but mix during network formation and display high heterogeneity (Regan & Aird 2012). A detailed schematic for venous EC nomenclature can be found in Figure 5-1.

Figure 5-1. Origin of venous ECs in vISVs

vISVs are composed of two EC-subtypes with arterial or venous origin. Venous ECs from the PCV form secondary sprouts. These ECs are called here vECs^{PCV}. After they intergrated into vISVs they are termed vECs^{PCV}. The other population of venous ECs in vISVs originates from the DA. Dorsal aorta ECs (aECs^{DA}) emanate sprouts and form the aISVs. aISV ECs are termed here aECs^{ISV}. When aISVs are remodeled into venous ISVs some arterial EC in the aISV become venularized which are called here v_aECs^{ISV}.

Interestingly, we could demonstrate using inducible *vegfc* gain-of-function experiments that vECs^{ISV} do not respond to Vegfc and instead acquire Vegfa responsiveness. It has been shown that ectopic Vegfc expression in the floor plate activates hypersprouting in the dorsal aspect of ISVs at 48hpf (Le Guen et al. 2014). It was reported that this phenotype can be enhanced if Ccbe1 and Vegfc are co-expressed in the floor plate. As Ccbe1 is expressed at the level of the HMS and is necessary for the maturation of Vegfc it may be that vISVs are only responsive to Vegfc expressed at the level of the HMS (source of Ccbe1) or at least close to it, such as floor plate expression (B. Hogan et al. 2009; Le Guen et al. 2014).

In conclusion, EC-characteristics do not seem to be determined by preset genetic programs but are dynamically programmed according their environment which is defined on both sides of the endothelium – the blood and the surrounding tissue. It would be of interest why vECs^{PCV} migrate against the flow direction dorsally into the vISVs whereas v_aECs^{ISV} never migrate ventrally into the PCV. It would therefore be interesting to elucidate how this directionality is governed and how EC-migration is regulated in endothelial sheets.

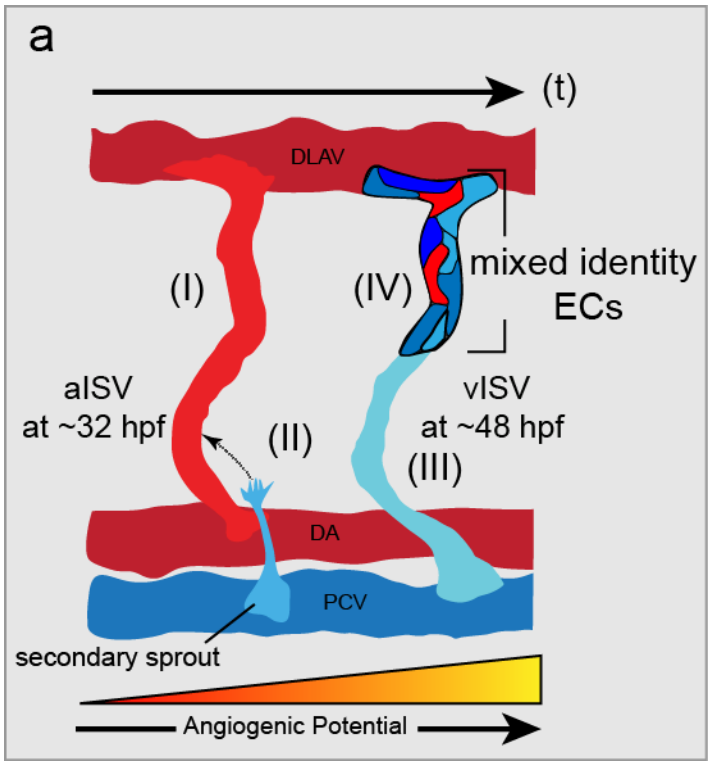

Figure 5-2. Purely venous and venularized arterial ECs display high angiogenic potential.

(**a**) The venous endothelial cells that give rise to the ectopic sprouts in *flt1*^{ka601} mutants show high heterogeneity and are either purely venous originating from the PCV vECs^{ISV} or venularized arterial ECs (v_aECs^{ISV}). During the trunk AV remodeling process, secondary venous sprouts connect (arrow) to the ventral part of the pre-existing aISV (I). As a consequence the ventral part of the aISV loses its connection to the dorsal aorta (II). The dorsal part forms a functional connection with the cardinal vein-derived ventral part (cells in blue), yielding an intersegmental vein carrying venous flow (III). Subsequently venous ECs from the PCV migrate dorsally to the DLAV and displace the majority of arterial ECs (aECs^{ISV}) (IV). Some arterial ECs remain and are venularized into venous ECs (a_vECs^{ISV}). Both EC subtypes can form *flt1*^{ka601} tertiary sprouts and are responsive to Vegfaa but not Vegfc. The dorsal aspect of intersegmental veins thus has mixed identity (blue and red cells, IV) whereas un-remodeled arterial ISVs contain only DA derived endothelium (I) (aECs^{ISV}). EC, endothelial cell; ISV, intersegmental vessel (a-arterial, v-venous); DA, dorsal aorta; PCV, posterior cardinal vein; DLAV, dorsal longitudinal anastomotic vessel; hpf, hours post fertilization.

In summary, tertiary sprouts exhibit greater similarity with physiological and pathological sprouting angiogenesis than primary and secondary sprouts and are not restricted to *flt1*^{ka601} mutants but give also rise to the spinal cord vasculature during normal development at 12-15dpf. Tertiary sprouts have venous origin, are blood flow sensitive and display high EC heterogeneity. In addition, they require nuclear positioning prior to sprout initiation, which is difficult to study in other models, hence *flt1*^{ka601} tertiary sprouting constitutes a novel type of sprouting depicting an exceptional model to study sprouting angiogenesis and would be well-suited for drug screening.

5.2 Neuronal Flt1 – a new cellular source of an old player

In zebrafish, mice and other vertebrates the most prominent expression domain of *flt1* is the endothelium of blood vessels (Fong et al. 1995; Bussmann et al. 2010; Krueger et al. 2011). Recent evidence however showed that *flt1* is also expressed in other cell types such as neurons, macrophages, monocytes and cancer cells (Sawano et al. 2001; Ohkubo et al. 2014; Selvaraj et al. 2015).

For instance, FLT1 signaling in macrophages has been proposed to facilitate macrophage guidance, as macrophage migration was impaired in *Flt1* KO mice (Hiratsuka et al. 1998; Hiratsuka et al. 2005). Similarly, expression of *Flt1* in various neuronal cell populations such as motor neurons, sensory neurons and dorsal root ganglia was shown to have neuronal cell-autonomous functions. These include sensing cancer pain in sensory neurons or neurodegenerative functions in motor neurons (Poesen et al. 2008; Storkebaum et al. 2005; Selvaraj et al. 2015). These processes are thought to involve mFLT1 signaling and the FLT1 ligand VEGFB. In the present study, we identified non-cell autonomous functions of neuronal sFlt1 and could show that neuronal sFlt1 affects vascular patterning by scavenging Vegfaa secreted from the spinal cord (a schematic of the neurovascular interface in the zebrafish spinal cord is shown in Figure 5-3).

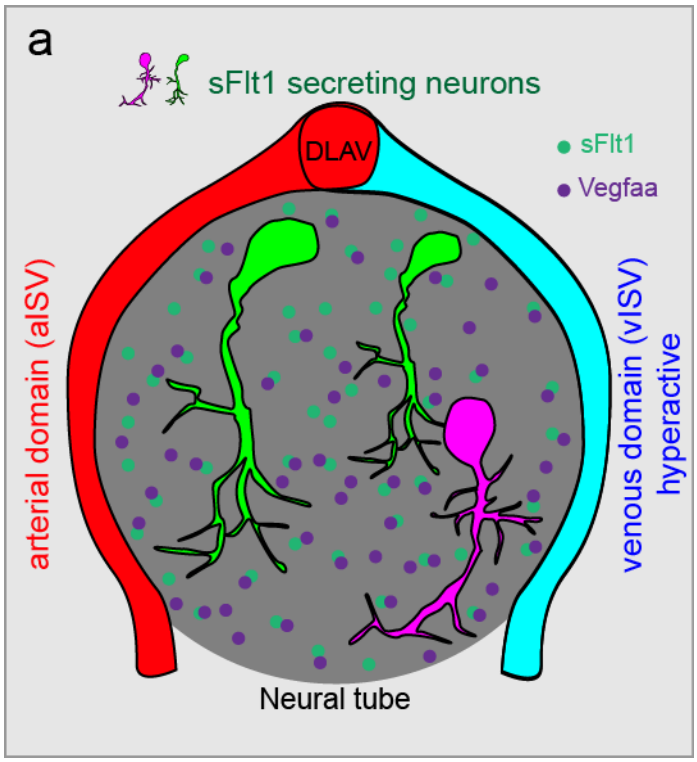

Figure 5-3. Flt1 and Vegfaa at the spinal cord neurovascular interface.

(**a**) Spinal cord neurons produce both Flt1 and Vegfaa in close proximity to the dorsal aspect of intersegmental arteries and veins. ISV, intersegmental vessel (a-arterial, v-venous).

We identified the spinal cord as an important and functionally relevant source of sFlt1. An outstanding question is which neuronal cell type produces physiologically relevant levels of sFlt1 and whether it is secreted at the cell soma, along axons and dendrites or only at the synapse? In our overexpression experiments with Vegfaa165 we observed that vessels align along Vegfaa165-secreting axons or soma, suggesting that not only the soma but also the axons themselves can secrete factors such as sFlt1 over the entire length of their projection. In line with our findings, mouse and quail studies indicate that loss of neuronal *Vegfa* or forced overexpression of *sFlt1* reduces neuronal vascularization and inhibits neuronal differentiation (Bautch & James 2009; Ruhrberg & Bautch 2013).

In current models it is assumed that vascular FLT1 is an important regulator of sprout guidance, although the experimental evidence is somewhat limited (Chappell et al. 2009; Jakobsson et al. 2010; Ho et al. 2012). We find that vascular *flt1* is dispensable for sprout directionality in all sprouting processes investigated in zebrafish. In *flt1*-depleted sprouts backsprouting to the parent vessel as suggested by Chappell and coworkers was not observed in the zebrafish model (Chappell et al. 2009).

One issue regarding the interpretation of data may involve the use of morpholinos, for further reading on this issue see introduction chapter “Morpholinos – friend or foe?”. In *flt1*^{ka601} zebrafish mutants we find that exclusively ectopic venous sprouting contributes to the formation of the organ-specific vasculature of the spinal cord. Previous studies suggest that with *flt1* targeting morpholinos one can also observe ectopic arterial sprouting (Krueger et al. 2011). In this morpholino setting, Flt1 morphants showed more tip cells and increased branching of primary aISV-sprouts. To uncover potential non-specific effects induced by morpholinos there is now largely consensus in the field to test different morpholinos dosages in the mutant background of the corresponding gene (Rossi et al. 2015; Stainier et al. 2015). We followed these new guidelines and show that low dosage *flt1* morpholino injection (1ng) recapitulates the *flt1*^{ka601} mutant phenotype and injection of this dosage into *flt1*^{ka601} mutants does not induce additional effects; in contrast injection of higher dosages (>3ng) causes both early arterial and later venous hypersprouting, and the former is not rescued in the *flt1*^{ka601} mutant background. This suggests that the vascular changes observed in previous studies may involve nonspecific side-effects related to the high MO dosage.

Zygmunt and colleagues report that sFlt1 acts downstream of the Sema3aa-PlexinD1

signaling pathway (Zygmunt et al. 2011). In the zebrafish trunk, vascular PlexinD1 and somatically expressed Sema3aa are considered repulsive guidance cues relevant for guiding arterial sprouts in between somites. At present, somites are also considered to be the physiologically relevant source of Vegfaa driving both the initiation of sprouting and the ventrodorsal expansion of the aISV. Loss of PlexinD1 or Sema3aa results in hyperbranching of aISVs into the somitic regions without penetrating the somites. The authors provided evidence suggesting that the repulsive actions of vascular PlexinD1 involve sFlt1. In *plxnd1*$^{Df(Chr08)fs31l/fs31l}$ mutants, hypersprouting occurs between 24-48hpf with ectopic sprouts branching from the aorta, and the aISVs. These authors show that morpholino mediated targeting of *sflt1* pre-mRNA induces a phenotype comparable to *plxnd1*$^{Df(Chr08)fs31l/fs31l}$ whereas sFlt1 gain-of-function rescues hypersprouting in *plxnd1*$^{Df(Chr08)fs31l/fs31l}$. If indeed sFlt1 is the crucial mediator of the PlexinD1 phenotype one would expect that the onset of hypersprouting, and cell-types involved should be comparable between *plxnd1*$^{Df(Chr08)fs31l/fs31l}$ and *flt1*^{ka601} mutants. We show that this is not the case, as the *flt1*^{ka601} mutant phenotype occurs 2 days after emergence of the *plxnd1*$^{Df(Chr08)fs31l/fs31l}$ phenotype. Moreover, the ectopic sprouts in *flt1*^{ka601} mutants arise from veins and not from arteries as reported in *plxnd1*$^{Df(Chr08)fs31l/fs31l}$. Additionally, experimental inadequacies may limit the reliability of the data presented by Zygmunt and colleagues. To show that indeed sFlt1 is the downstream effector of PlxnD1 they performed a knockdown of *sflt1* specifically targeting the I10E11a splice acceptor and verified the successful targeting of the *sflt1*-pre-mRNA by RT-PCR spanning E10-E11a. Successful depletion of *sflt1* splicing should in theory result in the complete loss of a PCR product. Instead a PCR band with a somewhat smaller size as expected could be observed, suggesting the presence and use of an upstream cryptic acceptor splice site. Since E11a codes only for the last 5 amino acids of sFlt1, cryptic splicing would most likely not result in protein truncation and loss-of-function. More likely the *sflt1* targeting morpholino used by Zygmunt induces side-effects or is not targeting sflt1.

For the future it will be important to determine (I) whether local sprout guidance is necessary for sprout elongation and (II) if blood flow shear stress and physical constraints in the tissue bed where the sprout extends give the sprout sufficient directionality. For instance, perpendicular blood flow pressure from the parent vessel could be an efficient mechanism to push the sprout away from the source as reported in vitro (Song & Munn 2011). In the case of tertiary sprouts, sprouting occurs from the vein toward the artery,

hence against the direction of the pressure gradient. Lumen formation does occur in the direction of the pressure gradient, yet the expansion of the tertiary sprouts could also be advanced by venous flow as long as they did not anastomose with a adjacent aISV (Gebala et al. 2016). Contradictory to this idea, primary and secondary sprouts in zebrafish can find their way and elongate away from the dorsal aorta even in the absence of flow (Lawson et al. 2003; Watson et al. 2013). Although it may well be that these cases physical constraints from the somites prevent backsprouting or directional changes. It is conceivable that some sprout species require blood flow, and blood pressure for directionality, whereas others sprouts may require Vegfa gradients.

Inducible depletion of *Flt1* in the mouse retinal plexus by crossing Rosa26 Cre mice or by injection of Ad-Cre constructs into *Flt1*$^{flox/flox}$ mice resulted in increased tip cell and filopodia numbers as well as increased numbers of bifurcations (Chappell et al. 2009; Ho et al. 2012). Tip cell numbers per area increased from approx. 4 in *Flt1*$^{flox/flox}$ to 5.5 in *Flt1*$^{\Delta/\Delta}$ mice. However, these changes are rather subtle and the definition of a tip cell in the respective statistical analyses is not clearly defined and therefore may be overinterpreted (Ho et al. 2012). Similarly, filopodia numbers and bifurcations were reported to be approx. 2 fold increased in Ad-Cre injected *Flt1*$^{flox/flox}$ retinas, although the overall vessel architecture remained intact (Chappell et al. 2009). These experiment show that loss of endogenous *Flt1* may mildly increase angiogenic potential in mouse neonates but it does not address the question, whether loss of neuronal or vascular *Flt1* or both contributes to increased sprouting potential (Chappell et al. 2009; Ho et al. 2012). In the mouse retinal vascular model astrocytes produce VEGF to activate retinal vascularization (Dorrell et al. 2002; Ruhrberg et al. 2002; Gerhardt et al. 2003). This is very similar to our findings in the spinal cord; where neuronal cells secrete Vegfaa to induce spinal cord vascularization. In astrocytes it has been shown that VEGFR-2 mediated uptake of VEGF limits sprouting angiogenesis, yet it is unknown whether neuronal FLT1 similarly restricts retinal angiogenesis (Okabe et al. 2014). To untangle the contribution of the neuronal and vascular FLT1, inducible *Flt1* loss-of-function experiments should be repeated with vascular- and neuronal-specific Cre lines.

Moreover, tightly controlled VEGF levels were shown to maintain neuronal integrity and safeguard neuronal survival and that decreases in VEGF levels in neurons can lead to neurodegenerative disease. We find that neuronal sFlt1 is important during embryonic

development but it is tempting to speculate that neuronal Flt1 in mature neurons in adults can also influence their integrity and survival. Hence, any pathological changes resulting in dysregulation of *flt1*, such as splice site mutations or mutations resulting in increased promoter activity or protein stability could in principle promote neurodegenerative disease and thus represent an important therapeutic target (Storkebaum & Carmeliet 2004; Lange, Storkebaum, et al. 2016).

5.3 The tip cell concept – we need new models for an old question

Selective tip cell activation is strictly necessary to facilitate an orchestrated formation of sprouts and vascular networks (Herbert & Stainier 2011; Siekmann et al. 2013). Hence, an important question in the angiogenesis field, which is still not entirely understood, is why only certain endothelial cells respond to growth factors whereas others do not. Following initial sprout formation, endothelial behavior within the sprout has to be coordinated in a way that the entire sprout migrates into a certain direction (Phng & Gerhardt 2009). The processes of selection and coordinated guidance have been explained with the "tip cell concept", proposing a model in which a leading tip cell is selected by lateral inhibition and guides the sprout towards a growth factor gradient (Ruhrberg et al. 2002; Gerhardt et al. 2003). Trailing stalk cells are considered to be the proliferative EC-population promoting sprout elongation.

We show here for the first time, that zebrafish vascular Flt1 is dispensable for sprouting angiogenesis. While our data show that during normal embryonic development, vascular Flt1 appears dispensable for tip/stalk differentiation, and branching morphogenesis, we cannot rule out that vascular Flt1 may play a role during different conditions. For instance, it is possible that during tumor growth or severe tissue hypoxia, VEGF levels exceed thresholds and vascular Flt1 can to some extent modulate vascularization and sprout activation. Thus, we do not exclude that vascular Flt1, especially under pathological conditions has important functions.

In reviews on sprouting angiogenesis it seems to be clear that vascular FLT1 is an important regulator of tip cell formation, limiting angiogenesis. However, careful analysis of the available literature reveals that this is by far not the case. The first *Flt1* loss-of-function

studies were conducted in non-inducible *Flt1* KO mice, in which over-commitment of angioblasts leads to early lethality, preventing the analysis of sprouting angiogenesis at later stages in these mice (Fong et al. 1995; Fong et al. 1996; Hiratsuka et al. 2005; Chappell et al. 2009). To elucidate the function of FLT1 during development and thus to overcome the first severe angioblast phenotype, FLT1 function in angiogenesis was addressed *in vivo* utilizing morula transplantation experiments with the *Flt1* KO mouse (Fong et al. 1999). This laborious technique was used because inducible loss-of-function tools were not available by the end of the 1990s. *Flt1*-depleted KO cells were transplanted into WT morulas at densities allowing the morula to overcome the lethal angioblast over-commitment phenotype. This study showed that vessels lacking *Flt1* ($lacZ^+$) can form normally and do not display severe abnormalities (Fong et al. 1999). As the lacZ staining used in these experiments allows only for low-resolution imaging and only yolk sac primary plexus formation has been analyzed, subtle phenotypes have possibly been overlooked in these mosaic analyses (Fong et al. 1999). Nonetheless, mosaic mice survive to adulthood giving some evidence that FLT1 is not strictly necessary for vascular development after angioblast formation.

As mentioned in the previous chapter, inducible Flt1 loss-of-function studies have been performed in the mouse. The authors reported that *Flt1* depleted retinal vessels exhibit increased filopodia numbers and bifurcations, albeit the overall structure of the retinal plexus is normal and even completely *Flt1* depleted neonates survive (Chappell et al. 2009; Ho et al. 2012). The authors deduced from these data that FLT1 has an important function in vessel formation; however if one compares these phenotypes with other vascular mutants such as *Dll4, Kdr* or *Vegf* the described phenotypes are rather mild suggesting that *Flt1* can influence VEGF levels and angiogenic potential but does not regulate local sprout guidance or tip cell formation (Suchting et al. 2007; Hellström et al. 2007; Carmeliet et al. 1996; Benedito et al. 2012). Other authors claim that FLT1 is specifically enriched in stalk cells (Jakobsson et al. 2010). We have no evidence in zebrafish for restricted expression. These authors possibly overinterpreted their data since analysis of *in vitro* data can be problematic as cells in culture do not carry flow and have no clear arterial or venous identity. This makes interpretation of data deduced from experiments using *in vitro* sprouting models extremely delicate. This is further enhanced by the fact that many factors thought to be involved in tip

cell selection are also involved in AVD (Lawson et al. 2001; Siekmann & Lawson 2007; Herbert & Stainier 2011).

In addition, the tip cell concept uses molecules, which are enriched or even restricted to the arterial or to the venous domain, such as FLT1, NOTCH1, DLL4 and FLT4 (Herbert & Stainier 2011). This expression difference of these genes is obvious in the mouse retinal plexus and very strict in the zebrafish vasculature (Lawson et al. 2001; Siekmann & Lawson 2007; Hogan et al. 2009). Here *flt1, dll4* and *notch1a* are strictly confined to the arterial domain, similarly *flt4* is mostly found in venous ECs. Therefore, it is unlikely that one concept can explain the tip cell selection process in the whole heterogenic landscape of endothelia. For instance, secondary sprout selection in zebrafish seems to be Kdrl, Notch and Dll4-independent because these factors are not expressed in the PCV (Küchler et al. 2006; Hogan et al. 2009; Koltowska et al. 2015). Thus, a different mechanism is responsible for the coordinated selection of tip cells in the PCV. It is possible that during evolution different selection mechanisms evolved independently but it is also conceivable that tip cell selection in arteries occurs indeed Dll4/Notch and Flt1 independent. Taking into account our data that veins and capillaries are the major side of angiogenesis we can even go a step further, and speculate that during tumor angiogenesis or wound healing, other mechanisms that are most likely Notch and Dll4-independent are utilized for tip cell selection and sprout guidance, which has obvious therapeutic implications. Accordingly, an alternative explanation for the increased tip cell formation in *Dll4*-depleted retinas would be that the deactivation of arterial genes downstream of NOTCH, results in increased venous remodeling and thus an overall higher angiogenic potential and vascular overgrowth (Suchting et al. 2007; Hellström et al. 2007). Not only our data disagree with the tip cell concept, other research groups recently showed that *Kdr* depleted retinal sprouts are also capable to make patent vessels and that *Dll4* is not even expressed in tip cells in the mouse retina (Benedito et al. 2012). As outlined above, more and more in vivo findings relativize the tip cell concept (Benedito et al. 2012) and evidence is accumulating that venous ECs are the major source of sprouting angiogenesis, as shown by us and others (Xu et al. 2014; Hen et al. 2015).

As discussed, the *Flt1* KO mouse exhibits a very severe phenotype with angioblast over-commitment, resulting in early lethality around E8.5 (Fong et al. 1995). Therefore, it is

surprising that *flt1*^{ka601} zebrafish mutants do not display angioblast formation defects. This has probably two reasons, first there is no vascular yolk plexus formed in zebrafish and secondly, angioblast differentiation, proliferation and migration seems to be independent of VEGF signaling in zebrafish, most likely involving APJ-elabela signaling and possibly other pathways (Helker et al. 2015). This species-specific difference could render the zebrafish insensitive to increased VEGF bioavailability during angioblast formation, overcoming this first phenotype in *flt1*^{ka601} mutants.

It will be interesting to investigate in future experiments if sprouting angiogenesis and spinal cord vascularization are affected in inducible loss-of-function mice, which have already exceeded angioblast differentiation and primary plexus formation, especially with regard to neuronal FLT1 contribution. *Flt1* is widely known as an arterial marker gene, but whether Flt1 has a function in AVD is unknown (Krueger et al. 2011). We could show that vISV sprouts aberrantly connect to aISVs in *flt1*^{ka601} mutants. Remarkably, shunt formation appears not to affect vascular development, since *flt1*^{ka601} mutants survive to adulthood and have no lymphatic or AVD defects. In zebrafish, parachordal lymphangioblasts differentiate directly form secondary sprouts or indirectly from vISVs after aISV-remodeling (Isogai et al. 2003). In *flt1*^{ka601} mutants only the direct contribution of secondary sprouts but not the indirect source from vISVs is inhibited. Therefore most likely, lymphatic differentiation from vISVs can compensate for the loss of lymphatic secondary sprout contribution to the lymphatic system. In conclusion, our data suggest that vascular Flt1 might have some role in arterialization and that aISVs in *flt1*^{ka601} mutants for this reason cannot fully block the anastomosis of venous sprouts in aISVs that are supposed to stay arterial and not to become remodeled into vISVs.

5.4 Veins not arteries make new vessels

We found that Vegfaa gain-of-function in *flt1*^{ka601} mutants does not equally activate arterial and venous sprouting but surprisingly exclusively promotes venous sprouting. Of note, there is accumulating evidence that vascular growth and angiogenesis occurs predominantly from the venular side (Risau 1995; Bergers & Benjamin 2003; Xu et al. 2014; Hen et al. 2015). For instance, formation of the gut vasculature is initiated from the PCV and all intestinal arteries and veins are formed from venous ECs originated from the PCV (Hen et al. 2015). However in

this model the PCV is the only vessel in close contact to the intestine, therefore it could be argued that arteries do not respond to Vegfa as they are too far away from the source. We in contrast, have a model in which vISVs and aISVs are both in close contact to the spinal cord, which we identified as the major source of Vegfaa after 2dpf. Therefore, the observation that ectopic sprouting in *flt1*^{ka601} mutants originates exclusively from venous ISVs, cannot be explained with the anatomical position of the source of Vegfaa or responder vessel. Thus the difference is most likely inherent to arterial and venous ECs (Figure 5-4).

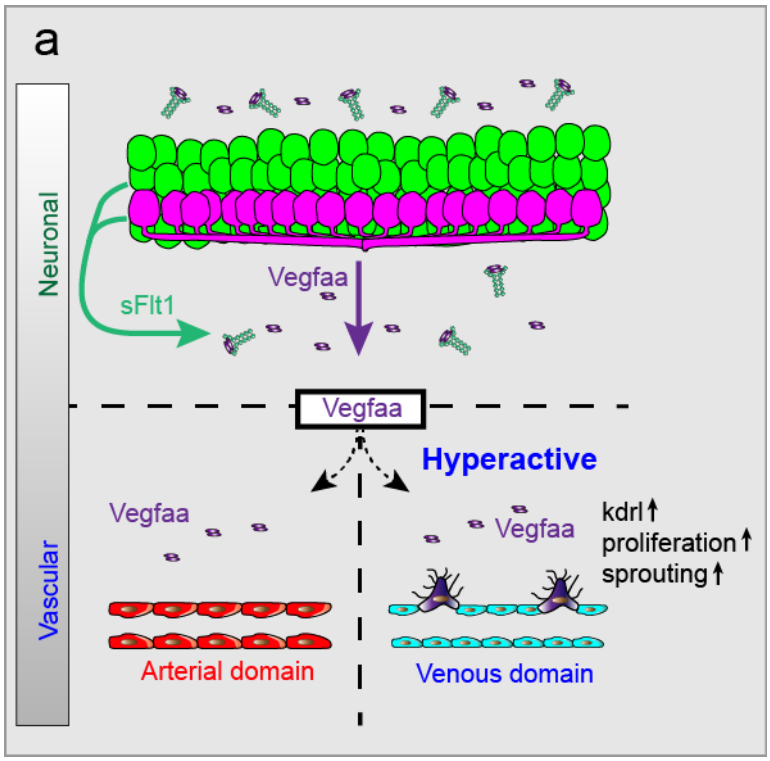

Figure 5-4. Neuronal sFlt1 and Vegfaa balance venous neuro-vascularization.

(**a**) Neuronal Flt1 determines the bioavailability of Vegfaa at the neurovascular interface. Loss of neuronal Flt1, or increases in neuronal Vegfaa augment Vegfaa at the neurovascular interface and promote ectopic venous sprouting. Ectopic venous sprouting involves endothelial cells with a high Vegfaa-Kdrl responsiveness. Arteries at this stage show a low Vegfaa responsiveness and do not respond to loss of Flt1.

Arterial ECs express Notch, which is the major driver of arterial differentiation (Lawson et al. 2001; Siekmann & Lawson 2007; Quillien et al. 2014). Therefore, we speculated that arterial depletion of Notch signaling in *flt1*^{ka601} mutants would result in dearterialization and initiation of sprouting in aISVs. Interestingly, arterial-specific Notch signaling inhibition in *flt1*^{ka601} mutants indeed activated some arterial sprouting, strongly suggesting that Notch decreases the angiogenic potential of arteries in an Flt1-independent manner. Flt1 is widely seen as a major effector activated by NOTCH (Funahashi et al. 2010; Jakobsson et al. 2010). Taking our data into account, it will be interesting to identify the true Notch downstream effectors inhibiting angiogenesis. It is possible that the arterialization of *notch* positive vessels is sufficient to render vessels non- or less responsive to angiogenic cues and that

arterioles are by definition not intended for vascular growth. Furthermore, the differences observed in sprouting potential between arteries and veins could additionally be regulated by other factors including blood flow shear stress, pericyte coverage, adherens and tight junctions-tightness or other unknown inhibitors or activators in arteries or veins, respectively. These factors could either directly affect sprouting or influence the *notch* status of the vessel. For instance, shear stress has been shown to activate NOTCH signaling, evidencing for a shear stress induced NOTCH-dependent inhibition of sprouting in arteries (Masumura et al. 2009; Tu et al. 2014). Adherens junctions and pericytes on the other hand, are known to have lower expression levels and lower vascular coverage in veins compared to arteries (Bergers & Song 2005; Orsenigo et al. 2012; Vestweber 2015).

5.5 Finding the balance – safeguarding supply without disrupting neuronal differentiation

It is widely accepted that neural stem cells need a low oxygen environment for their expansion. During early mouse development this is achieved by keeping the stem cell niches devoid of blood vessels. During later stages, upon vascularization of the brain oxygen delivery is augmented and neural stem cell differentiation is promoted (Panchision 2009; Mannello et al. 2011; Lange, Turrero Garcia, et al. 2016). We propose that the spatio-temporal control of spinal cord vascularization is achieved via neuronal titration of sFlt1-Vegfaa levels at the neurovascular interface. High sFlt1 levels during early spinal cord formation keep blood vessels away from stem cells, whereas low sFlt1 and high Vegfaa attract blood vessels towards differentiating neurons. Hence, it is a compelling option that radial glia cells, the stem cells in the spinal cord, produce sFlt1 and thereby prevent vascularization during early spinal cord development, thus ensuring sufficient expansion of neuronal stem cells. To test this hypothesis, the sFlt1 producing neuronal subpopulations need to be identified and it should be verified whether premature spinal cord vascularization in *flt1*^{ka601} mutants influences neuronal development, stem cell numbers and neuronal regenerative capacities. Furthermore, it will be important to identify the factors regulating *flt1* expression and splicing in neurons in order to obtain a better understanding of neuronal stem cell niches and how they regulate vessel recruitment and oxygen tension.

Flt1^{ka601} mutants as well as other mutants with neuronal Vegfaa gain-of-function phenotype, such as *ptena*$^{-/-}$*;ptenb*$^{-/-}$, *dll4*^{j16e1} and *vhl*^{hu2117} display massive hypersprouting at the level of the spinal cord (Rooijen et al. 2009; van Rooijen et al. 2011; Choorapoikayil et al. 2013; Leslie et al. 2007). Interestingly, the sprouts elongate along the spinal cord and vascularization thus occurs laterally forming a PNVP in these mutants. Strikingly, we found that if Vegfaa levels are increased further, using *flt1*^{ka601}; *vhl*^{hu2117} double mutants, tertiary sprouts do not only laterally vascularize the spinal cord but also penetrate into the spinal cord. These double mutants die at ~5dpf possibly due to premature internal invasion and destruction of the spinal cord neuronal architecture. These data substantiate that (I) the neural tube is the major source of Vegfaa after 2dpf and (II) that these mutants affect different levels of VEGF biology, namely transcription and protein bioavailability (Figure 5-5).

Studying spinal cord vascularization in WT embryos we could show that the spinal cord is laterally vascularized by a process we termed tertiary sprouting at ~11-15dpf predominantly from the venous side, analogous to *flt1*^{ka601} mutants but ~7dpf later. In mice, the spinal cord is internally vascularized by sprout invasion form the PNVP (Bautch & James 2009; Ruhrberg & Bautch 2013). It will be important to determine in future studies, if the primitive spinal cord vasculature formed at 11-15dpf in zebrafish is analogous to the PNVP in mice, and whether the zebrafish spinal cord is analogously to the mouse spinal cord, internally vascularized at later stages (James et al. 2009; Ruhrberg & Bautch 2013). Neuronal vascularization promotes neural stem cell differentiation and untimely or excessive vascularization may disrupt the highly orchestrated neuronal differentiation and specification processes (Lange, Turrero Garcia, et al. 2016; Lange, Storkebaum, et al. 2016).

We propose a two-tiered checkpoint mechanism involving neuronal Vegfaa and sFlt1 regulating timely lateral vascularization and spinal cord invasion according to the demands and neurodevelopmental processes (the model is depicted in Figure 5-5).

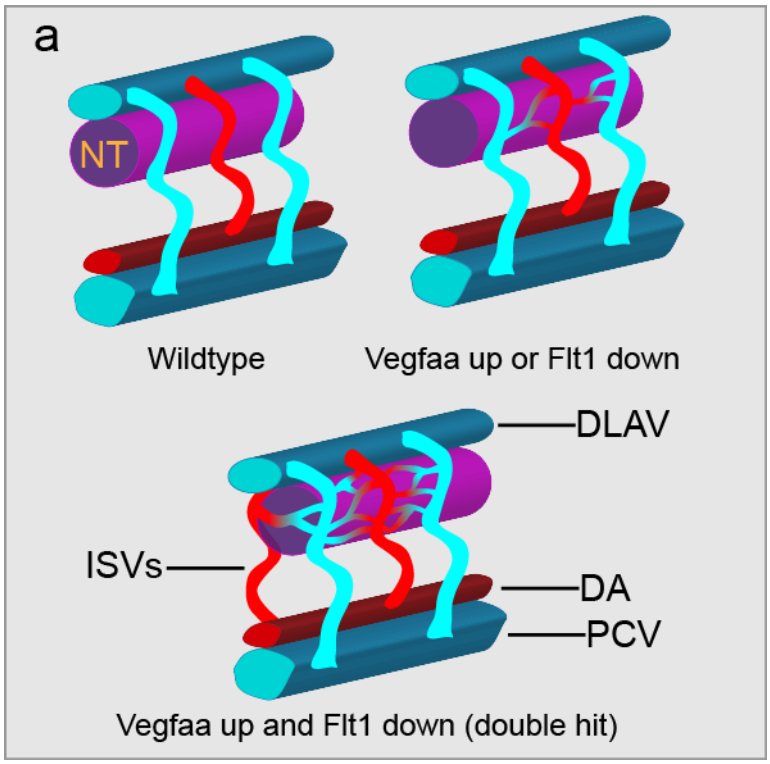

Figure 5-5. A two-tiered sFlt1-Vegfaa mechanism regulates lateral vascularization and sprout invasion in the developing spinal cord.

(**a**) Schematic representation of lateral vascularization around the neural tube in WT (top left), *flt1*^{ka601} single mutant or *vhl*^{hu2114} single mutant (top right), and *flt1*^{ka601};*vhl*^{hu2114} double mutant (bottom). Loss of *flt1* or *vhl* induces the formation of a peri-neural tube network, and combining both mutants in addition promotes sprout invasion into the neural tube. NT, neural tube; ISV, intersegmental vessel; DA, dorsal aorta; PCV, posterior cardinal vein; DLAV, dorsal longitudinal anastomotic vessel.

6 Materials and Methods

6.1 Materials

6.1.1 Transgenic lines

The transgenic reporter lines *Tg(fli1a:EGFP)^{y1}*, *Tg(kdrl:hsa.-HRAS-mcherry)^{s916}*, *TgBAC(flt1:YFP)^{hu4624}*, *Tg(fli1a:nGFP)^{y7}*, *Tg(Xla.Tubb:DsRed)^{zf148}*, *Tg(kdrl:EGFP)^{s843}*, *Tg(HuC:EGFP)^{as8}*, *Tg(mnx1:GFP)^{ml2}*, *Tg(flt1^{enh}:tdTomato)*, *Tg(flt4:mCitrine)^{hu7135}*, *Tg(kdrl:nlskikGR)^{hsc7}* and *vhl^{hu2117}* mutants were used as published (B. Hogan et al. 2009; Peri & Nüsslein-Volhard 2008; Bussmann et al. 2010; van Impel et al. 2014); *ptena$^{-/-}$;ptenb$^{-/+}$* zebrafish mutants were a gift from Jeroen den Hertog (Choorapoikayil et al. 2013). Details about the reporter lines used in this work can be found in Table 6-1.

Table 6-1. Zebrafish transgenic reporter lines

Transgenic line	Fluorescent organs/cells	Features
Tg(kdrl:EGFP)^{s843}	Green vascular reporter	Well suited for vascular phenotype analysis
Tg(fli1a:EGFP)^{y1}	Green fluorescence in the vasculature and neural crest cells (NCC)	Strong fluorescence, not suitable for late trunk or brain analysis due to strong NCC background
Tg(kdrl:hsa.-HRAS-mcherry)^{s916}	Red fluorescence restricted to the membrane of ECs	Suitable for analysis of vascular phenotypes, high resolution due to membrane fixation of mcherry
Tg(flt1^{enh}:tdTomato)	Arterial specific expression (not expressed in neurons)	Very strong arterial marker
TgBAC(flt1:YFP)^{hu4624}	Yellow fluorescence restricted to the arterial domain and flt1^{+} neurons	Can be used to identify arteries and to analyze flt1^{+} neurons
Tg(flt4:mCitrine)^{hu7135}	Venous enriched reporter	Strongly expressed in the PCV, lower expression in ISVs, very weak expression in the DA
Tg(fli1a:nGFP)^{y7}	Nuclei of blood vessels and NCCs	Suitable for nuclei number counting or EC migrational analysis
Tg(kdrl:nlskikGR)^{hsc7}	Expression of the photoswitchable kikGR in the nuclei of ECs	Suitable for cell tracking and counting after photoconversion
Tg(Xla.Tubb:DsRed)^{zf148}	Reporter for mature neurons	Very strong neuronal reporter, well

		suited for analysis of axonal projections or moto- and sensory neurons
Tg(HuC:EGFP)^{as8}	Pan-neuronal reporter	Strong expression in neurons of the brain and spinal cord, not suitable for axon analysis
Tg(mnx1:GFP)^{ml2}	Motoneuron reporter	Expressed in primary and secondary motoneurons

Table 6-2. Commercial kits

Product/Kit	**Manufacturer**
QuatiTect Whole Trascriptome kit	QIAGEN
QIAprep Spin Miniprep Kit	QIAGEN
QIAprep Spin Midiprep Kit	QIAGEN
RNeasy Mini Kit	QIAGEN
QIAquick Gel Extraction Kit	QIAGEN
QIAquick PCR Purification Kit	QIAGEN
Maxima cDNA First Strand Synthesis Kit	Thermo Fisher
mMessage Machine SP6 Transcription Kit	Thermo Fisher
mMessage Machine T7 ULTRA Transcription Kit	Thermo Fisher
Maxi Script T7 Transcription Kit	Thermo Fisher
PowerUp SYBR Green Master Mix	Thermo Fisher

Table 6-3. Inhibitors and chemicals

Product	**Manufacturer**
Ki8751	Sigma-Aldrich
Maz51	Merck
DMSO	Sigma-Aldrich
DAPT	Sigma-Aldrich
LY-411575	Sigma-Aldrich

Table 6-4. Kits and chemicals for RNAseq

Product/Kit	**Manufacturer**
Random Hexamer Primer	Thermo Fisher
RNAse out	Thermo Fisher
SuperScriptII OR III Reverse Transcriptase	Thermo Fisher

5xSecond Strand Buffer	Thermo Fisher
DNA Polymerase I	Thermo Fisher
Agencourt AMPure XP Reagent	Beckman coulter
RiboMinus™ Eukaryote Kit v2	Thermo Fisher
TruSeqIllumina RNA sample prepv2 kit	Illumina

Table 6-5. Plasmids

Plasmid	**Manufacturer or provider**
PGEM-T Easy	Promega
pCR8/GW/TOPO	Thermo Fisher
pminiTol_flt1-0.9	Schulte-Merker S, University of Münster, Germany
DR274	DR274 was a gift from Keith Joung (Addgene plasmid # 42250)
MLM3613	MLM3613 was a gift from Keith Joung (Addgene plasmid # 42251)
-3.8NBT_tauGFP	Amaya lab, University of Manchester, UK
p5E_NBT	Cloned from from -3.8NBT_tauGFP into p5E_MCS (this work)
pME_gal4ERt2	pME-geta4 was a gift from Strähle U, KIT, Germany
p5E_3.2elavl	p5E_-3.2HuC was a gift from Strähle U, KIT, Germany
Tol2Kit	The Tol2kit was a gift from Kawakami K, NIG, Japan
pME_MAML-GFP	Was a gift from Burns C, CRC, Charlestown, USA
pME_GFP-p2A_SmaI	Cloned from Tol2Kit plasmid #455 (this work)
pME_GFP-p2A_vegfaa121	Cloned by Anna Klaus using pME_GFP-p2A_SmaI
pME_GFP-p2A_vegfaa165	Cloned by Anna Klaus using pME_GFP-p2A_SmaI
pME_GFP-p2A_vegfc	Cloned by Anna Klaus using pME_GFP-p2A_SmaI
pME_GFP-p2A_sFlt1	Cloned from pME_GFP-p2A_SmaI (this work)
pME-Cas9-T2A-GFP	pME-Cas9-T2A-GFP was a gift from Leonard Zon (Addgene plasmid # 63155)
pDestTol2CG2-U6:gRNA	pDestTol2CG2-U6:gRNA was a gift from Leonard Zon (Addgene plasmid # 63156)
pDestTol2CG2-U6:flt1E3	Cloned from pDestTol2CG2-U6:gRNA (this work)
pDestTol2CG2-U6:flt1E3_ Cas9-T2A-GFP	Cloned by gateway cloning using pME_Cas9-T2A-GFP and pDestTol2CG2-U6:flt1E3 (this work)
pCG2_elavl3.2_gal4ERt2	Cloned by gateway cloning using pME_gal4ERt2 and p5E_elavl3.2 (this work)
pCG2_UAS_GFP-p2A-vegfaa165	Cloned by gateway cloning using pME_GFP-p2A-

	vegfaa165 and p5E_UAS (tol2kit) (this work)
pCG2_UAS_GFP-p2A-vegfaa121	Cloned by gateway cloning using pME_GFP-p2A-vegfaa121 and p5E_UAS (tol2kit) (this work)
pCG2_UAS_GFP-p2A-vegfc	Cloned by gateway cloning using pME_GFP-p2A-vegfc and p5E_UAS (tol2kit) (this work)
pCG2_UAS_GFP-p2A-sFlt1	Cloned by gateway cloning using pME_GFP-p2A-sFlt1 and p5E_UAS (tol2kit) (this work)
pCG2_NBT_GFP-p2A-sFlt1	Cloned by gateway cloning using pME_GFP-p2A-sFlt1 and p5E_NBT (tol2kit) (this work)

Table 6-6. Morpholino sequences

Target gene	MO sequence	Injection amount	MO type
flt1	5'ATATCGAACATTCTCTTGGTCTTGC-3'	1-3ng	ATG-MO
vhl	5'-GCATAATTTCACGAACCCACAAAAG-3'	6ng	E1i1 splice MO
vegfaa	5'-GTATCAAATAAACAACCAAGTTCAT-3'	0.3ng	ATG-MO
flt4	5'-CTCTTCATTTCCAGGTTTCAAGTCC-3'	4ng	ATG-MO
Ctrl MO	5'-CTCTTACCTCAGTTACAATTTATA-3'	10ng	

Table 6-7. Real-time qPCR primer sequences

gene	name	forward primer	reverse primer
vegfaa	zvegfaa-E4-E5	5'-CAACGCGTATCGCAGCATAA-3'	5'-TGCCTTTGGCCTGCATTC-3'
vegfab	zvegfab-E3-E4	5'-TGCTGGGTGCTGCAATGAT-3'	5'-CTCTTAATCTCCAAGGTAATGTTGTATGTG-3'
ef1a	zef1a-E4-E5	5'-GTTGCCTTCGTCCCAATTTC-3'	5'-CAATCTTCCATCCCTTGAACCA-3'
mflt1	zflt1-E19	5'-GTGAACACAAGGCTCTAATGACAGA-3'	5'-TGCGCCGAGGAGATTGAC-3'
sflt	z-sflt-E11a	5'-TCCGTCCCAATTTACCATTCC-3'	5'-TCTTGGGTGGCTGGATGAG-3'
plgf	z-plgf-E4-E6	5'-CACAAAGCCTGTGAATGTAGACT-3'	5'-TTCTCCTTCCTTTTTCTCCCTCTAT-3'
lyve1a	zlyve1a_E4/5-E5/6	5'-GGCTCCACTGAAGCTGTTCC-3'	5'-GCCTTGCAGGGTCTTTTCGT-3'
angpt2a	zanpt2a-E4/5-E6	5'-TGTGACAAGGCAAGGTAGCAA-3'	5'-GTCCCCATGTCACAGTAGGC -3'
aplnra	zaplnra_E1	5'-GGACAAAACTCTGGGGGTGAA-3'	5'-ACACTCGCATCCACTCATCG -3'
esm1	zesm1_E2-E2/3	5'-TTGTGACAGAGAAACCGGCG -3'	5'-AACCCACTTCATTACCTGCTTCA-3'

hbbe2	zhbbe1_E1/2-E2	5'-ACTGCAGAGGGCTTTGATTGT-3'	5'-TGGCCTCAGCATTGTACAGG -3'

Table 6-8. sgRNA sequences used for CRISPR/Cas

Target gene	sgRNA sequence (without PAM)
sflt1 and mflt1	sgRNAflt1E3: 5'-GGGACGGTGGGAGCTCCAGT-3'
sflt1 and mflt1	sgRNAflt1E5: 5'-GGAATATCATCTGGAACAGC-3'
mflt1	sgRNAflt1E11#1:5'-GGCAGTCCAGGACGAAGGAGG-3'
mflt1	sgRNAflt1E11#2:5'-GGTGATGGTCAAGATGGGATTG-3'
mflt1	sgRNAflt1E11#3:5'-GGTCAAGATGGGATTGTGGG-3'
mflt1	sgRNAflt1E11#4:5'-GGAGAAGCCTCCTCCTTCGTCC-3'
mflt1	sgRNAflt1E11#5:5'-GGATGGTCAAGATGGGATTGT-3'

Table 6-9. sgRNA oligos for oligo-cloning into DR274

oligo1	oligo2
Flt1_E3_sgRNA_1+: TAGGGACGGTGGGAGCTCCAGT	Flt1_E3_sgRNA_1-: AAACACTGGAGCTCCCACCGTC
Flt1_E5_sgRNA_1+: TAGGAATATCATCTGGAACAGC	Flt1_E5_sgRNA_1-: AAACGCTGTTCCAGATGATATT
Flt1_E11b_sgRNA_1+: TAGGCAGTCCAGGACGAAGGAGG	Flt1_E11b_sgRNA_1-: AAACCCTCCTTCGTCCTGGACTG
Flt1_E11b_sgRNA_2+: TAGGTGATGGTCAAGATGGGATTG	Flt1_E11b_sgRNA_2-: AAACCAATCCCATCTTGACCATCA
Flt1_E11b_sgRNA_3+: TAGGTCAAGATGGGATTGTGGG	Flt1_E11b_sgRNA_3-: AAACCCCACAATCCCATCTTGA
Flt1_E11b_sgRNA_4+: TAGGAGAAGCCTCCTCCTTCGTCC	Flt1_E11b_sgRNA_4-: AAACGGACGAAGGAGGAGGCTTCT
Flt1_E11b_sgRNA_5+: TAGGATGGTCAAGATGGGATTGT	Flt1_E11b_sgRNA_5-: AAACACAATCCCATCTTGACCAT

Table 6-10. Primer sequences used for construct cloning and genotyping

primer name	primer sequence
pME_GFP_p2A_fw	5'-GCAGGAGACGTGGAGGAGAACCCTGGACCCGGGGAATTCAAGGCCTCTCGAGCCTCTAGAT-3'
pME_GFP_p2A_rev	5'-TTGCTTTAACAGAGAGAAGTTAGTAGCTCCGCTTCCTGAATTCCCAGATCTTCCACCGCC-3'
vegfc_p2A_fw	5'-ATCAGCGCTCACTTATTTGGATTTTCTGTC-3'
vegfc_p2A_rev	5'-AGTCTCGAGTTAGTCCAGTCTTCCCCAGTATGTG-3'
sflt1_p2A_fw	5'-ATGTTCGATATATTATTTGTGATGATATTTGG-3'
sflt1_p2A_rev	5'-AAGTCTCGAGTCAGGCCAGCCGCGCCGGG-3'
Vegfaa_p2A_fw	5'-AACTTGGTTGTTTATTTGATACAGTTATTTCTCGC-3'
Vegfaa_p2A_rev	5'-AGTCTCGAGTCATCTTGGCTTTTCACATCT-3'
U6_flt1E3_1	5'-GGGACGGTGGGAGCTCCAGTGT-3'
U6_flt1E3_2	5'-ACTGGAGCTCCCACCGTCCCGA-3'
Flt1_E3_gDNA_f	5'-CAGCTCAACACACACAGTATTGTTTTA-3'
Flt1_E3_gDNA_r	5'-ACACCTGAAGCATCTTACCTGTGA-3'

Flt1E11A2386576F	5'-ATTCCCAAGAGACCTGAAATCGGAA-3'
Flt1E11A2386151R	5'-GCTTGATTGCAGTTATCTTGAGGCA-3'

6.2 Methods

6.2.1 Ethics statement

Zebrafish husbandry and experimental procedures were performed in accordance with the German animal protection standards and were approved by the Government of Baden-Württemberg, Regierungspräsidium Karlsruhe, Germany (Akz.: 35-9185.81/G-93/15).

6.2.2 Morpholino injections

Morpholino antisense oligomers (MOs; Gene Tools) were prepared at a stock concentration of 1mM according to the manufacturer. MOs were injected into the yolk of one-cell stage embryos as described (Krueger et al. 2011; Hogan et al. 2009; Santhakumar et al. 2012; Childs et al. 2002). MO sequences can be found in Table 6-3.

6.2.3 mRNA injection and generation of transgenic/mutant lines

For the generation of mutants 1nl of a mixture containing 600ng μl^{-1} capped and polyadenylated Cas9-nls mRNA and 50ng μl^{-1} sgRNA was injected into one-cell stage embryos (Hwang et al. 2013). Cas9 mRNA was produced by *in vitro* transcription using the mMessage mMachine T7 Ultra Kit (Ambion). For the generation of transgenic lines 1nl of a mixture of 12,5ng μl^{-1} Transposase mRNA and 25ng μl^{-1} plasmid DNA was injected into one-cell stage embryos.

6.2.4 Generating *flt1* mutants

The zebrafish *flt1* gene consists of 34 exons encoding membrane-bound *Flt1* (mFlt1) and a shorter soluble Flt1 (sFlt1) form. Soluble Flt1 is generated through alternative splicing of *flt1* mRNA at the exon 10 - Intron 10 boundary (Supplementary Figure 2a). To annihilate the

production of both *mflt1* and *sflt1* and obtain *flt1* mutants, we targeted exon 3, using a CRISPR/Cas approach. We designed five sgRNAs targeting exon 3, encoding the extracellular Ig1 domain relevant for Vegfaa binding. Oligonucleotides containing the GG-N18 targeting sequence and overhangs were purchased from Eurofins (Ebersberg, Germany). The annealed oligos were ligated into DR274 which was a gift from Keith Joung (Addgene plasmid # 42250) (Hwang et al. 2013). The corresponding genomic region (surrounding exon 3) was amplified by PCR using primer pair Flt1_E3_gDNA_r and Flt1_E3_gDNA_f and indels were quantified with T7EI assay or direct Sanger sequencing of the PCR product as described (for primer sequences see Supplementary Table 6)(Hwang et al. 2013). The T7EI cleavage products of 211 and 249 bp were quantified using ImageJ. The sgRNA^{flt1E3} (see Supplementary Table 4) with the highest cleavage rate (~70%) was used to generate the *flt1* mutants. WT embryos were coinjected with sgRNA^{flt1E3} plus capped and polyadenylated Cas9 mRNA. Four independent lines with frame shift mutations were investigated in more detail. The *flt1^{ka601} (exon 3 -1nt allele), flt1^{ka602} (exon 3 -5nt allele), flt1^{ka603} (exon 3 +5nt allele) and flt1^{ka604} (exon 3 -14nt allele)* have a premature termination codon (PTC) resulting in a truncated protein devoid of a functional extracellular Vegfaa binding domain. Embryos carrying the mutation were raised and outcrossed to vascular and neuronal reporter lines (*Tg(kdrl:eGFP)^{s843}, Tg(fli1a:eGFP)^{y1}, Tg(fli1a:nGFP)^{y7}, Tg(kdrl:hsa.HRAS-mcherry)^{s916}, and Tg(Xla.Tubb:DsRed)^{zf148}*).

6.2.5 Generation of *mflt1 specific* mutants

To generate *mflt1* mutants we used a CRISPR/Cas approach and designed an sgRNA targeting E11b, the first specific *mflt1* exon (Krueger et al. 2011). In this scenario splicing of intron 10 and exon 11a relevant for generating *sflt1* mRNA remains unaffected. Oligos Flt1E11_O1_A_15 and Flt1E11_O2_A_15 were annealed and cloned into DR274 as described for *flt1* mutants. Founders were identified by PCR and subsequent Sanger sequencing, using primers Flt1E11A2386576F and Flt1E11A2386151R. We identified four frame shift mutants harboring a PTC in exon 11b. *Flt1^{ka605} (exon 11b +28nt), flt1^{ka606} (exon 11b +20nt), flt1^{ka607} (exon 11b -1nt)* and *flt1^{ka608} (exon 11b -1nt and one mutation) mflt1* mutants were outcrossed to *Tg(kdrl:EGFP)^{s843}* and *Tg(Xla.Tubb:DsRed)^{zf148}*. All four *mflt1* mutants were phenotypically comparable and in this manuscript only the *mflt1* mutant *flt1^{ka605}* is shown.

All sgRNA sequences and oligos used for annealed oligo cloning into DR274 are listed in Supplementary Table 4,5.

6.2.6 Generation of p5E_ Xla.Tubb-3.8 and p5E_flt1^{enh}

The NBT_tauGFP plasmid was a kind gift by Enrique Amaya(Huang et al. 2007). The 3.8kb regulatory element derived from neural specific beta tubulin was removed from the NBT_tauGFP using SalI and HindIII and subcloned into SalI and HindIII digested and dephosphorylated p5E_MCS (Kwan et al. 2007). The 1kb *flt1* enhancer/promoter fragment from the pMiniTol2_flt1_ECR5a_pro_181_YFP (Bussmann et al. 2010) construct was subcloned into p5E_MCS using KpnI and HindIII. The resulting plasmids were named p5E_ Xla.Tubb-3.8 and p5E_flt1^{enh}.

6.2.7 Generation of pME_eGFP-p2A_SmaI

To easily detect transgenic cells the pME_eGFP (#455) from the Tol2kit (Kwan et al. 2007) was modified by site-directed mutagenesis PCR. The p2A sequence was added before the stop codon of GFP using pME_eGFP specific primer with 5'end extension coding for the p2A peptide and a SmaI restriction site just downstream of p2A for convenient subcloning (pME_eGFP_p2A_fw and pME_eGFP_p2A_rev primer).

6.2.8 pME_eGFP-p2A_*vegfaa* 165, vegfc and *sflt1* cloning

pME_eGFP-p2A_SmaI was digested with SmaI and XhoI. The inserts *vegfaa 165*, *vegfC* and *sflt1* were amplified from zebrafish cDNA using primers *vegfaa* _p2A_fw/rev, vegfc_p2A_fw/rev and *sflt1* _p2A_fw/rev. The PCR products were digested with XhoI and gel purified. Vector and inserts were ligated following the manufactures instructions (NEB T4 DNA Ligase). The resulting plasmids were named pME_eGFP-p2A_*vegfaa* 165, pME_eGFP-p2A_vegfc and pME_eGFP-p2A_*sflt1* .

6.2.9 Generation of gateway expression clones

pME_DN-MAML-eGFP was kindly provided by Caroline Burns(Zhao et al. 2014). p5E_flt1^{enh}, pME_DN-MAML-eGFP and p3E_polyA were recombined into pDestTol2CG2 according to the manufactures instructions (Thermo Fisher, LR Clonase II plus). The resulting plasmid was named pCG2_flt1_ DN-MAML-eGFP. p5E_Xla.Tubb-3.8, pME_eGFP-p2A_*sflt1* and p3E_polyA were recombined into pDestTol2CG2 (pCG2_Xla.Tubb-3.8_eGFP-p2A-*sflt1*). p5E_Xla.Tubb-3.8, pME_eGFP-p2A_*sflt1* and p3E_polyA were recombined into pDestTol2CG2 (pCG2_Xla.Tubb-3.8_eGFP-p2A-*sflt1*). p5E_elavl-3.2 (unpublished), pME_gal4ERT2 and p3E_polyA were recombined into pDestTol2CG2 (pCG2_elavl-3.2_gal4-ERT2). p5E_flt1^{enh} , pME_gal4ERT2 and p3E_polyA were recombined into pDestTol2CG2 (pCG2_ flt1^{enh}_gal4-ERT2).

6.2.10 Generation of tissue-specific KO constructs

pME-Cas9-T2A-GFP and pDestTol2pA2-U6:gRNA were a gift from Leonard Zon (Addgene plasmid # 63157 and # 63155) (Ablain et al. 2015). pDestTol2pA2-U6:gRNA^{flt1E3} was generated by annealed oligo cloning. Oligos U6_flt1E3_1 and U6_flt1E3_2 were cloned into pDestTol2pA2-U6:gRNA as described(Ablain et al. 2015). To drive Cas9 expression specifically in neurons, the Gal4 driver construct pCG2_Xla:Tubb-3.8_gal4ERT2 was generated by recombining p5E_Xla.Tubb-3.8, pME_gal4ERT2, p3E_polyA and pDestTol2CG2. For the Gal4 effector construct, p5E_UAS, pME_cas9-t2a-eGFP and p3E_polyA were recombined into pDestTol2pA2-U6:sgRNA^{flt1E3} (pCG2_UAS_Cas9-t2A-eGFP_U6_gRNA^{flt1E3}).

6.2.11 FACS analysis

Approximately 500 embryos *Tg(mnx1:GFP)*^{ml2}, *Tg(HuC:EGFP)*^{as8}, *Tg(Xla.Tubb:DsRed)*^{zf148} or vhl MO injected *Tg(Xla.Tubb:DsRed)*^{zf148} embryos were dechorionated at 24 hpf using pronase (0.5 mg/ml). Cells were dissociated using FACSMax as described (Manoli & Driever 2012). *Tg(mnx1:GFP)*^{ml2}, *Tg(HuC:EGFP)*^{as8} embryos were dissociated and sorted at 24hpf, control and *vhl* MO injected *Tg(Xla.Tubb:DsRed)*^{zf148} embryos were dissociated and sorted at 3dpf. Dissociated cells were FACS-sorted using BD-FACS-Aria I and Aria II. The sorted cells (approx. 0.5 x 10^6 cells per experiment) were spinned down at 310g for 5 min and resuspended in lysis buffer contained in the RNeasy mini kit (Qiagen). RNA was extracted as described in the manual. Due to limited amounts of RNA the QuantiTect Whole Transcriptome Kit (Qiagen) was used to preamplify and reverse transcribe the RNA to make cDNA. cDNA was diluted 1:250 for real-time qPCR.

6.2.12 Gene expression analysis by real-time qPCR

Total RNA of zebrafish embryos was isolated with TRIzol, purified with RNeasy mini kit (Qiagen) and quantity and quality were measured using an Agilent 2100 Bioanalyzer (Agilent Technologies) according to the manufacturer's instructions. We performed DNase on-column digestion using RNase-free DNase Set (Qiagen) according to the manufacturer, followed by cDNA synthesis using the Thermoscript First-Strand Synthesis System (Thermo Fisher Scientific). qPCR was conducted with SYBR® Green PCR Master Mix (Thermo Scientific) in a StepOnePlus™ real-time qPCR system (Applied Biosystems). Primers for real-time qPCR were ordered from Eurofins Genomics. Gene expression data were normalized against zebrafish elongation factor 1-alpha. Primers and probes are listed in Table 1-3.

6.2.13 RNA-Seq library preparation and sequencing

Zebrafish RNA was isolated and purified from 4dpf zebrafish larvae using TRIzol and RNeasy mini kit (Qiagen) as recommended by the manufacturers. A cDNA library was generated using the TruSeq Ilumina RNA sample prepv2 kit according to the manufacturer's protocol. The cDNA library was sequenced on a HiSeq2000 according to the manufacturer's protocols (Illumina).

6.2.14 Identification of differentially expressed genes

Raw sequencing reads were mapped to the transcriptome and the zebrafish reference genome (GRCz10 danRer10) using Bowtie2.0 and TopHat 2.0 (Trapnell et al. 2012). On average 44,490,573 reads (81,6% of total reads) were assigned to genes with Cufflinks and HTSeq software package (Anders et al. 2014). Differentially expressed genes (control vs. mutant) were identified using DESeq and Cuffdiff (Anders & Huber 2010; Trapnell et al. 2012). Genes were defined as differentially expressed if ≥ 2 fold significantly regulated *(P< 0.05)* with two independent methods (DEseq and Cuffdiff).

6.2.15 Zebrafish histological sectioning

Dechorionated larvae were fixed in 4%PFA for 2h and subsequently transferred to 20% DMSO/ 80% Methanol and incubated overnight at -20°C. Larvae were then washed in 100mM NaCl, 100mMTris-HCl, pH7.4 for 30 min at room temperature. Washed larvae were embedded in gelatin from cold water fish skin/ sucrose (Sigma) as described (Fagotto & Gumbiner 1994). Larvae were sectioned (20µm) in a cryomicrotome.

6.2.16 Inhibitor treatments

All stock solutions were prepared in DMSO. Embryos were dechorionated at 24hpf using Pronase (Roche, Basel, Switzerland). Embryos were incubated from 2.5dpf with 100µM of DAPT (Sigma, St Louis, MO, USA), 25µM MAZ51 (Merck Millipore, Billerica, Massachusetts, USA) or 0.125µM ki8751 (Sigma, St Louis, MO, USA). Control embryos were mock treated with DMSO (Sigma, St Louis, MO, USA). Embryos were randomly assigned to experimental groups. Investigators were blinded to inhibitor treatment.

6.2.17 Gal4ERT2 endoxifen activation

Endoxifen (Sigma) was solved in DMSO. Zebrafish embryos expressing Gal4ERT2 were incubated from 52hpf onwards in 0.5µM endoxifen in E3 medium in the dark. GFP positive cells could be observed approximately 1.5 hours after induction.

6.2.18 Vascular network analysis

To assess sprout number and length, we developed a semi-automated analysis of the DLAV-ISV vessel network using ImageJ (Supplementary Figure 1e). Image-stacks of ISVs were acquired using the Leica SP8 confocal microscope. Stack projections of one side of the trunk were generated. Dorsal region of the ISVs was used for analysis. Using ImageJ a Gaussian blur filter was applied followed by a black/white threshold and subsequent skeletonization to generate a skeleton of the vasculature. Segment number, branch point number and total branch length were calculated using the "analyze skeleton" plugin. The semi-automated pipeline was applied for analysis of 4dpf vascular networks, while sprout numbers in 2-3dpf zebrafish embryos were counted manually.

6.2.19 Imaging

Zebrafish larvae were embedded in 0.7% low melting agarose with 0.112mg/mL Tricaine (E10521, Sigma) and 0.003% PTU (P7629, Sigma) in glass bottom dishes (MatTek, P35G-0.170-14-C). Images presented in this study were acquired using a Leica SP8 confocal microscope with LAS X software. Images were processed using ImageJ. Vascular branching was quantified using a semi-automated ImageJ pipeline (Supplementary Figure 1e). Animal numbers used are indicated in figure legends. For zebrafish mutants more than 100 embryos per genotype were analyzed. In morpholino experiments morphologically malformed embryos were excluded from analysis.

6.2.20 Statistical analysis

Statistical analysis was performed using GraphPad Prism 6. Each dataset was tested for normal distribution (D'Agostino and Pearson test). Parametric method (unpaired Students t-test) was only applied if the data were normally distributed. For non-normal distributed data sets, a non-parametric test (Mann Whitney U test) was applied. When appropriate in case of multiple comparisons, Bonferroni correction was applied. P values <0.05 were considered significant. Data are represented as mean ± s.e.m., unless otherwise indicated. *P< 0.05, **P< 0.01 and ***P< 0.001.

7 Bibliography

Ablain, J. et al., 2015. A CRISPR/Cas9 Vector System for Tissue-Specific Gene Disruption in Zebrafish. *Developmental Cell*, 32(6), pp.756–64.

Adams, R.H. & Alitalo, K., 2007. Molecular regulation of angiogenesis and lymphangiogenesis. *Nature Reviews. Molecular Cell Biology*, 8(6), pp.464–478.

Adams, R.H. & Eichmann, A., 2010. Axon guidance molecules in vascular patterning. *Cold Spring Harbor perspectives in biology*, 2(5).

Agarwal, I. & Karumanchi, S.A., 2011. Preeclampsia and the Anti-Angiogenic State. *Pregnancy hypertension*, 1(1), pp.17–21.

Aird, W.C., 2005. Spatial and temporal dynamics of the endothelium. *Journal of thrombosis and haemostasis : JTH*, 3(7), pp.1392–406.

Al-Husein, B. et al., 2012. Antiangiogenic therapy for cancer: an update. *Pharmacotherapy*, 32(12), pp.1095–111.

Ambati, B.K. et al., 2006. Corneal avascularity is due to soluble VEGF receptor-1. *Nature*, 443(7114), pp.993–7.

Ambrose, J. & Singh, M., 2015. Pathophysiology of coronary artery disease leading to acute coronary syndromes. *F1000Prime Reports*, 7(8).

Anders, S. & Huber, W., 2010. Differential expression analysis for sequence count data. *Genome biology*, 11(10), p.R106.

Anders, S., Pyl, P.T. & Huber, W., 2014. HTSeq - A Python framework to work with high-throughput sequencing data. *Bioinformatics (Oxford, England)*, 31(2), pp.166–9.

Arany, Z. et al., 2008. HIF-independent regulation of VEGF and angiogenesis by the transcriptional coactivator PGC-1α. *Nature*, 451(7181), pp.1008–1012.

Auer, T. & Bene, F. Del, 2014. CRISPR/Cas9 and TALEN-mediated knock-in approaches in zebrafish. *Methods*.

Autiero, M. et al., 2003. Placental growth factor and its receptor, vascular endothelial growth factor receptor-1: novel targets for stimulation of ischemic tissue revascularization and inhibition of angiogenic and inflammatory disorders. *Journal of thrombosis and haemostasis : JTH*, 1(7), pp.1356–70.

Bautch, V.L. & James, J.M., 2009. Neurovascular development: The beginning of a beautiful friendship. *Cell adhesion & migration*, 3(2), pp.199–204.

Bazzoni, G. & Dejana, E., 2004. Endothelial cell-to-cell junctions: molecular organization and role in vascular homeostasis. *Physiological reviews*, 84(3), pp.869–901.

Ben-Zvi, A. et al., 2008. The Semaphorin receptor PlexinA3 mediates neuronal apoptosis during dorsal root ganglia development. *The Journal of neuroscience : the official journal of the Society for Neuroscience*, 28(47), pp.12427–32.

Del Bene, F., 2011. Interkinetic nuclear migration: cell cycle on the move. *The EMBO journal*, 30(9), pp.1676–7.

Benedito, R. et al., 2012. Notch-dependent VEGFR3 upregulation allows angiogenesis without VEGF-VEGFR2 signalling. *Nature*, 484(7392), pp.110–4.

Benedito, R. et al., 2009. The Notch Ligands Dll4 and Jagged1 Have Opposing Effects on Angiogenesis. *Cell*,

137(6), pp.1124–1135.

Bentley, K. et al., 2014. The role of differential VE-cadherin dynamics in cell rearrangement during angiogenesis. *Nature cell biology*, 16(4), pp.309–21.

Bergers, G. & Benjamin, L.E., 2003. Tumorigenesis and the angiogenic switch. *Nature reviews. Cancer*, 3(6), pp.401–10.

Bergers, G. & Song, S., 2005. The role of pericytes in blood-vessel formation and maintenance. *Neuro-oncology*, 7(4), pp.452–64.

Bill, B.R. et al., 2009. A Primer for Morpholino Use in Zebrafish. *Zebrafish*, 6(1), pp.69–77.

Blanco, R. & Gerhardt, H., 2013. VEGF and Notch in tip and stalk cell selection. *Cold Spring Harbor perspectives in medicine*, 3(1), p.a006569.

Blum, M. et al., 2015. Morpholinos: Antisense and Sensibility. *Developmental Cell*, 35(2), pp.145–149.

De Bock, K. et al., 2013. Role of endothelial cell metabolism in vessel sprouting. *Cell metabolism*, 18(5), pp.634–47.

Boeckel, J.-N. et al., 2011. Jumonji domain-containing protein 6 (Jmjd6) is required for angiogenic sprouting and regulates splicing of VEGF-receptor 1. *Proceedings of the National Academy of Sciences of the United States of America*, 108(8), pp.3276–3281.

Brozzo, M.S. et al., 2012. Thermodynamic and structural description of allosterically regulated VEGFR-2 dimerization. *Blood*, 119(7), pp.1781–8.

Burke, S.D. et al., 2016. Soluble fms-like tyrosine kinase 1 promotes angiotensin II sensitivity in preeclampsia. *Journal of Clinical Investigation*, 126(7), pp.2856–2869.

Burri, P.H., Hlushchuk, R. & Djonov, V., 2004. Intussusceptive angiogenesis: its emergence, its characteristics, and its significance. *Developmental dynamics : an official publication of the American Association of Anatomists*, 231(3), pp.474–88.

Buschmann, I. et al., 2010. Pulsatile shear and Gja5 modulate arterial identity and remodeling events during flow-driven arteriogenesis. *Development (Cambridge, England)*, 137(13), pp.2187–96.

Bussmann, J. et al., 2010. Arteries provide essential guidance cues for lymphatic endothelial cells in the zebrafish trunk. *Development (Cambridge, England)*, 137(16), pp.2653–7.

Bussmann, J. et al., 2008. Zebrafish VEGF receptors: A guideline to nomenclature. *PLoS Genetics*, 4(5), pp.4–5.

Bussmann, J., Bakkers, J. & Schulte-Merker, S., 2007. Early endocardial morphogenesis requires Scl/Tal1. *PLoS genetics*, 3(8), p.e140.

Bussmann, J., Wolfe, S.A. & Siekmann, A.F., 2011. Arterial-venous network formation during brain vascularization involves hemodynamic regulation of chemokine signaling. *Development (Cambridge, England)*, 138(9), pp.1717–1726.

Carmeliet, P. et al., 1996. Abnormal blood vessel development and lethality in embryos lacking a single VEGF allele. *Nature*, 380(6573), pp.435–9.

Carmeliet, P., 2003. Angiogenesis in health and disease. *Nature Medicine*, 9(6), pp.653–660.

Carmeliet, P., 2005. Angiogenesis in life, disease and medicine. *Nature*, 438(7070), pp.932–6.

Carmeliet, P. et al., 1998. Role of HIF-1alpha in hypoxia-mediated apoptosis, cell proliferation and tumour angiogenesis. *Nature*, 394(6692), pp.485–90.

Carmeliet, P. & Tessier-Lavigne, M., 2005. Common mechanisms of nerve and blood vessel wiring. *Nature*, 436(7048), pp.193–200.

Chappell, J.C. et al., 2016. Flt-1 (VEGFR-1) Coordinates Discrete Stages of Blood Vessel Formation. *Cardiovascular research*, p.cvw091–.

Chappell, J.C. et al., 2009. Local guidance of emerging vessel sprouts requires soluble Flt-1. *Developmental Cell*, 17(3), pp.377–386.

Chappell, J.C., Mouillesseaux, K.P. & Bautch, V.L., 2013. Flt-1 (vascular endothelial growth factor receptor-1) is essential for the vascular endothelial growth factor-Notch feedback loop during angiogenesis. *Arteriosclerosis, Thrombosis, and Vascular Biology*, 33(8), pp.1952–1959.

Childs, S. et al., 2002. Patterning of angiogenesis in the zebrafish embryo. *Development (Cambridge, England)*, 129(4), pp.973–82.

Choorapoikayil, S. et al., 2013. Loss of Pten promotes angiogenesis and enhanced vegfaa expression in zebrafish. *Disease models & mechanisms*, 6(5), pp.1159–66.

Christinger, H.W. et al., 2004. The crystal structure of placental growth factor in complex with domain 2 of vascular endothelial growth factor receptor-1. *The Journal of biological chemistry*, 279(11), pp.10382–8.

Clauss, M. et al., 1996. The Vascular Endothelial Growth Factor Receptor Flt-1 Mediates Biological Activities: IMPLICATIONS FOR A FUNCTIONAL ROLE OF PLACENTA GROWTH FACTOR IN MONOCYTE ACTIVATION AND CHEMOTAXIS. *Journal of Biological Chemistry*, 271(30), pp.17629–17634.

Cohen, T. et al., 1995. VEGF121, a vascular endothelial growth factor (VEGF) isoform lacking heparin binding ability, requires cell-surface heparan sulfates for efficient binding to the VEGF receptors of human melanoma cells. *The Journal of biological chemistry*, 270(19), pp.11322–6.

Covassin, L. et al., 2006. Global analysis of hematopoietic and vascular endothelial gene expression by tissue specific microarray profiling in zebrafish. *Developmental Biology*, 299(2), pp.551–562.

Covassin, L.D. et al., 2009. A genetic screen for vascular mutants in zebrafish reveals dynamic roles for Vegf/Plcg1 signaling during artery development. *Developmental biology*, 329(2), pp.212–226.

Covassin, L.D. et al., 2006. Distinct genetic interactions between multiple Vegf receptors are required for development of different blood vessel types in zebrafish. *Proceedings of the National Academy of Sciences of the United States of America*, 103(17), pp.6554–9.

Cui, X. et al., 2015. Venous Endothelial Marker COUP-TFII Regulates the Distinct Pathologic Potentials of Adult Arteries and Veins. *Scientific Reports*, 5, p.16193.

Davis, G.E. & Camarillo, C.W., 1996. An alpha 2 beta 1 integrin-dependent pinocytic mechanism involving intracellular vacuole formation and coalescence regulates capillary lumen and tube formation in three-dimensional collagen matrix. *Experimental cell research*, 224(1), pp.39–51.

Davis, R.H., 2004. Timeline: The age of model organisms. *Nature Reviews Genetics*, 5(1), pp.69–76.

Degen, A., Millenaar, D. & Schirmer, S.H., 2014. Therapeutic approaches in the stimulation of the coronary collateral circulation. *Current cardiology reviews*, 10(1), pp.65–72.

Dejana, E., 2004. Endothelial cell-cell junctions: happy together. *Nature reviews. Molecular cell biology*, 5(4), pp.261–70.

Dejana, E., Tournier-Lasserve, E. & Weinstein, B.M., 2009. The control of vascular integrity by endothelial cell

junctions: molecular basis and pathological implications. *Developmental cell*, 16(2), pp.209–21.

Dewerchin, M. & Carmeliet, P., 2012. PlGF: A multitasking cytokine with disease-restricted activity. *Cold Spring Harbor Perspectives in Medicine*, 2(8), pp.1–24.

Dorrell, M.I., Aguilar, E. & Friedlander, M., 2002. Retinal vascular development is mediated by endothelial filopodia, a preexisting astrocytic template and specific R-cadherin adhesion. *Investigative ophthalmology & visual science*, 43(11), pp.3500–10.

Dumont, D.J. et al., 1998. Cardiovascular failure in mouse embryos deficient in VEGF receptor-3. *Science (New York, N.Y.)*, 282(5390), pp.946–9.

Eichmann, A., 2010. Regulation of blood vessel patterning and guidance. *The FASEB Journal*, 24(1 Supplement), pp.62.3–62.3.

Eisen, J.S., 1991. Motoneuronal development in the embryonic zebrafish. *Development Supplement*, 2, pp.141–147.

Eisen, J.S. & Smith, J.C., 2008. Controlling morpholino experiments: don't stop making antisense. *Development*, 135(10), pp.1735–1743.

Eliasson, P. & Jönsson, J.-I., 2010. The hematopoietic stem cell niche: low in oxygen but a nice place to be. *Journal of cellular physiology*, 222(1), pp.17–22.

Ellertsdóttir, E. et al., 2010. Vascular morphogenesis in the zebrafish embryo. *Developmental Biology*, 341(1), pp.56–65.

Eremina, V. et al., 2003. Glomerular-specific alterations of VEGF-A expression lead to distinct congenital and acquired renal diseases. *The Journal of clinical investigation*, 111(5), pp.707–16.

Fagotto, F. & Gumbiner, B.M., 1994. Beta-catenin localization during Xenopus embryogenesis: accumulation at tissue and somite boundaries. *Development (Cambridge, England)*, 120(12), pp.3667–79.

Fantin, A. et al., 2010. Tissue macrophages act as cellular chaperones for vascular anastomosis downstream of VEGF-mediated endothelial tip cell induction. *Blood*, 116(5), pp.829–40.

Ferrara, N. et al., 1996. Heterozygous embryonic lethality induced by targeted inactivation of the VEGF gene. *Nature*, 380(6573), pp.439–42.

Ferrara, N., 2005. The role of VEGF in the regulation of physiological and pathological angiogenesis. *EXS*, (94), pp.209–31.

Flamme, I., Frölich, T. & Risau, W., 1997. Molecular mechanisms of vasculogenesis and embryonic angiogenesis. *Journal of cellular physiology*, 173(2), pp.206–10.

Folkman, J., 1971. Tumor Angiogenesis: Therapeutic Implications. *http://dx.doi.org/10.1056/NEJM197111182852108*.

Folkman, J. & Haudenschild, C., 1980. Angiogenesis in vitro. *Nature*, 288(5791), pp.551–556.

Folkman, J. & Shing, Y., 1992. Angiogenesis. *The Journal of biological chemistry*, 267(16), pp.10931–4.

Fong, G.-H.H. et al., 1996. Regulation of flt-1 expression during mouse embryogenesis suggests a role in the establishment of vascular endothelium. *Developmental Dynamics*, 207(1), pp.1–10.

Fong, G.-H.H. et al., 1995. Role of the Flt-1 receptor tyrosine kinase in regulating the assembly of vascular endothelium. *Nature*, 376(6535), pp.66–70.

Fong, G.H. et al., 1999. Increased hemangioblast commitment, not vascular disorganization, is the primary

defect in flt-1 knock-out mice. *Development (Cambridge, England)*, 126(13), pp.3015–3025.

Füller, T. et al., 2003. Forward EphB4 signaling in endothelial cells controls cellular repulsion and segregation from ephrinB2 positive cells. *Journal of cell science*, 116(Pt 12), pp.2461–70.

Funahashi, Y. et al., 2010. Notch regulates the angiogenic response via induction of VEGFR-1. *Journal of angiogenesis research*, 2(1), p.3.

Furne, C. et al., 2008. Netrin-1 is a survival factor during commissural neuron navigation. *Proceedings of the National Academy of Sciences of the United States of America*, 105(38), pp.14465–70.

Galie, P.A. et al., 2014. Fluid shear stress threshold regulates angiogenic sprouting. *Proceedings of the National Academy of Sciences*, 111(22), pp.7968–7973.

Gay, C.M., Zygmunt, T. & Torres-Vázquez, J., 2011. Diverse functions for the semaphorin receptor PlexinD1 in development and disease. *Developmental biology*, 349(1), pp.1–19.

Gebala, V. et al., 2016. Blood flow drives lumen formation by inverse membrane blebbing during angiogenesis in vivo. *Nature Cell Biology*, 18(4), pp.443–450.

Gerhardt, H., 2008. VEGF and endothelial guidance in angiogenic sprouting. *Organogenesis*, 4(4), pp.241–6.

Gerhardt, H. et al., 2003. VEGF guides angiogenic sprouting utilizing endothelial tip cell filopodia. *The Journal of Cell Biology*, 161(6), pp.1163–1177.

Glasauer, S.M.K. & Neuhauss, S.C.F., 2014. Whole-genome duplication in teleost fishes and its evolutionary consequences. *Molecular genetics and genomics : MGG*, 289(6), pp.1045–60.

Gordon, W.R. et al., 2015. Mechanical Allostery: Evidence for a Force Requirement in the Proteolytic Activation of Notch. *Developmental Cell*, 33(6), pp.729–736.

Gore, A. V. et al., 2011. Rspo1/Wnt signaling promotes angiogenesis via Vegfc/Vegfr3. *Development*, 138(22), pp.4875–4886.

Götz, M. & Huttner, W.B., 2005. The cell biology of neurogenesis. *Nature reviews. Molecular cell biology*, 6(10), pp.777–88.

Goulding, M., 2009. Circuits controlling vertebrate locomotion: moving in a new direction. *Nature reviews. Neuroscience*, 10(7), pp.507–18.

Guarani, V. et al., 2011. Acetylation-dependent regulation of endothelial Notch signalling by the SIRT1 deacetylase. *Nature*, 473(7346), pp.234–8.

Le Guen, L. et al., 2014. Ccbe1 regulates Vegfc-mediated induction of Vegfr3 signaling during embryonic lymphangiogenesis. *Development (Cambridge, England)*, 141(6), pp.1239–49.

Gundersen, G.G. & Worman, H.J., 2013. Nuclear positioning. *Cell*, 152(6), pp.1376–89.

Haigh, J.J., 2008. Role of VEGF in organogenesis. *Organogenesis*, 4(4), pp.247–56.

Hanahan, D. & Folkman, J., 1996. Patterns and Emerging Mechanisms of the Angiogenic Switch during Tumorigenesis. *Cell*, 86(3), pp.353–364.

Helker, C.S.M. et al., 2015. The hormonal peptide Elabela guides angioblasts to the midline during vasculogenesis. *eLife*, 4, p.e06726.

Hellström, M. et al., 2007. Dll4 signalling through Notch1 regulates formation of tip cells during angiogenesis. *Nature*, 445(7129), pp.776–80.

Hen, G. et al., 2015. Venous-derived angioblasts generate organ-specific vessels during zebrafish embryonic

development. *Development (Cambridge, England)*, 142(24), pp.4266–78.

Herbert, S.P. et al., 2009. Arterial-Venous Segregation by Selective Cell Sprouting: An Alternative Mode of Blood Vessel Formation. *Science*, 326(5950), pp.294–298.

Herbert, S.P. & Stainier, D.Y.R., 2011. Molecular control of endothelial cell behaviour during blood vessel morphogenesis. *Nature Reviews Molecular Cell Biology*, 12(9), pp.551–564.

Herley, M.T. et al., 1999. Characterization of the VEGF Binding Site on the Flt-1 Receptor. *Biochemical and Biophysical Research Communications*, 262(3), pp.731–738.

Herwig, L. et al., 2011. Distinct cellular mechanisms of blood vessel fusion in the zebrafish embryo. *Current biology : CB*, 21(22), pp.1942–8.

Hirashima, M. et al., 2003. A chemically defined culture of VEGFR2+ cells derived from embryonic stem cells reveals the role of VEGFR1 in tuning the threshold for VEGF in developing endothelial cells. *Blood*, 101(6), pp.2261–7.

Hiratsuka, S. et al., 1998. Flt-1 lacking the tyrosine kinase domain is sufficient for normal development and angiogenesis in mice. *Proceedings of the National Academy of Sciences of the United States of America*, 95(16), pp.9349–54.

Hiratsuka, S. et al., 2001. Involvement of Flt-1 tyrosine kinase (vascular endothelial growth factor receptor-1) in pathological angiogenesis. *Cancer research*, 61(3), pp.1207–13.

Hiratsuka, S. et al., 2005. Membrane fixation of vascular endothelial growth factor receptor 1 ligand-binding domain is important for vasculogenesis and angiogenesis in mice. *Molecular and cellular biology*, 25(1), pp.346–54.

Ho, V.C. et al., 2012. Elevated vascular endothelial growth factor receptor-2 abundance contributes to increased angiogenesis in vascular endothelial growth factor receptor-1-deficient mice. *Circulation*, 126(6), pp.741–52.

Hogan et al., 2009. Vegfc/Flt4 signalling is suppressed by Dll4 in developing zebrafish intersegmental arteries. *Development (Cambridge, England)*, 136(23), pp.4001–9.

Hogan, B. et al., 2009. ccbe1 is required for embryonic lymphangiogenesis and venous sprouting. *Nature Genetics*, 41(4), pp.396–398.

Holmqvist, K. et al., 2003. The Shb adaptor protein causes Src-dependent cell spreading and activation of focal adhesion kinase in murine brain endothelial cells. *Cellular signalling*, 15(2), pp.171–9.

Huang, J.K. et al., 2007. BDNF promotes target innervation of Xenopus mandibular trigeminal axons in vivo. *BMC developmental biology*, 7, p.59.

Hwang, W.Y. et al., 2013. Efficient genome editing in zebrafish using a CRISPR-Cas system. *Nature Biotechnology*, 31(3), pp.227–229.

Iijima, M. et al., 2002. Tumor Suppressor PTEN Mediates Sensing of Chemoattractant Gradients. *Cell*, 109(5), pp.599–610.

Ikeda, T. et al., 2011. Hypoxia down-regulates sFlt-1 (sVEGFR-1) expression in human microvascular endothelial cells by a mechanism involving mRNA alternative processing. *The Biochemical journal*, 436(2), pp.399–407.

van Impel, A. et al., 2014. Divergence of zebrafish and mouse lymphatic cell fate specification pathways.

Development (Cambridge, England), 141(6), pp.1228–38.

Isogai, S. et al., 2003. Angiogenic network formation in the developing vertebrate trunk. *Development (Cambridge, England)*, 130(21), pp.5281–90.

Isogai, S., Horiguchi, M. & Weinstein, B.M., 2001. The vascular anatomy of the developing zebrafish: an atlas of embryonic and early larval development. *Developmental biology*, 230(2), pp.278–301.

Jahnsen, E.D. et al., 2015. Notch1 is pan-endothelial at the onset of flow and regulated by flow. *PloS one*, 10(4), p.e0122622.

Jakobsson, L. et al., 2010. Endothelial cells dynamically compete for the tip cell position during angiogenic sprouting. *Nature cell biology*, 12(10), pp.943–53.

James, J.M., Gewolb, C. & Bautch, V.L., 2009. Neurovascular development uses VEGF-A signaling to regulate blood vessel ingression into the neural tube. *Development (Cambridge, England)*, 136(5), pp.833–41.

Jensen, L.D. et al., 2015. VEGF-B-Neuropilin-1 signaling is spatiotemporally indispensable for vascular and neuronal development in zebrafish. *Proceedings of the National Academy of Sciences of the United States of America*, 112(44), pp.E5944–53.

Jin, S.-W. et al., 2005. Cellular and molecular analyses of vascular tube and lumen formation in zebrafish. *Development (Cambridge, England)*, 132(23), pp.5199–209.

Jones, E.A. V et al., 2008. Separating genetic and hemodynamic defects in neuropilin 1 knockout embryos. *Development (Cambridge, England)*, 135(14), pp.2479–88.

Joukov, V. et al., 1997. Proteolytic processing regulates receptor specificity and activity of VEGF-C. *The EMBO journal*, 16(13), pp.3898–911.

Kamei, M. et al., 2006. Endothelial tubes assemble from intracellular vacuoles in vivo. *Nature*, 442(7101), pp.453–456.

Kamei, M. & Weinstein, B.M., 2005. Long-term time-lapse fluorescence imaging of developing zebrafish. *Zebrafish*, 2(2), pp.113–23.

Kania, A. & Klein, R., 2016. Mechanisms of ephrin-Eph signalling in development, physiology and disease. *Nature reviews. Molecular cell biology*, 17(4), pp.240–256.

Kawasaki, J. et al., 2014. RASA1 functions in EPHB4 signaling pathway to suppress endothelial mTORC1 activity. *The Journal of clinical investigation*, 124(6), pp.2774–84.

Kearney, J.B. et al., 2004. The VEGF receptor flt-1 (VEGFR-1) is a positive modulator of vascular sprout formation and branching morphogenesis. *Blood*, 103(12), pp.4527–35.

Kemp, H.A., Carmany-Rampey, A. & Moens, C., 2009. Generating chimeric zebrafish embryos by transplantation. *Journal of visualized experiments : JoVE*, (29).

Kimura, E., Isogai, S. & Hitomi, J., 2015. Integration of vascular systems between the brain and spinal cord in zebrafish. *Developmental biology*, 406(1), pp.40–51.

Kimura, H. et al., 2000. Hypoxia response element of the human vascular endothelial growth factor gene mediates transcriptional regulation by nitric oxide: control of hypoxia-inducible factor-1 activity by nitric oxide. *Blood*, 95(1), pp.189–97.

Koch, S. & Claesson-Welsh, L., 2012. Signal transduction by vascular endothelial growth factor receptors. *Cold Spring Harbor perspectives in medicine*, 2(7), p.a006502.

Kok, F.O. et al., 2014. Reverse Genetic Screening Reveals Poor Correlation between Morpholino-Induced and Mutant Phenotypes in Zebrafish. *Developmental Cell*, 32(1), pp.97–108.

Koltowska, K. et al., 2015. Vegfc Regulates Bipotential Precursor Division and Prox1 Expression to Promote Lymphatic Identity in Zebrafish. *Cell reports*, 13(9), pp.1828–41.

Krueger, J. et al., 2011. Flt1 acts as a negative regulator of tip cell formation and branching morphogenesis in the zebrafish embryo. *Development (Cambridge, England)*, 138(10), pp.2111–20.

Küchler et al., 2006. Development of the zebrafish lymphatic system requires VEGFC signaling. *Current biology*, 16(12), pp.1244–8.

Kwan, K.M. et al., 2007. The Tol2kit: a multisite gateway-based construction kit for Tol2 transposon transgenesis constructs. *Developmental dynamics: an official publication of the American Association of Anatomists*, 236(11), pp.3088–3099.

Kwon, H.-B.H.-B. et al., 2013. The parallel growth of motoneuron axons with the dorsal aorta depends on Vegfc/Vegfr3 signaling in zebrafish. *Development*, 140(19), pp.4081–4090.

Lange, C., Turrero Garcia, M., et al., 2016. Relief of hypoxia by angiogenesis promotes neural stem cell differentiation by targeting glycolysis. *The EMBO journal*.

Lange, C., Storkebaum, E., et al., 2016. Vascular endothelial growth factor: a neurovascular target in neurological diseases. *Nature Reviews Neurology*, 12(8), pp.439–454.

Lawson, N.D. et al., 2001. Notch signaling is required for arterial-venous differentiation during embryonic vascular development. *Development (Cambridge, England)*, 128(19), pp.3675–3683.

Lawson, N.D. et al., 2003. phospholipase C gamma-1 is required downstream of vascular endothelial growth factor during arterial development. *Genes & Development*, 17(11), pp.1346–1351.

Lawson, N.D., Vogel, A.M. & Weinstein, B.M., 2002. Sonic hedgehog and vascular endothelial growth factor act upstream of the Notch pathway during arterial endothelial differentiation. *Developmental Cell*, 3(1), pp.127–136.

Lee, S. et al., 2007. Autocrine VEGF signaling is required for vascular homeostasis. *Cell*, 130(4), pp.691–703.

Lee, S. et al., 2005. Processing of VEGF-A by matrix metalloproteinases regulates bioavailability and vascular patterning in tumors. *The Journal of cell biology*, 169(4), pp.681–91.

Lenard, A. et al., 2013. In vivo analysis reveals a highly stereotypic morphogenetic pathway of vascular anastomosis. *Developmental cell*, 25(5), pp.492–506.

Leppänen, V.-M. et al., 2013. Structural and mechanistic insights into VEGF receptor 3 ligand binding and activation. *Proceedings of the National Academy of Sciences of the United States of America*, 110(32), pp.12960–5.

Leslie, J.D. et al., 2007. Endothelial signalling by the Notch ligand Delta-like 4 restricts angiogenesis. *Development*, 134(5), pp.839–844.

Lewis, K.E. & Eisen, J.S., 2003. From cells to circuits: development of the zebrafish spinal cord. *Progress in Neurobiology*, 69(6), pp.419–449.

Liang, D. et al., 2001. The role of vascular endothelial growth factor (VEGF) in vasculogenesis, angiogenesis, and hematopoiesis in zebrafish development. *Mechanisms of Development*, 108(1-2), pp.29–43.

Lieschke, G.J. & Currie, P.D., 2007. Animal models of human disease: zebrafish swim into view. *Nature Reviews*

Genetics, 8(5), pp.353–367.

Liu, Y. et al., 1995. Hypoxia Regulates Vascular Endothelial Growth Factor Gene Expression in Endothelial Cells : Identification of a 5' Enhancer. *Circulation Research*, 77(3), pp.638–643.

Liu, Z.-J. et al., 2003. Regulation of Notch1 and Dll4 by vascular endothelial growth factor in arterial endothelial cells: implications for modulating arteriogenesis and angiogenesis. *Molecular and cellular biology*, 23(1), pp.14–25.

Makita, T. et al., 2008. Endothelins are vascular-derived axonal guidance cues for developing sympathetic neurons. *Nature*, 452(7188), pp.759–763.

Mannello, F., Medda, V. & Tonti, G.A., 2011. Hypoxia and neural stem cells: from invertebrates to brain cancer stem cells. *The International journal of developmental biology*, 55(6), pp.569–81.

Manoli, M. & Driever, W., 2012. Fluorescence-activated cell sorting (FACS) of fluorescently tagged cells from zebrafish larvae for RNA isolation. *Cold Spring Harbor Protocols*, 7(8), pp.879–886.

Masumura, T. et al., 2009. Shear Stress Increases Expression of the Arterial Endothelial Marker EphrinB2 in Murine ES Cells via the VEGF-Notch Signaling Pathways. *Arteriosclerosis, Thrombosis, and Vascular Biology*, 29(12), pp.2125–2131.

Miller, L.C. et al., 2010. Separating early sensory neuron and blood vessel patterning. *Developmental dynamics : an official publication of the American Association of Anatomists*, 239(12), pp.3297–302.

Moran, A.E. et al., 2014. Temporal trends in ischemic heart disease mortality in 21 world regions, 1980 to 2010: the Global Burden of Disease 2010 study. *Circulation*, 129(14), pp.1483–92.

Mukouyama, Y.-S. et al., 2005. Peripheral nerve-derived VEGF promotes arterial differentiation via neuropilin 1-mediated positive feedback. *Development (Cambridge, England)*, 132(5), pp.941–52.

Mukouyama, Y.S. et al., 2002. Sensory nerves determine the pattern of arterial differentiation and blood vessel branching in the skin. *Cell*, 109(6), pp.693–705.

Muller, Y.A. et al., 1997. The crystal structure of vascular endothelial growth factor (VEGF) refined to 1.93 A resolution: multiple copy flexibility and receptor binding. *Structure (London, England : 1993)*, 5(10), pp.1325–38.

Nakayama, M. et al., 2013. Spatial regulation of VEGF receptor endocytosis in angiogenesis. *Nature cell biology*, 15(3), pp.249–260.

Nguyen, V. et al., 2000. Dorsal and intermediate neuronal cell types of the spinal cord are established by a BMP signaling pathway. *Development*, 127(6), pp.1209–1220.

le Noble, F. et al., 2004. Flow regulates arterial-venous differentiation in the chick embryo yolk sac. *Development (Cambridge, England)*, 131(2), pp.361–75.

Noctor, S.C. et al., 2001. Neurons derived from radial glial cells establish radial units in neocortex. *Nature*, 409(6821), pp.714–20.

Noguera-Troise, I. et al., 2006. Blockade of Dll4 inhibits tumour growth by promoting non-productive angiogenesis. *Nature*, 444(7122), pp.1032–1037.

Nolan, D.J.D.J. et al., 2013. Molecular signatures of tissue-specific microvascular endothelial cell heterogeneity in organ maintenance and regeneration. *Developmental cell*, 26(2), pp.204–19.

Nowak-Sliwinska, P., Segura, T. & Iruela-Arispe, M.L., 2014. The chicken chorioallantoic membrane model in

biology, medicine and bioengineering. *Angiogenesis*, 17(4), pp.779–804.

Nyholm, M.K., Abdelilah-Seyfried, S. & Grinblat, Y., 2009. A novel genetic mechanism regulates dorsolateral hinge-point formation during zebrafish cranial neurulation. *Journal of cell science*, 122(Pt 12), pp.2137–48.

Ohkubo, H. et al., 2014. VEGFR1-positive macrophages facilitate liver repair and sinusoidal reconstruction after hepatic ischemia/reperfusion injury. *PloS one*, 9(8), p.e105533.

Okabe, K. et al., 2014. Neurons Limit Angiogenesis by Titrating VEGF in Retina. *Cell*, 159(3), pp.584–596.

Okuda, K.S. et al., 2012. lyve1 expression reveals novel lymphatic vessels and new mechanisms for lymphatic vessel development in zebrafish. *Development (Cambridge, England)*, 139(13), pp.2381–91.

Olsson, A.-K. et al., 2006. VEGF receptor signalling - in control of vascular function. *Nature reviews. Molecular cell biology*, 7(5), pp.359–71.

Oosthuyse, B. et al., 2001. Deletion of the hypoxia-response element in the vascular endothelial growth factor promoter causes motor neuron degeneration. *Nature genetics*, 28(2), pp.131–8.

Orsenigo, F. et al., 2012. Phosphorylation of VE-cadherin is modulated by haemodynamic forces and contributes to the regulation of vascular permeability in vivo. *Nature communications*, 3, p.1208.

Panchision, D.M., 2009. The role of oxygen in regulating neural stem cells in development and disease. *Journal of cellular physiology*, 220(3), pp.562–8.

Park, H.C. et al., 2000. Analysis of upstream elements in the HuC promoter leads to the establishment of transgenic zebrafish with fluorescent neurons. *Developmental biology*, 227(2), pp.279–93.

Patterson, L.J. & Patient, R., 2006. The “Ets” factor: vessel formation in zebrafish--the missing link? *PLoS biology*, 4(1), p.e24.

Peri, F. & Nüsslein-Volhard, C., 2008. Live imaging of neuronal degradation by microglia reveals a role for v0-ATPase a1 in phagosomal fusion in vivo. *Cell*, 133(5), pp.916–27.

Pham, V.N. et al., 2007. Combinatorial function of ETS transcription factors in the developing vasculature. *Developmental biology*, 303(2), pp.772–83.

Phng, L.-K., Stanchi, F. & Gerhardt, H., 2013. Filopodia are dispensable for endothelial tip cell guidance. *Development (Cambridge, England)*, 140(19), pp.4031–40.

Phng, L.K. & Gerhardt, H., 2009. Angiogenesis: A Team Effort Coordinated by Notch. *Developmental Cell*, 16(2), pp.196–208.

Piper, M. et al., 2002. N-terminal Slit2 promotes survival and neurite extension in cultured peripheral neurons. *Neuroreport*, 13(17), pp.2375–8.

Poesen, K. et al., 2008. Novel role for vascular endothelial growth factor (VEGF) receptor-1 and its ligand VEGF-B in motor neuron degeneration. *The Journal of neuroscience : the official journal of the Society for Neuroscience*, 28(42), pp.10451–9.

Proulx, K., Lu, A. & Sumanas, S., 2010. Cranial vasculature in zebrafish forms by angioblast cluster-derived angiogenesis. *Developmental biology*, 348(1), pp.34–46.

Pugh, C.W. & Ratcliffe, P.J., 2003. Regulation of angiogenesis by hypoxia: role of the HIF system. *Nature Medicine*, 9(6), pp.677–684.

Quillien, A. et al., 2014. Distinct Notch signaling outputs pattern the developing arterial system. *Development*,

141(7), pp.1544–1552.

Rafii, S., Butler, J.M. & Ding, B.-S., 2016. Angiocrine functions of organ-specific endothelial cells. *Nature*, 529(7586), pp.316–325.

Rafii, S. & Lyden, D., 2003. Therapeutic stem and progenitor cell transplantation for organ vascularization and regeneration. *Nature Medicine*, 9(6), pp.702–712.

Ramasamy, S.K. et al., 2014. Endothelial Notch activity promotes angiogenesis and osteogenesis in bone. *Nature*, 507(7492), pp.376–380.

Regan, E.R. & Aird, W.C., 2012. Dynamical Systems Approach to Endothelial Heterogeneity. *Circulation Research*, 111(1), pp.110–130.

Reischauer, S. et al., 2016. Cloche is a bHLH-PAS transcription factor that drives haemato-vascular specification. *Nature*, 535(7611), pp.294–298.

Ribatti, D., 2008. Judah Folkman, a pioneer in the study of angiogenesis. *Angiogenesis*, 11(1), pp.3–10.

Risau, W., 1995. Differentiation of endothelium. *FASEB journal : official publication of the Federation of American Societies for Experimental Biology*, 9(10), pp.926–33.

Risau, W. & Flamme, I., 1995. Vasculogenesis. *Annual review of cell and developmental biology*, 11, pp.73–91.

Robciuc, M.R. et al., 2016. VEGFB/VEGFR1-Induced Expansion of Adipose Vasculature Counteracts Obesity and Related Metabolic Complications. *Cell metabolism*, 23(4), pp.712–24.

Roca, C. & Adams, R.H., 2007. Regulation of vascular morphogenesis by Notch signaling. *Genes & development*, 21(20), pp.2511–24.

Rocha, S.F. et al., 2014. Esm1 modulates endothelial tip cell behavior and vascular permeability by enhancing VEGF bioavailability. *Circulation research*, 115(6), pp.581–90.

van Rooijen, E. et al., 2011. *A zebrafish model for VHL and hypoxia signaling.* Third Edit., Elsevier Inc.

van Rooijen, E. et al., 2010. von Hippel-Lindau tumor suppressor mutants faithfully model pathological hypoxia-driven angiogenesis and vascular retinopathies in zebrafish. *Disease Models & Mechanisms*, 3(5-6), pp.343–353.

Rooijen, E. van et al., 2009. Zebrafish mutants in the von Hippel-Lindau tumor suppressor display a hypoxic response and recapitulate key aspects of Chuvash polycythemia. *Blood*, 113(25), pp.6449–60.

Rossi, A. et al., 2015. Genetic compensation induced by deleterious mutations but not gene knockdowns. *Nature*, 524(7564), pp.230–233.

Rottbauer, W. et al., 2005. VEGF-PLC 1 pathway controls cardiac contractility in the embryonic heart. *Genes & Development*, 19(13), pp.1624–1634.

Rubanyi, G.M., 2013. Mechanistic, Technical, and Clinical Perspectives in Therapeutic Stimulation of Coronary Collateral Development by Angiogenic Growth Factors. *Molecular Therapy*, 21(4), pp.725–738.

Ruhrberg, C. et al., 2002. Spatially restricted patterning cues provided by heparin-binding VEGF-A control blood vessel branching morphogenesis. *Genes & development*, 16(20), pp.2684–2698.

Ruhrberg, C. & Bautch, V.L., 2013. Neurovascular development and links to disease. *Cellular and molecular life sciences : CMLS*, 70(10), pp.1675–84.

Ruiz de Almodovar, C. et al., 2009. Role and therapeutic potential of VEGF in the nervous system. *Physiological reviews*, 89(2), pp.607–48.

Sabin, F., 1917. Origin and Development of the Primitive Vessels of the Chick and of the Pig.

Saharinen, P. et al., 2004. Lymphatic vasculature: development, molecular regulation and role in tumor metastasis and inflammation. *Trends in immunology*, 25(7), pp.387–95.

Santhakumar, K. et al., 2012. A zebrafish model to study and therapeutically manipulate hypoxia signaling in tumorigenesis. *Cancer research*, 72(16), pp.4017–27.

Sawamiphak, S. et al., 2010. Ephrin-B2 regulates VEGFR2 function in developmental and tumour angiogenesis. *Nature*, 465(7297), pp.487–91.

Sawano, A. et al., 2001. Flt-1, vascular endothelial growth factor receptor 1, is a novel cell surface marker for the lineage of monocyte-macrophages in humans. *Blood*, 97(3), pp.785–791.

Schaper, W. et al., 1988. The collateral circulation of the heart. *Progress in cardiovascular diseases*, 31(1), pp.57–77.

Schmidt, R., Strähle, U. & Scholpp, S., 2013. Neurogenesis in zebrafish – from embryo to adult. *Neural Development*, 8(1), p.3.

Schulte-Merker, S. & Stainier, D.Y.R., 2014. Out with the old, in with the new: reassessing morpholino knockdowns in light of genome editing technology. *Development*, 141(16), pp.3103–3104.

Sela, S. et al., 2008. A novel human-specific soluble vascular endothelial growth factor receptor 1: Cell type-specific splicing and implications to vascular endothelial growth factor homeostasis and preeclampsia. *Circulation Research*, 102(12), pp.1566–1574.

Selvaraj, D. et al., 2015. A Functional Role for VEGFR1 Expressed in Peripheral Sensory Neurons in Cancer Pain. *Cancer cell*, 27(6), pp.780–96.

Senger, D.R. et al., 1993. Vascular permeability factor (VPF, VEGF) in tumor biology. *Cancer metastasis reviews*, 12(3-4), pp.303–24.

Shalaby, F. et al., 1995. Failure of blood-island formation and vasculogenesis in Flk-1-deficient mice. *Nature*, 376(6535), pp.62–6.

Shibuya, M. et al., 1990. Nucleotide sequence and expression of a novel human receptor-type tyrosine kinase gene (flt) closely related to the fms family. *Oncogene*, 5(4), pp.519–24.

Shibuya, M., 2001. Structure and dual function of vascular endothelial growth factor receptor-1 (Flt-1). *The international journal of biochemistry & cell biology*, 33(4), pp.409–20.

Siekmann, A.F., Affolter, M. & Belting, H.-G., 2013. The tip cell concept 10 years after: New players tune in for a common theme. *Experimental Cell Research*, 319(9), pp.1255–1263.

Siekmann, A.F. & Lawson, N.D., 2007. Notch signalling limits angiogenic cell behaviour in developing zebrafish arteries. *Nature*, 445(7129), pp.781–4.

Sigurbjörnsdóttir, S., Mathew, R. & Leptin, M., 2014. Molecular mechanisms of de novo lumen formation. *Nature reviews. Molecular cell biology*, 15(10), pp.665–76.

Simons, M., 2005. Angiogenesis: where do we stand now? *Circulation*, 111(12), pp.1556–66.

De Smet, F. et al., 2009. Mechanisms of vessel branching: filopodia on endothelial tip cells lead the way. *Arteriosclerosis, thrombosis, and vascular biology*, 29(5), pp.639–49.

Song, J.W. & Munn, L.L., 2011. Fluid forces control endothelial sprouting. , 2011, pp.1–6.

Spear, P.C. & Erickson, C.A., 2012. Interkinetic nuclear migration: a mysterious process in search of a function.

Development, growth & differentiation, 54(3), pp.306–16.

Stahlhut, C. et al., 2012. miR-1 and miR-206 regulate angiogenesis by modulating VegfA expression in zebrafish. *Development (Cambridge, England)*, 139(23), pp.4356–64.

Stainier, D.Y. et al., 1995. Cloche, an early acting zebrafish gene, is required by both the endothelial and hematopoietic lineages. *Development (Cambridge, England)*, 121(10), pp.3141–50.

Stainier, D.Y.R., Kontarakis, Z. & Rossi, A., 2015. Making sense of anti-sense data. *Developmental cell*, 32(1), pp.7–8.

Stefater, J.A. et al., 2011. Regulation of angiogenesis by a non-canonical Wnt-Flt1 pathway in myeloid cells. *Nature*, 474(7352), pp.511–5.

Stone, J. & Dreher, Z., 1987. Relationship between astrocytes, ganglion cells and vasculature of the retina. *The Journal of comparative neurology*, 255(1), pp.35–49.

Storkebaum, E. et al., 2005. Treatment of motoneuron degeneration by intracerebroventricular delivery of VEGF in a rat model of ALS. *Nature neuroscience*, 8(1), pp.85–92.

Storkebaum, E. & Carmeliet, P., 2004. VEGF: a critical player in neurodegeneration. *The Journal of clinical investigation*, 113(1), pp.14–8.

Strzyz, P.J. et al., 2015. Interkinetic nuclear migration is centrosome independent and ensures apical cell division to maintain tissue integrity. *Developmental cell*, 32(2), pp.203–19.

Suchting, S. et al., 2007. The Notch ligand Delta-like 4 negatively regulates endothelial tip cell formation and vessel branching. *Proceedings of the National Academy of Sciences of the United States of America*, 104(9), pp.3225–30.

Sumanas, S. & Lin, S., 2006. Ets1-related protein is a key regulator of vasculogenesis in zebrafish. *PLoS biology*, 4(1), p.e10.

Suto, K. et al., 2005. Crystal structures of novel vascular endothelial growth factors (VEGF) from snake venoms: insight into selective VEGF binding to kinase insert domain-containing receptor but not to fms-like tyrosine kinase-1. *The Journal of biological chemistry*, 280(3), pp.2126–31.

Swift, M.R. & Weinstein, B.M., 2009. Arterial-venous specification during development. *Circulation research*, 104(5), pp.576–88.

Takahashi, H. & Shibuya, M., 2005. The vascular endothelial growth factor (VEGF)/VEGF receptor system and its role under physiological and pathological conditions. *Clinical science (London, England : 1979)*, 109(3), pp.227–41.

Tammela, T. et al., 2008. Blocking VEGFR-3 suppresses angiogenic sprouting and vascular network formation. *Nature*, 454(7204), pp.656–60.

Tammela, T. & Alitalo, K., 2010. Lymphangiogenesis: Molecular mechanisms and future promise. *Cell*, 140(4), pp.460–76.

Tata, M., Ruhrberg, C. & Fantin, A., 2015. Vascularisation of the central nervous system. *Mechanisms of development*, 138 Pt 1, pp.26–36.

Tchaikovski, V., Fellbrich, G. & Waltenberger, J., 2008. The molecular basis of VEGFR-1 signal transduction pathways in primary human monocytes. *Arteriosclerosis, thrombosis, and vascular biology*, 28(2), pp.322–8.

Thoma, R., 1873. *Die Ueberwanderung farbloser Blutkörper von dem Blut - in das Lymphgefässsystem.*,

Thurston, G., Noguera-Troise, I. & Yancopoulos, G.D., 2007. The Delta paradox: DLL4 blockade leads to more tumour vessels but less tumour growth. *Nature reviews. Cancer*, 7(5), pp.327–31.

del Toro, R. et al., 2010. Identification and functional analysis of endothelial tip cell-enriched genes. *Blood*, 116(19), pp.4025–33.

Torres-Vázquez, J. et al., 2004. Semaphorin-plexin signaling guides patterning of the developing vasculature. *Developmental cell*, 7(1), pp.117–23.

Torres-Vázquez, J., Kamei, M. & Weinstein, B.M., 2003. Molecular distinction between arteries and veins. *Cell and tissue research*, 314(1), pp.43–59.

Trapnell, C. et al., 2012. Differential gene and transcript expression analysis of RNA-seq experiments with TopHat and Cufflinks. *Nature protocols*, 7(3), pp.562–578.

Tu, J. et al., 2014. Notch1 and 4 signaling responds to an increasing vascular wall shear stress in a rat model of arteriovenous malformations. *BioMed research international*, 2014, p.368082.

Ulrich, F. et al., 2011. Neurovascular development in the embryonic zebrafish hindbrain. *Developmental Biology*, 357(1), pp.134–151.

Veldman, M.B. & Lin, S., 2008. Zebrafish as a developmental model organism for pediatric research. *Pediatric research*, 64(5), pp.470–6.

Vestweber, D., 2015. How leukocytes cross the vascular endothelium. *Nature Reviews Immunology*, 15(11), pp.692–704.

Wallez, Y. & Huber, P., 2008. Endothelial adherens and tight junctions in vascular homeostasis, inflammation and angiogenesis. *Biochimica et biophysica acta*, 1778(3), pp.794–809.

Wang, H.U., Chen, Z.-F. & Anderson, D.J., 1998. Molecular Distinction and Angiogenic Interaction between Embryonic Arteries and Veins Revealed by ephrin-B2 and Its Receptor Eph-B4. *Cell*, 93(5), pp.741–753.

Wang, Y. et al., 2010. Ephrin-B2 controls VEGF-induced angiogenesis and lymphangiogenesis. *Nature*, 465(7297), pp.483–6.

Watson, O. et al., 2013. Blood flow suppresses vascular Notch signalling via dll4 and is required for angiogenesis in response to hypoxic signalling. *Cardiovascular research*, 100(2), pp.252–61.

Webby, C.J. et al., 2009. Jmjd6 catalyses lysyl-hydroxylation of U2AF65, a protein associated with RNA splicing. *Science (New York, N.Y.)*, 325(5936), pp.90–93.

Weidemann, A. & Johnson, R.S., 2008. Biology of HIF-1α. *Cell Death and Differentiation*, 15(4), pp.621–627.

Welti, J. et al., 2013. Recent molecular discoveries in angiogenesis and antiangiogenic therapies in cancer. *The Journal of clinical investigation*, 123(8), pp.3190–200.

Wiesmann, C. et al., 1997. Crystal Structure at 1.7 Å Resolution of VEGF in Complex with Domain 2 of the Flt-1 Receptor. *Cell*, 91(5), pp.695–704.

Wiley, D.M. et al., 2011. Distinct signalling pathways regulate sprouting angiogenesis from the dorsal aorta and the axial vein. *Nature cell biology*, 13(6), pp.686–92.

Wilson, L. & Maden, M., 2005. The mechanisms of dorsoventral patterning in the vertebrate neural tube. *Developmental biology*, 282(1), pp.1–13.

Winberg, M.L. et al., 1998. Plexin A is a neuronal semaphorin receptor that controls axon guidance. *Cell*, 95(7),

pp.903–16.

Woolard, J. et al., 2004. VEGF165b, an inhibitory vascular endothelial growth factor splice variant: mechanism of action, in vivo effect on angiogenesis and endogenous protein expression. *Cancer research*, 64(21), pp.7822–35.

Xu, C. et al., 2014. Arteries are formed by vein-derived endothelial tip cells. *Nature communications*, 5, p.5758.

Y C Fung, and & Zweifach, B.W., 1971. Microcirculation: Mechanics of Blood Flow in Capillaries. *http://dx.doi.org/10.1146/annurev.fl.03.010171.001201*.

Yamaguchi, S., Iwata, K. & Shibuya, M., 2002. Soluble Flt-1 (soluble VEGFR-1), a potent natural antiangiogenic molecule in mammals, is phylogenetically conserved in avians. *Biochemical and biophysical research communications*, 291(3), pp.554–9.

Yaniv, K. et al., 2007. Imaging the developing lymphatic system using the zebrafish. *Novartis Foundation symposium*, 283, pp.139–48; discussion 148–51, 238–41.

Yaniv, K. et al., 2006. Live imaging of lymphatic development in the zebrafish. *Nature Medicine*, 12(6), pp.711–716.

Yao, J. et al., 2011. Expression of a functional VEGFR-1 in tumor cells is a major determinant of anti-PlGF antibodies efficacy. *Proceedings of the National Academy of Sciences*, 108(28), pp.11590–11595.

You, L.-R. et al., 2005. Suppression of Notch signalling by the COUP-TFII transcription factor regulates vein identity. *Nature*, 435(7038), pp.98–104.

Young, B.C., Levine, R.J. & Karumanchi, S.A., 2010. Pathogenesis of preeclampsia. *Annual review of pathology*, 5, pp.173–92.

Zarkada, G. et al., 2015. VEGFR3 does not sustain retinal angiogenesis without VEGFR2. *Proceedings of the National Academy of Sciences of the United States of America*, 112(3), pp.761–6.

Zhao, L. et al., 2014. Notch signaling regulates cardiomyocyte proliferation during zebrafish heart regeneration. *Proceedings of the National Academy of Sciences of the United States of America*, 111(4), pp.1403–8.

Zhao, W. et al., 2012. Binding affinities of vascular endothelial growth factor (VEGF) for heparin-derived oligosaccharides. *Bioscience reports*, 32(1), pp.71–81.

Zygmunt, T. et al., 2011. Semaphorin-PlexinD1 Signaling Limits Angiogenic Potential via the VEGF Decoy Receptor sFlt1. *Developmental cell*, 21(2), pp.301–314.

8 Abbreviations

aISV	arterial intersegmental vessel
Alk2/3	activin receptor-like kinase
ANG-2	Angiopoetin 2
APLN	Apelin
APLNR	Apelin receptor
AV	arteriovenous
AVD	arteriovenous differentiation
BAD	Bcl-2-associated death promoter
BCL-2	B cell lymphoma 2
BMP	bone morphogenic protein
BMPR	bone morphogenic protein receptor
CDH5	cadherin 5 (VE-Cadherin)
CNS	central nervous system
COUP-TFII	chicken ovalbumin upstream promoter transcription factor 2
CRISPR/Cas	Clustered Regularly Interspaced Short Palindromic Repeats/Cas
CV	cardinal vein
DA	dorsal aorta
DAG	diacylglycerol
DLAV	dorsal longitudinal anastomotic vessel
DLL4	delta like 4 (mouse/human protein)
Dll4	delta like 4 (mouse gene)
Dll4	delta like 4 (zebrafish protein)
dll4	delta like 4 (zebrafish gene)
dpf	days post fertilization
EC	endothelial cell
ECM	extracellular matrix
Ela	Elabela (zebrafish protein)
eNOS	endothelial nitric oxide synthase
ER	Endoplasmatic reticulum
ERK1/2	extracellular-signal-regulated kinase 1/2
ERR-α	Estrogen-related receptor alpha
ETS domain	E26 transformation-specific domain
etsrp	Ets1-related protein (zebrafish gene aka etv2)
etv2	ETS variant 2 (zebrafish gene)
F-actin	filamentous actin
FAK	focal adhesion kinase
FDA	Food and Drug Administration
FGF	Fibroblast Growth Factor
Fli1a	Fli1 proto-oncogene
FLT1	Fms-related tyrosine kinase 1 (mouse/human protein)

Flt1	Fms-related tyrosine kinase 1 (mouse gene)
Flt1	Fms-related tyrosine kinase 1 (zebrafish protein)
flt1	Fms-related tyrosine kinase 1 (zebrafish gene)
FLT4	Fms-related tyrosine kinase 4 (mouse/human protein)
Flt4	Fms-related tyrosine kinase 4 (mouse gene)
Flt4	Fms-related tyrosine kinase 4 (zebrafish protein)
flt4	Fms-related tyrosine kinase 4 (zebrafish gene)
foxc1a/b	forkhead box C1a/b
FOXO1	Forkhead box protein O1
Gja5	gap junction protein alpha 5 (connexin-40)
HDAC	histone deacetylase
HMS	horizontal myoseptum
hpf	hours post fertilization
HRE	hypoxia response element
HSPGs	heparane sulfate proteoglycans
Ig	immunoglobulin
IP3	inositol-1,4,5-triphosphate
ISV	intersegmental vessel
JMJD6	Jumonji domain-containing protein 6 (mouse/ human protein)
kDa	kilo Dalton
KDR/VEGFR2	kinase insert domain receptor (mouse/human protein)
Kdr	kinase insert domain receptor (mouse gene)
Kdrl	kinase insert domain receptor-like (zebrafish protein)
kdrl	kinase insert domain receptor-like (zebrafish gene)
LECs	lymphatic endothelial cells
PLs	parachordal lymphangioblasts
MAPK	mitogen-activated protein kinase
mFlt1	membrane-bound Flt1 (zebrafish protein)
mflt1	membrane-bound Flt1 (zebrafish gene)
MMP	matrix metalloproteases
MTOC	microtubule organizing center
NC	notochord
NCK	non-catalytic region of tyrosine kinase adaptor protein 1
NGF	nerve growth factor
NICD	Notch intercellular domain
NO	nitric oxide
NRPs	non-ribosomal peptides
NT	neural tube

PCV	posterior cardinal vein
PDK	phosphoinositide-dependent kinase
PGC-1α	Peroxisome proliferator-activated receptor-gamma coactivator
PHDs	prolyl hydroxylase domain 1,2,3
PI3K	phosphoinisitide-3 kinase
PIGF	placental growth factor
PIP2	phosphatidyllinositol (4,5)-biphosphate
PIP3	phosphatidyllinositol (3,4,5)-triphosphate
PKC	protein kinase C
PLCy	Phospholipase C gamma 1
PLGF	placental growth factor
Plxnd1	PlexinD1 (zebrafish protein)
PNVP	perineural vascular plexus
PTEN	phosphate and tensin homolog
pVHL	von Hippel-Lindau protein
R	tyrosine
RGC	radial glia cell
RTK	receptor tyrosine kinase
Sema3a	Semaphorin 3a (zebrafish protein)
Sema3aa	Semaphorin 3aa (zebrafish specific isoform a)
sENG	soluble endoglin
sFlt1	soluble Flt1 (zebrafish protein)
sflt1	soluble Flt1 (zebrafish gene)
SHB	SH2 domain containing protein B
shh	sonic hedgehog
TSAd	T cell-specific adapter protein
VE-cadherin	vascular endothelial cadherin (cdh5)
VEGF	Vascular Endothelial Growth Factor (VEGFA – human/mouse protein)
Vegfa	Vascular Endothelial Growth Factor A (mouse gene)
Vegfa	Vascular Endothelial Growth Factor A (zebrafish protein-isoform a or b)
vegfa	Vascular Endothelial Growth Factor A (zebrafish gene)
Vegfaa	Vascular Endothelial Growth Factor A (zebrafish protein-isoform a)
vegfaa	Vascular Endothelial Growth Factor A (zebrafish gene-isoform a)
VEGFR	Vascular Endothelial Growth Factor Receptor (human/mouse protein)
vISV	venous intersegmental vessel
VPF	vascular permeability factor (VEGF)
VRAP	VEGF receptor associated protein
WASP	Wiskott-Aldrich syndrome protein
WAVE	WASP-family verprolin-homologous protein

9 Publications

Wild, R., Klems, A., Takamiya, M., Hayashi, Y., Strähle, U., van Impel, A., Schulte-Merker, S., Krueger, J., Preau, J., le Noble, F. Neuronal sFlt1 and Vegfaa determine venous sprouting and spinal cord vascularization. **Nature Communications**, in press.

10 Curriculum Vitae

Personal records

Name:	Raphael Wild
Date of birth:	September 25th, 1986
Place of birth:	Berlin, Germany

Education and research experience

04/2015 – present	Karlsruhe Institute of Technology (Karlsruhe, Germany) PhD student Research group: Prof. Dr. Ferdinand le Noble
09/2012 – 03/2015	Max-Delbrueck-Centrum for Molecular Medicine (Berlin, Germany) PhD student Research group: Prof. Dr. Ferdinand le Noble
10/2011 – 03/2012	Max-Delbrueck-Centrum for Molecular Medicine (Berlin, Germany) Master thesis Research group: Prof. Dr. Ferdinand le Noble
10/2010 – 08/2012	Humboldt University of Berlin (Berlin, Germany) M.Sc. Molecular Life Sciences
10/2007 - 06/2010	University of Vienna (Vienna, Austria) B.Sc. Biology (Focus: Molecular Biology)
07/2006 - 07/2007	Voluntary Social Year (Moscow, Russia) General hospital no. 15, intensive care
06/2006	Dreilinden-Gymnasium; (Berlin, Germany) Abitur (high-school diploma)

Conferences and Meetings

07/2016	Endothelial Cell Phenotypes in Health & Disease Gordon Research Conference (Girona, Spain) Poster presentation
10/2015	Joint Dutch-German Microcirculation Meeting 2015 (Hannover, Germany) Poster presentation
09/2015	8th Regional Meeting on Fish Genetics and Development (Klingenmünster, Germany) Oral presentation
05/2015	ZF-Health Symposium (Paris, France)
12/2014	Angiomeeting 2015 (Münster, Germany) Oral presentation
06/2014	POF evaluation MDC (Berlin, Germany) Poster presentation